Anti-filarial drug discovery: targeting the *Wolbachia* endosymbiont

Thesis submitted in accordance with the requirements of the University of Liverpool
for the degree of Doctor in Philosophy
by

Rachel Clare

November 2018

Abstract

The diseases onchocerciasis and lymphatic filariasis (LF) are a leading cause of global morbidity affecting over 85.5 million people throughout the tropics. Clinical pathology for these diseases ranges from localised pain to hydrocele, lymphoedema and elephantiasis for LF and skin disease to blindness for onchocerciasis. Both filarial diseases are caused by parasitic filarial worm infections. Treatments for these diseases are limited to just three drugs (ivermectin (IVM), albendazole (ALB) and diethylcarbamazine citrate (DEC)), all of which principally kill only the larval stages (microfilaricidal) of these worms leaving adult worms able to re-populate the microfilarial (mf) reservoirs and subsequently continue the transmission cycle. Macrofilaricidal drugs which target the adult stages are urgently needed to aid elimination. The Anti-*Wolbachia* Consortium (A·WOL) is working on such treatments by targeting the endosymbiotic bacteria which reside within the filarial worms. Clinical field trials have provided proof of concept evidence of targeting *Wolbachia* with the antibiotic doxycycline. However, doxycycline requires a prolonged treatment course of 4-6 weeks and is contraindicated in pregnancy and children under 8 years old, therefore there is an urgent need for repurposed or novel drugs with a shorter treatment timeframe and utility in excluded populations. This study presents the development of a high content screen which enabled a 25-fold increase in throughput in screening capacity for the A·WOL drug discovery programme, from 1,000 to 25,000 compounds per month. This screen was instrumental in allowing the programme to initiate a medicinal chemistry 'hit to lead' and lead optimization development programme. Following this assay development, a collaboration with A·WOL and AstraZeneca allowed for a paradigm shift in the evolution of this screen to an industrial scale high-throughput assay (HTS). This validated assay was used to screen over 1.8 million compounds: 1.3 million from the AstraZeneca collection and 0.5 million from the Medicines for Malaria Venture (MMV). This HTS resulted in ~20,000 'hit' compounds with anti-*Wolbachia* activity. Triaging of the compounds was carried out through secondary dose response screens of ~6,000 compounds followed by further triaging through both bioinformatic assessment as well as tertiary larval (mf) testing. The resultant hit chemotypes were tested within a newly developed time kill assay validated as part of this study. This assay identified 5 novel chemotypes with faster acting anti-*Wolbachia* activity than the existing portfolio of A·WOL drugs and lead candidates.

Contents

Table of Figures

Table of Tables

Acknowledgements

I have been very fortunate to have had huge support throughout the length of my part-time self-funded PhD from both colleagues, family and friends. First, I would like to thank my Supervisor, Professor Mark Taylor and secondary supervisors Professor Stephen Ward and Professor Giancarlo Biagini, for their support and advice throughout, for the many opportunities I have had during my PhD and also allowing for this part time PhD by supporting my role as a research assistant within the A·WOL Consortium. Throughout the years there have been numerous members of the Consortium who have supported me, namely Kelly Johnston, Louise Ford and David Hong as great mentors and Gemma Molyneux, Hayley Tyrer, Amy Marriott and Andy Steven with plenty of moral support. Within the lab we are very fortunate to have a great team who are always willing to help each other out, most notably Andy Steven and John Archer whose help is always just a '….Andy/John? Would you be able to……' for which the answer has never been no. Although extremely challenging from a work, commute and personal perspective my secondment to AstraZeneca was instrumental in my PhD and career development both on a personal level and dramatic increase in my scientific and management skill set. The success of this work would not have been made possible if I had not been made to feel so welcome within AstraZeneca, with so many people taking the time to help train me on various pieces of equipment. Special thanks go to Roger Clark with the development of the HTS assay and Catherine Bardelle for validation and completion of this screen not forgetting the commitment from Matthew Collier, Andrew Cassidy and Laura Myhill. I will be forever grateful to Laura Myhill for the laughter and effort that kept me going through the array of daily problem solving. I am so proud and excited about the data and publications which have come from this collaboration which would not have been possible without the triaging and advice from my supervisors, mentors and the A·WOL chemistry team especially David Hong, Neil Berry and Paul O'Neil.

The encouragement and support from my friends Becky and Hannah, Sarah and Kathryn and my family has been never ending. The willingness of my husband to not only take shared leave but pretty much being a sole parent over the last month leading up to my submission has been crucial to allow me to complete this PhD. My parents have been as supportive as ever, including their willingness to attempt to read sections for me, numerous babysitting offers and excitement that they get to go to another graduation. Finally, and most importantly I would like to thank my son Ben who although didn't want me to have even a single day of my maternity leave to myself and liked to challenge me to review papers and write my thesis on very little sleep, has been my inspiration since returning from maternity leave. He has taught me how to be very efficient with short spells of time!

Contributor's Statements

Chapter 1: Rachel Clare wrote this under the supervision of Professor Mark Taylor.

Chapter 2: Rachel Clare wrote this under the supervision of Professor Mark Taylor. Rachel Clare designed the experiments and completed the scientific experiments under the supervision of Professor Mark Taylor, Dr Darren Cook and Dr Kelly Johnston.

Chapter 3: Rachel Clare wrote this under the supervision of Professor Mark Taylor. Rachel Clare designed the experiments with assistance from AstraZeneca collaborators (Mark Wigglesworth, Roger Clark, Dr Catherine Bardelle and Paul Harper) and A·WOL colleagues (Dr Kelly Johnston). Rachel Clare performed the scientific experiments with assistance from Roger Clark, Dr Catherine Bardelle, Matthew Collier, Paul Harper and A·WOL colleagues (Laura Myhill and Andrew Cassidy). Rachel Clare analysed the results with assistance from Mark Wigglesworth, Roger Clark and Dr Catherine Bardelle. The selection of the A·WOL compound validation set was provided by the A·WOL chemistry team. All assay plates were provided by the AstraZeneca compound management team with the platform and related HTS support provided by the AstraZeneca's Global HTS centre.

Chapter 4: Rachel Clare wrote this with supervision from Professor Mark Taylor. Rachel Clare designed and completed the AstraZeneca HTS screening with the assistance of AstraZeneca collaborators (Mark Wigglesworth, Roger Clark, Dr Catherine Bardelle and Paul Harper) and A·WOL colleagues (Laura Myhill and Andrew Cassidy). The HTS results were processed by AstraZeneca with their Genedata Screener software, the outputs of which were analysed by Rachel Clare and Dr Catherine Bardelle under the supervision of Mark Wigglesworth, Professor Mark Taylor and Professor Stephen Ward. Bioinformatic triaging was

carried out by the A·WOL (Dr Neil Berry, Dr David Hong, Professor Paul O'Neill) and AstraZeneca (Börjesson) chemists. Rachel Clare completed the experimental design, work and analysis of the MMV HTS screening with the assistance of Kevin Cross, Laura Myhill and Andrew Cassidy. The secondary HTS screen was completed by AstraZeneca. The mf assay was optimised by Dr Darren Cook. The mf assay scientific experiments were completed and analysed by Rachel Clare with support from Andy Steven and John Archer. The time kill assay was developed, validated, completed and analysed by Rachel Clare under the supervision of Dr Kelly Johnston, Dr David Hong, Professor Mark Taylor and Professor Stephen Ward. The mf production and qPCRs were set up by Andrew Steven and John Archer.

Chapter 5: Rachel Clare wrote this and Professor Mark Taylor supervised the writing.

Publications, Presentations and Conferences

Publications from this thesis

Chapter 2:

RH Clare et al. 2014 Development and validation of a high-throughput anti-*Wolbachia* whole-cell screen: a route to macrofilaricidal drugs against onchocerciasis and lymphatic filariasis. *Journal of Biomolecular Screening,* 20(1), 64–69.

Chapter 3:

RH Clare, R Clark et al. Development of a high-throughput cytometric screen to identify anti-*Wolbachia* compounds - a successful collaboration between A·WOL and AstraZeneca. *SLAS Discovery,* 2019b, in press.

Chapter 4:

RH Clare et al. 2019a Industrial scale high-throughput screening delivers multiple fast acting macrofilaricides. *Nature Communications,* 10, 11.

RH Clare, J Bibby et al. Screening the 500,000 Medicine for Malaria Venture compound library against the *Wolbachia* endosymbiont drug target for lymphatic filariasis and onchocerciasis. *Awaiting submission*

Presentations

Conference oral presentations

ISNTD d3 meeting – 2017 London

PerkinElmer User Group meeting – 2016 London

British Society of Parasitology (BSP) – 2016 London and 2015 Liverpool

LSTM Student conference – 2015 and 2016 Liverpool

The European Laboratory Research & Innovation Group (ELRIG): research and innovation – 2015 – Nottingham

Society for Laboratory Automation and Screening (SLAS) – 2015 – Washington

Departmental talk at AstraZeneca – 2014 – Alderley Park

AstraZeneca 'Freshers' lunch and learn – 2014 – Alderley Park

LSTM PGR induction day – 2013 – LSTM

Regular talks at weekly lab meetings and monthly A·WOL group meetings at LSTM in addition to presenting at 2 of the A·WOL international annual meetings

Conference poster presentation

American Society for Tropical Medicine & Hygiene (ASTM&H) – 2016 - Atlanta

BSP – 2015 Liverpool and 2014 Cambridge

LSTM student conference – 2014 and 2013 Liverpool

Additional conference attendance

ISNTD d3 – London 2018, 2016, 2015

ASTM&H – Atlanta 2012, Philadelphia 2011

ELRIG drug discovery - Liverpool 2016

Perkin Elmer High Content Screening User Group meeting – London 2014

List of Abbreviations and Acronyms

A·WOL	Anti-*Wolbachia* Consortium
AFRO	WHO Regional Office for Africa
ALB	albendazole
APOC	African Programme for Onchocerciasis Control
ARC	assay ready cryopreserved
ARPs	assay ready plates
AZT	azithromycin
BSA	bovine serum albumin
CDTI	community directed treatment with ivermectin
CV	coefficient of variation
DEC	diethylcarbamazine citrate
DMPK	drug metabolism and pharmacokinetics
DMSO	dimethyl sulfoxide
DNA	deoxyribonucleic acid
DNDi	Drugs for Neglected Diseases initiative
EC50	concentration of a drug that gives half the maximal response
ESPEN	Expanded Special Project for Elimination of Neglected Tropical Diseases
FCS	foetal calf serum
FDA	the Food and Drug Administration
FTE	full time employee
GNF	Genomics Institute of the Novartis Research Foundation
GHIT	Global Health Innovative Technology Fund
gst	Glutathione S-Transferase
GPELF	Global Programme to Eliminate Lymphatic Filariasis
GSK	GlaxoSmithKline
HAT	Human African Trypanosomiasis
HCS	high content screen
HTS	high-throughput screen
Hum Mics	human microsome clearance
IVM	ivermectin
IC50	concentration of an

	inhibitor where the response is reduced by half
IDA	IVM/DEC/ALB triple combination
LCMS	liquid chromatography mass spectrometry
LF	lymphatic filariasis
LogD	a descriptor of the lipophilicity of a molecule
LogS	a descriptor of the solubility of a molecule
LSTM	Liverpool School of Tropical Medicine
MDA	mass drug administration
mf	microfilaria
MMV	the Medicines for Malaria Venture
NEC	new chemical entities
NTD	neglected tropical diseases
OCP	Onchocerciasis Control Programme in West Africa
OEPA	Onchocerciasis Elimination Program for the Americas
PDP	Product Development Partnership
PKPD	pharmacodynamics/ pharmacokinetics
POC	proof of concept
QC	quality control
Rat Heps	rat hepatocyte clearance
RNA	ribonucleic acid
SAE	serious adverse events
SAR	structural activity relationships
SER	Spot Edge Ridge
StDev	Standard Deviation
TB	tuberculosis
TPP	target product profile
WHO	World Health Organization
wsp	*Wolbachia* Surface Protein

<u>*Species*</u>

A. albopictus - Aedes albopictus

A. viteae - Acanthocheilonema viteae

B. malayi - Brugia malayi

B. pahangi – Brugia pahangi

B. timori - Brugia timori

C. pneumoniae - Chlamydia pneumoniae

Mtb - Mycobacterium tuberculosis

O. volvulus - Onchocerca volvulus

W. bancrofti - Wuchereria bancrofti

Chapter 1 - Introduction

1.1. Filarial diseases

Lymphatic filariasis and onchocerciasis are two tropical diseases caused by filarial nematodes. These diseases are highly disabling, with the latest estimates for the number of cases at 85.5 people million affected throughout the tropics, making these diseases one of the leading causes of global morbidity (James et al. 2018).

1.1.1. Lymphatic filariasis

Lymphatic filariasis (LF) is mainly caused by the nematode *Wuchereria bancrofti* which is distributed in tropical areas including South America, Africa, Southeast Asia and the Pacific (Figure 1.1), while the nematode *Brugia malayi* is restricted to South Asia and *Brugia timori* is found in a minor focus in South-eastern Indonesia (Molyneux et al. 2003; Taylor et al. 2010, 2014). These nematodes account for an estimated 64.6 million cases of LF (James et al. 2018) with 856 million people at risk across 52 countries (World Health Organization 2018a). The larval stages of the nematode (microfilariae (mf)) are transmitted from humans to multiple species of mosquitoes, within which they develop into third-stage infective larvae (L3) over two weeks (World Health Organization 2017 and Figure 1.2). At the next blood meal of the vector the L3 larvae infect the human host, where they develop into fourth-stage larvae, moulting to the adult L5 stage after about a year. Once they have matured within the human host the adult nematodes live within the lymphatic vessels and are reproductively active for 5-8 years, producing millions of mf which migrate from the lymphatics to the blood (Figure 1.2). These mf periodically migrate to the peripheral blood to coincide with the feeding habits of the local mosquito vectors (Hawking 1951, 1967). These nematodes cause pathology which exacerbates with age, from children with subclinical pathology through to adults with overt disease, including localised pain and swellings due to inflammatory responses against dead or dying worms (Dreyer et al. 2000; Melrose 2002). This can lead to hydrocele, lymphoedema and elephantiasis, with the latter resulting in the common name for this disease (World Health Organization 2017).

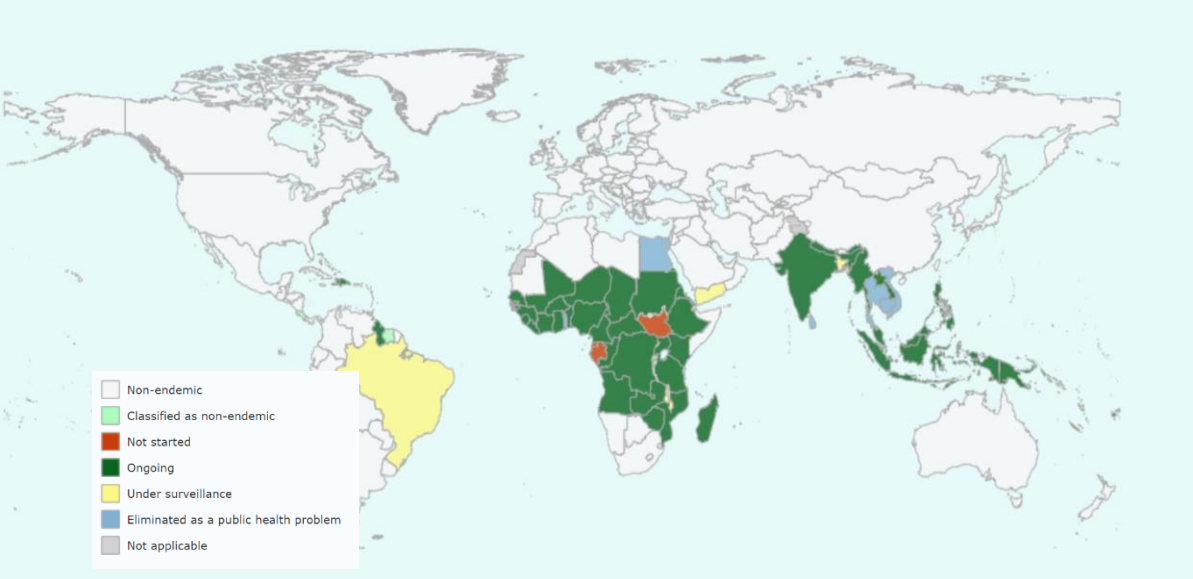

Figure 1.1 Lymphatic filariasis. Status of Mass Drug Administration (MDA) 2018. Data source: http://apps.who.int/neglected_diseases/ntddata/lf/lf.html (World Health Organization 2018b). The MDA status for each country (indicated by the colour key), is a simplification of the overall country status, however this does not represent the heterogeneity in the focal distribution of the disease within the country.

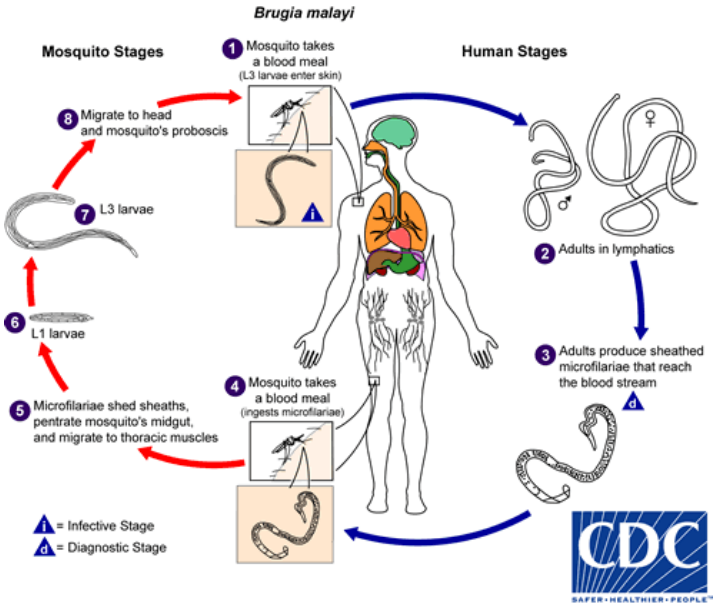

Figure 1.2. The lifecycle of *Brugia malayi*. During a blood meal, an infected mosquito introduces third-stage filarial larvae onto the skin of the human host, where they penetrate into the bite wound ❶. The L3 develop into adults that commonly reside in the lymphatics ❷. Adults produce microfilariae (mf), which are sheathed and have nocturnal periodicity. The mf migrate into lymph and enter the blood stream reaching the peripheral blood ❸. A mosquito ingests the mf during a blood meal ❹. After ingestion, the mf lose their sheaths and work their way through the wall of the proventriculus and cardiac portion of the midgut to reach the thoracic muscles ❺. There the mf develop into first-stage larvae ❻ and subsequently into third-stage larvae ❼. The third-stage larvae migrate through the hemocoel to the mosquito's proboscis ❽ and can infect another human when the mosquito takes a blood meal ❶. Reproduced from the data source: CDC https://www.cdc.gov/parasites/lymphaticfilariasis/biology_b_malayi.html

1.1.2. Onchocerciasis

Onchocerciasis is caused by the nematode *Onchocerca volvulus* which affects nearly 21 million people in 31 countries worldwide but is mostly found in Africa, with small foci in the Americas (Brazil and Venezuela) and Yemen (Figure 1.3) (World Health Organization 2018c; World Health Organization 2018d). The larvae are transmitted by day-biting blackflies which breed in rivers and streams, giving rise to the common name for this disease, 'river blindness'. Once matured within the human host, these long-lived adult worms (Plaisier et al. 1991 have estimated the mean reproductive life span of adult female worms at 9 - 11 years) reside in subcutaneous and deep tissues, forming nodules (Figure 1.4). The mf produced from adult females within these nodules migrate to the skin (and other tissues such as the eyes), which allows for their transmission by their blackfly vector. The death of these mf induces inflammatory-mediated skin disease and blindness (Burnham 1998; Keiser et al. 2002; Slatko et al. 2010; Taylor et al. 2010; Turner et al. 2014). These skin diseases range from; intense and troublesome itching, acute and chronic papular dermatitis, lichenified onchodermatitis through to leopard skin, lizard skin and hanging groin. Sowda can also occur in rare cases. Ocular lesions occur due to the death of mf within the eye, with chronic exposure leading to sclerosing keratitis, iridocyclitis and permanent visual impairment and blindness (Hall and Pearlman 1999; World Health Organization 2018c).

Both of these filarial diseases are listed as the World Health Organization's (WHO) Neglected Tropical Diseases (NTDs) (World Health Organization 2018e). The NTD term was adopted in the early 2000s (Molyneux 2004, 2012) to highlight the global lack of funding for "other diseases" than the big three; tuberculosis, HIV/AIDS and malaria. NTDs also inflict suffering on neglected communities, which includes the poorest people in the world, with almost all of the people in the 'bottom billion' having at least one of these NTDs (Hotez et al. 2009). NTDs have a disproportionate impact on the world's poor, further enhancing poverty through detriment to worker productivity and child development (Hotez et al. 2016; Molyneux 2017).

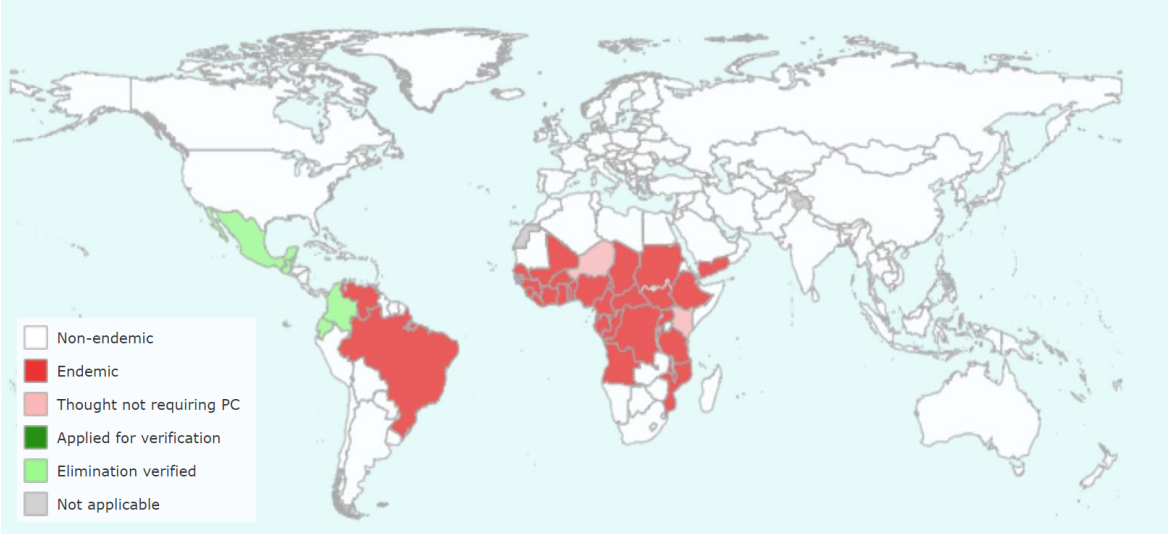

Figure 1.3. Onchocerciasis. Status of endemicity: 2018. Data source: http://apps.who.int/neglected_diseases/ntddata/oncho/onchocerciasis.html (World Health Organization 2018d). The status for each country (indicated by the colour key), is a simplification of the overall country status, however this does not represent the heterogeneity in the focal distribution of the disease within the country.

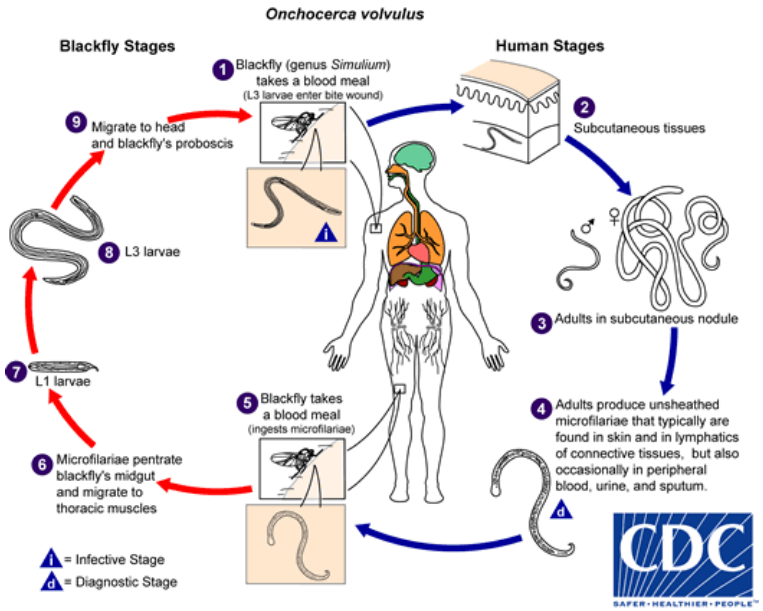

Figure 1.4. The lifecycle of *Onchocerca volvulus*. During a blood meal, an infected blackfly (genus *Simulium*) introduces third-stage filarial larvae onto the skin of the human host, where they penetrate into the bite wound ❶. In subcutaneous tissues the larvae ❷ develop into adult filariae, which commonly reside in nodules in subcutaneous connective tissues ❸. Adults can live in the nodules for approximately 15 years. Some nodules may contain numerous male and female worms. In the subcutaneous nodules, the female worms are capable of producing microfilariae (mf) for approximately 9 years. The mf are occasionally found in peripheral blood, urine, and sputum but are typically found in the skin and in the lymphatics of connective tissues ❹. A blackfly ingests the mf during a blood meal ❺. After ingestion, the mf migrate from the blackfly's midgut through the hemocoel to the thoracic muscles ❻. There the mf develop into first-stage larvae ❼ and subsequently into third-stage infective larvae ❽. The third-stage infective larvae migrate to the blackfly's proboscis ❾ and can infect another human when the fly takes a blood meal ❶. Reproduced from the data source: CDC https://www.cdc.gov/parasites/onchocerciasis/biology.html

1.2. Current treatments

Current treatments for filarial diseases focus on long term mass drug administration (MDA) implementation. This strategy incorporates the treatment of the entire at-risk community regardless of the infected status of individuals within these communities, resulting in a high demand on the drug quantities (World Health Organization 2018a, 2018b, 2018c). However, MDA eliminates the need for diagnostics for test-and-treat or test-to-exclude which require additional operational costs and logistics (Boussinesq et al. 2018).

The first large scale efforts to combat onchocerciasis were consolidated through the launch of the Onchocerciasis Control Programme in West Africa (OCP) in 1974 - 1975. Through the use of treating blackfly breeding sites with larvicides throughout initially seven West African countries, the OCP aimed to eliminate the disease (river blindness) as a public health problem through vector control (Boatin 2008). In 1989, the OCP adopted annual treatment with the then recently licenced drug ivermectin (IVM). Large-scale community trials in Ghana provided evidence for feasible and safe use of this drug to treat the microfilarial reservoir within humans (Remme et al. 1989, 1990). By the end of the programme in 2002, this intervention had expanded to cover 11 countries in West Africa (Boatin 2008). The work by the OCP was extended to cover the remaining endemic African countries by the African Programme for Onchocerciasis Control (APOC), launched in 1995, which pioneered the use of community directed treatment with ivermectin (CDTI) (Boatin 2008). The success of CDTI allowed, in 2012, for a shift in the programme goals, from control of morbidity to elimination of the parasite reservoir in feasible locations. In 2015, APOC came to a close, and control activities were devolved to the national programmes of the endemic countries. Between 2016 and 2020, these country programme-led activities receive technical support from the Expanded Special Programme for Elimination of Neglected Tropical Diseases (ESPEN), hosted and managed by the WHO Regional Office for Africa (AFRO) (Hopkins 2016). The elimination programme throughout the Americas was initiated in 1993 by the Onchocerciasis Elimination Program for the Americas (OEPA). OEPA's regional strategy was to implement biannual mass distribution of IVM across all 13 endemic foci within 6 countries (Mexico, Guatemala, Colombia, Ecuador, Brazil and Venezuela). The aim of this programme focused on the elimination of new (ocular) morbidity by 2007 and elimination of transmission of the parasite wherever feasible (Sauerbrey 2008).

WHO began its commitment to eliminating LF in 1997. To support this goal, the Global Programme to Eliminate Lymphatic Filariasis (GPELF) was established in 2000. The broad partnership within this programme included two pharmaceutical companies, namely, Merck & Co., Inc. and GlaxoSmithKline (GSK). These two companies donate drugs as well as financial, programmatic and management support for the global efforts to eliminate LF (Ottesen 2000).

The current MDA for both filarial diseases, as discussed above, relies on three drugs; ivermectin (IVM), albendazole (ALB) and diethylcarbamazine citrate (DEC). IVM is donated through the Mectizan Donation Program, with Merck & Co., Inc., pledging an unlimited supply for as long as needed for LF and onchocerciasis (Gustavsen et al. 2018). GlaxoSmithKline have also pledged 600 million ALB tablets annually for LF until it is eliminated as a public health problem (Gustavsen et al. 2018). Eisai Co., Ltd., have offered up to 2.2 billion DEC tablets for the period of 2013-2020 (Eisai Access to Medicines, 2014) .

These three donated drugs all principally target the progeny stage (mf) of these filarial worms (Taylor et al. 2010, 2014; World Health Organization 2018a). The primary aim of MDA is to interrupt transmission of LF and onchocerciasis, and to avoid the development of skin disease and blindness in onchocerciasis. However, MDA programmes require sustained and consistent implementation to cover the adult worm life span, with effective population coverage to break the transmission cycle (Verver et al. 2018). For example, the WHO recommendation for LF is at least 5 years of annual MDA with effective coverage of > 65% of the total population taking the medicine (World Health Organization 2017). For onchocerciasis the WHO recommendation is over 10 years of annual treatment (World Health Organization 2018a). Such prolonged treatments are required to sustain the blocking of transmission due to rebound of the microfilarial reservoir (Ottesen et al. 1990; Turner et al. 2014). Without widespread elimination, remaining populations will have the potential to be a source for re-introduction of transmission, at both small and large scale, especially when considering the movement of both the infected vectors and people (Molyneux et al. 2003; Verver et al. 2018).

Ivermectin is the sole MDA therapy for onchocerciasis, which is usually implemented through CDTI (World Health Organization 2018c). For LF the treatment is dependent on co-endemic diseases: ALB and DEC in areas where LF alone is endemic, IVM + ALB in areas co-

endemic with onchocerciasis, and ALB alone biannually in *Loa loa* co-endemic areas (World Health Organization 2018a). These restrictions to treatment are due to the risk of serious adverse events (SAEs) in particular settings. IVM treatment of *Loa loa* co-infected patients with high microfilaraemia can lead to encephalopathy, coma and death due to rapid death of microfilariae occluding the microvasculature in the brain (Gardon et al. 1997). This factor therefore dramatically limits CDTI treatment for onchocerciasis in areas co-endemic with *Loa loa* (Kamgno et al. 2017). DEC is contraindicated in onchocerciasis endemic areas due to the risk of adverse events including severe ocular inflammatory reactions and Mazzotti reactions (Francis et al. 1985; Ottesen 2006; Taylor et al. 2010; Fischer et al. 2017). Perceived or real adverse events associated with MDA creates stigma and fear within a population resulting in a drop of compliance and treatment coverage. The increased proportions of the population refusing treatment therefore has a big impact on the success of MDA (Turner et al. 2013; Wanji et al. 2015; Senyonjo et al. 2016; Boussinesq et al. 2018; Verver et al. 2018).

Despite this substantial worldwide burden, there has been very limited development of new drugs to treat these diseases, with no new chemical entity (NCE) approved for the use against helminth infections in the past decade (Burrows et al. 2014; Panic et al. 2014). However, although not a NCE, in June 2018 the veterinary drug moxidectin (a macrocyclic lactone like IVM) was approved for human use in the treatment of onchocerciasis (Medicines Development for Global Health 2018; Opoku et al. 2018). This treatment along with new regimens of triple combinations of IVM, DEC and ALB (IDA) may help in reaching some of the global targets outlined in the 2012 WHO roadmap for NTDs, endorsed by the London Declaration (Savioli and Daumerie 2012). The target for onchocerciasis was originally set as elimination in Yemen and regions of Latin America by 2015, with further selected countries in Africa by 2020, later extended by APOC to 2025 (APOC 2012, World Health Organization 2012). Elimination has been verified in Colombia, Ecuador, Guatemala and Mexico. However, the two remaining target countries in the Americas (Brazil and Venezuela) continue to be endemic for onchocerciasis (World Health Organization 2018c, 2018d). However, this is an over simplification with the status based on political rather than geographic boundaries, such as the Amazonian focus for this disease which straddles the two countries. This focus includes the challenges of implementing treatments for hard-to-

reach communities, such as the Yanomami communities, especially when considering the 6- and 3-monthly treatment strategies which have been implemented (Botto et al. 2016). By contrast, the two northern endemic foci in Venezuela are under post-treatment surveillance to confirm the successful elimination of the infection (Convit et al. 2013). No countries in Africa and Yemen have had elimination verified or applied for verification (World Health Organization 2018d). For LF the target is to achieve global elimination, with 100% of all endemic countries verified as free of transmission or to have entered post-intervention surveillance by 2020 (Savioli and Daumerie 2012; Cano et al. 2014). WHO's status report for LF as of October 2018, states that the elimination of LF as a public health problem has been achieved in 14 countries: Cambodia, Cook Islands, Egypt, Maldives, Marshall Islands, Niue, Palau, Sri Lanka, Thailand, Togo, Tonga, Vanuatu, Viet Nam and Wallis and Futuna. Furthermore, 7 countries are under post-intervention surveillance; American Samoa, Bangladesh, Brazil, Brunei Darussalam, Kiribati, Malawi, and Yemen.

However, 46 countries worldwide still have ongoing MDA and 5 countries have not yet started MDA (Equatorial Guinea, Gabon, São Tome and Principe, New Caledonia and South Sudan) (World Health Organization 2018b). These data clearly indicate that although progress has been impressive, the elimination targets for these diseases by 2020 appear unlikely to be met, and that new tools and approaches are required (Molyneux 2017, Molyneux et al. 2017).

Transmission dynamics models and empirical evidence demonstrate the requirement for these MDA programmes to be sustained for a long time in order to interrupt transmission and therefore lead to the target of elimination of these diseases. Prediction models for both diseases suggest that even with intensification of treatments (biannually or even quarterly) and simultaneous vector control, elimination of these diseases cannot be guaranteed in all areas by 2025 (Stolk et al. 2015; Basáñez et al. 2016; Verver et al. 2018). There is also growing concern of the potential for drug resistance to IVM (Osei-Atweneboana et al. 2011; Frempong et al. 2016).

1.3. Alternative approaches for the treatment of filariasis

Alternative or complementary therapies to the standard MDA are currently being tested in the field, including increasing the periodicity of treatment e.g. IVM bi- or pluri-annually or triple combination therapy with IVM, DEC and ALB (IDA) (King et al. 2018). These methods may have a greater effect on reducing mf and subsequent transmission as well as potential macrofilaricidal activity against LF (Cano et al. 2014; World Health Organization 2017; Boussinesq et al. 2018). However, for these strategies the risk of SAEs is still of great concern, therefore pre-treatment testing will be required, complicating and increasing the cost of this MDA strategy. This testing may include 'pre-treat-and-treat' or 'test-and-not-treat'. A co-infection with onchocerciasis and LF would result from the 'Pre-treat-and-treat' option and allow for onchocerciasis treatment with IVM prior to IDA treatment for LF. A co-infection with *Loa loa* would be identified via 'test-and-not-treat' to avoid the potential SAE related to IVM (Kamgno et al. 2017, 2018; Gedge et al. 2018).

Alternative microfilaricidal drugs are also being assessed such as moxidectin, which was approved by the Food and Drug Administration (FDA) in June 2018 (Medicines Development for Global Health 2018). Moxidectin is a macrocyclic lactone similar to IVM. However, clinical trials have shown it has superiority over IVM with modelling predicting that the impact of annual dosing would match that of biannual treatment with IVM (Turner et al. 2015). Therefore, resources could focus on maximising coverage of annual moxidectin over biannual IVM (Boussinesq et al. 2018; Opoku et al. 2018). However, the same limitations as using IVM occur, including Mazzotti reactions, and further data are required to assess the approach to use in *Loa loa* co-endemic areas where ivermectin MDA is contraindicated (Opoku et al. 2018).

Other compounds are entering clinical trials including the re-purposed veterinary drug emodepside (originated by Astellas and out-licensed to Bayer). This drug is currently in a phase 1 study of its safety, tolerability and pharmacokinetics in healthy volunteers by the Drugs for Neglected Diseases initiative (DNDi) (Boussinesq et al. 2018; DNDi 2018).

Such direct-acting drugs as described above have had limited success in the filarial drug discovery field. Janssen's promising candidate flubendazole (orally bioavailable formulation), which is in the same benzimidazole class as ALB, has proven macrofilaricidal

activity. However, it was discontinued in 2017 due to toxicological effects (Geary et al. 2019; Lachau-Durand et al. 2019). Similarly, a boron derived benzimidazole AN15470 originally from Anacor Pharmaceuticals was also discontinued. Oxfendazole (a veterinary drug) is the only remaining benzimidazole in the DNDi pipeline, currently in preclinical testing (DNDi 2018).

Although new drugs are progressing, none of the drugs described above have activity against a novel target, the endosymbiotic bacteria, *Wolbachia pipientis* (discussed further in Chapter 1.4 below). The Anti-*Wolbachia* Consortium (A·WOL), combining partners from academia and industry led by the Liverpool School of Tropical Medicine (LSTM), was established in 2007 to discover and develop new anti-*Wolbachia* drugs (Taylor et al. 2010; Burrows et al. 2014; Johnston et al. 2014a). The first such designer macrofilaricidal drug, TylAMac™, is a derivative of the veterinary drug tylosin, a 16-membered macrolide, which was identified during the screening of a focused anti-infective compound library by A·WOL. Following the identification of this highly active compound in A·WOL's *in vitro* cell screen (discussed further in Chapter 1.5 below), anti-*Wolbachia* activity was confirmed *in vivo* against *Litomosoides sigmodontis* and *Brugia malayi*, when delivered parenterally. However, oral administration had almost no activity, due to poor oral bioavailability. The creation of analogs through medicinal chemistry efforts, ultimately developed TylaMac™, an oral compound with anti-*Wolbachia* efficacy *in vivo*. TylaMac™ also has a pharmacology and safety profile that is compatible with a short-term treatment regimen and has completed phase I trials, currently progressing to phase II testing (Drugs for Neglected Diseases Initiative 2018; Taylor et al. 2019; Table 1.1). In addition, new therapies are awaiting clinical trials including high-dose rifampicin treatment, predicted to have clinically relevant exposure in humans, which has been shown to be well-tolerated over one to two weeks. This dosage depletes *Wolbachia* more rapidly than doxycycline in pre-clinical animal models, suggesting improved activity in clinical trials (Aljayyoussi et al. 2017a). A·WOL have developed these *in-vivo* animal models, to better inform the clinical relevance of potential new drugs using a pharmacokinetic/ pharmacodynamic (PKPD) modelling approach. These PKPD models are based on both L3-L4 larval (short term) and adult (long-term) *Brugia malayi* infected immunodeficient mice. This model system has been developed to related pharmacokinetic parameters to pharmacodynamic outcomes using clinically relevant doses

in humans. These clinically relevant human-mouse bioequivalent bridging studies (Johnston 2014a; Sharma et al. 2016; Aljayyoussi et al. 2017a; Hong et al. 2019) have been well characterised via drug development through to clinical application (Debrah et al. 2006b, 2007, 2011, 2015). Further details on new anti-*Wolbachia* therapies are discussed in this thesis.

1.4. *Wolbachia* – a novel drug target

The intracellular bacterium *Wolbachia* infects a remarkable range of arthropods, with estimates ranging from 40-66% (Hilgenboecker et al. 2008; Zug et al. 2012). *Wolbachia* has a range of consequences for its hosts, ranging from parasitic to beneficial; the former includes reproductive manipulation to promote its transmission, and the latter the affording of protection from pathogens (Barr 1980; O'Neill et al. 1992; Rousset et al. 1992; Stouthamer et al. 1993; Taylor et al. 2018). There has been an explosion of interest in the protective role that *Wolbachia* can provide, in relation to the mosquito vectors of arboviruses such as dengue, Zika, chikungunya, West Nile and yellow fever (Frentiu et al. 2010; Glaser and Meola 2010; Walker et al. 2011; van den Hurk et al. 2012; Blagrove et al. 2013; Hussain et al. 2013; Aliota et al. 2016a, 2016b; Dutra et al. 2016). Research by the World Mosquito Program, is testing whether the artificial introduction of *Wolbachia* into the mosquito, *Aedes aegypti*, can be used as a control tool to reduce the transmission of these life-threatening viruses (World Mosquito Program 2019).

In addition to the widespread presence of *Wolbachia* in insects, all filarial worms causing human onchocerciasis and LF harbour *Wolbachia*. However, within these hosts *Wolbachia* has a mutualistic association, as it is vital for the nematode's survival, growth and fertility (Taylor et al. 2010; Slatko et al. 2014). Bacterial-like structures were first discovered in filariae in the 1970s with the advent of electron microscopy (McLaren et al. 1975; Kozek & Marroquin 1977; Kozek 1977). This observation gained little attention until 1995 when molecular genetic techniques enabled the identification of the bacteria as *Wolbachia* in a veterinary filarial worm, *Dirofilaria immitis* (dog heartworm). This was the first time *Wolbachia* had been found in any non-arthropod species (Sironi et al. 1995). Subsequent studies detected *Wolbachia* in *Dirofilaria immitis*, *Dirofilaria repens*, *Brugia malayi*, *Brugia pahangi*, *Onchocerca gibsoni*, *Onchocerca gutturosa*, *Onchocerca ochengi*, *Wuchereria bancrofti* and *Litomosoides sigmodontis* (Bandi et al. 1998). *Wolbachia* has been found in all

developmental stages of filarial worms (Kozek and Marroquin 1977; Kozek 1977; Sironi et al. 1995; Hoerauf et al. 1999; Taylor et al. 1999a, 1999b; McGarry et al. 2004; Foster et al. 2005). Almost all filarial parasites of humans have been shown to harbour *Wolbachia* (Taylor et al. 1999b; Bandi et al. 2001; Foster et al. 2005; Lefoulon et al. 2016). To date, 20 species of filariae appear to be devoid of *Wolbachia*, these range throughout all subfamilies and have been isolated from a breadth of hosts included mammals, bird and reptiles. From a medical perspective in relation to filarial diseases, the most important species to lack *Wolbachia* is *Loa loa* (Büttner et al. 2003; McGarry et al. 2003).

Wolbachia pipientis are alpha-proteobacteria closely related to *Ehrlichia* and *Anaplasma* species (Sironi et al. 1995; Lefoulon et al. 2016). Phylogenetic analyses by Lefoulon et al. (2016) support the separation of this species into the 7 supergroups A to Q (excluding G) (Lo et al. 2007; Ros et al. 2009; Bing et al. 2014; Glowska et al. 2015). Filarial *Wolbachia* are found within supergroups C, D, F and J. The filariae causing LF (*W. bancrofti*, *B. malayi* and *B. timori*) are hosts for supergroup D, alongside other *Brugia* species, as well as *Litomosoides* species. The symbiont of *O. volvulus* is found in supergroup C, alongside other *Onchocerca* species, as well as *Dirofilaria* species and *Loxodontofilaria caprini* (Lefoulon et al. 2016).

Within filarial nematodes, *Wolbachia* are found principally in the hypodermal lateral chords within host-derived vacuoles, at varying quantities between individuals (McGarry et al. 2004). They have also been identified in the ovaries, embryos and secretory-excretory canal (Kozek and Marroquin 1977; McGarry et al. 2004; Landmann et al. 2010; Fischer et al. 2011).

Bosshardt et al. (1993) were the first to show that treating *Brugia pahangi*-infected jirds with the antibiotic tetracycline inhibited the maturation of 3rd stage larvae to adult worms and the development of microfilaraemia. The direct association between tetracycline treatment leading to depletion of *Wolbachia* and inhibiting parasite development was identified by Hoerauf et al. (1999). They showed that 28 days of treatment with tetracycline (compared to penicillin, known to lack activity against rickettsial bacteria) in a *Litomosoides sigmodontis* mouse model led to the elimination of *Wolbachia* judged by immunohistology and electron microscopy (Hoerauf et al. 1999). Furthermore, this resulted in blocking worm establishment and growth as well as rendering the adult worms infertile. Conversely, there was no impact on *Wolbachia*-free *Acanthocheilonema viteae*. This highlighted the

nematodes' relationship with *Wolbachia* as mutualistic in contrast to the largely parasitic association found in arthropods. Work by Bandi et al. (1999) identified similar inhibition of development within embryos when treating *B. pahangi* in jirds with tetracycline, as well as associating this inhibition to *Wolbachia* reduction. This work was extended to testing doxycycline in dogs infected with *Dirofilaria immitis* with similar results. Beyond the mutualism of *Wolbachia* essentiality for development and fertility, several studies have suggested other metabolic provisions provided by *Wolbachia* to their filarial nematode hosts. Comparative analysis of *Wolbachia* (*wBm*) and *Brugia malayi* genomic sequences by Wu et al. (2009), highlighted the heme biosynthesis pathway as one such provision. From this pathway, which is conserved in eukaryotes and prokaryotes, all but one of the heme biosynthetic genes (protoporphyrinogen- IX oxidase (PPO)) can be identified in the *wBm* genome. Conversely, all but the last heme biosynthetic gene in the pathway (ferrochelatase (FC)) are absent from the *B. malayi* genome, suggesting these nematodes are incapable of *de novo* heme biosynthesis. This is common to most nematodes including *Caenorhabditis elegans*, suggesting that they salvage heme or intermediates from their environment, or in the case of filarial worms, acquisition from their *Wolbachia* endosymbiont (Wu et al. 2009). ATP has also been proposed to be provided to the host for energy generation by *Wolbachia*. Evidence for this hypothesis is based on the analysis of the gene expression of *Wolbachia* from *Onchocerca ochengi* by Darby et al. (2012). Their work suggests that *Wolbachia* could have a mitochondrion-like function based on the high profile of ATP synthase in the transcriptome and proteome, as well as elevated expression of respiratory chain components. This work by Darby et al. (2012) also supports the suggestion that *Wolbachia* modulates the mammalian immune system to allow their filarial host to withstand the mammalian immune response for their long lifespan, thus providing a defensive as well as a metabolite provisioning mutualism. This theory has been supported by *in vivo* studies by Hansen et al. (2011). In their work, depletion of *Wolbachia* in *O. ochengi* by oxytetracycline resulted in the infiltration of eosinophils into the nodule resulting in the eventual death of the worms. This was specific to *Wolbachia* and not the nematode death, as this response was not observed for melarsomine (a conventional adulticide with no anti-*Wolbachia* activity). Landmann et al. (2011) also discuss the role that *Wolbachia* has with apoptosis within the host. They suggest that *Wolbachia* has a defensive role in limiting apoptosis which could be vital to allow the nematode to develop through crucial life stages. In

comparison, depletion of *Wolbachia* induces non-cell autonomous apoptosis which leads to arresting the development of otherwise motile and viable mf and L4 (Landmann et al. 2011). This mutualistic relationship between filarial nematodes and *Wolbachia* can therefore be exploited as a drug target for LF and onchocerciasis. The concept of *Wolbachia* as a drug target has subsequently been validated by an extensive series of clinical trials using antibiotics such as doxycycline (Table 1.2 and Table 1.3). Field trials with doxycycline have shown efficacy of a 4-6 weeks course of treatment with 100/200 mg per day resulting in long-term sterilisation and macrofilaricidal (death of adult worm) activity. Further to this, work by Albers et al. (2012) on *O. volvulus*, identified that the impact of doxycycline treatment can extend to limiting transmission, through delaying larval development within the vector (though delayed development was also due to seasonal trends toward lower ambient temperatures that lengthened the extrinsic incubation period). Doxycycline has subsequently become adopted as a policy drug, in particular as an alternative treatment for onchocerciasis in *Loa loa* co-endemic areas, due to the absence of SAE risk compared with IVM treatment of loiasis patients (Turner et al. 2010; Tamarozzi et al. 2012; Taylor et al. 2014; Aljayyoussi et al. 2017a; Boussinesq et al. 2018). Although a community-based delivery of doxycycline for onchocerciasis has been shown to be feasible and with a long-term impact in Cameroon (Wanji et al. 2009; Tamarozzi et al. 2012), with therapeutic coverage of 73.8% and compliance at 97.5%, doxycycline is not deemed suitable for MDA. This is due to the long course of treatment (daily for 4-6 weeks) as well as contraindication in children and women of a child-bearing age (Taylor et al. 2014). It is believed that the high level of adherence to the treatment regimen was aided by positive feed-back from community members who took part and subsequently motivated reluctant individuals based on their personal experience of treatment benefits, including relief from body itches and nodules, improved vision, appetite and sexual desire as well as curing boils and wounds (Wanji et al. 2009). Some of these benefits are likely to be due to the broad spectrum antibiotic activity of doxycycline. In addition to these benefits for onchocerciasis, trials with doxycycline treatment for LF demonstrated clinical improvements in the severity of lymphoedema and hydrocoele (Debrah et al. 2006a, 2009; Mand et al. 2009, 2012; Taylor et al. 2010).

Table 1.1. Summary of ongoing clinical trials using anti-*Wolbachia* therapy.

Ongoing trials	Phase	Disease	Drug	Intervention	trial start - end date	location
ISRCTN14042737: Doxycycline to improve filarial lymphedema (LEDoxy Ghana)	2	LF	DOX	200 mg/day DOX for 6 weeks 100 mg/day DOX for 6 weeks	Jan 17 - Jun 20	Ghana
ISRCTN65756724: Doxycycline to improve filarial lymphedema (LEDoxy Tanzania)	2	LF	DOX	200 mg/day DOX for 6 weeks 100 mg/day DOX for 6 weeks	Jan 17 - Dec 20	Tanzania
NCT02929121 A 24 Month Study to Compare Efficacy of Doxycycline vs Placebo for Improving Filarial Lymphedema in India	3	Filariasis	DOX	200 mg/day for 6 weeks (patients < 50 kg would receive 100 mg)	Aug 17 – Dec 19	India
NCT02927496 A 24 Month Study, to Compare the Efficacy of Doxycycline vs. Placebo for Improving Filarial Lymphedema in Mali	3	Filariasis	DOX	200 mg/day for 6 weeks (patients < 50 kg would receive 100 mg)	Aug 17 – Dec 19	Mali
NCT02929134 A 24 Month Study to Compare Efficacy of Doxycycline vs Placebo for Improving Filarial Lymphedema in Sri Lanka	3	Filariasis	DOX	200 mg/day for 6 weeks (patients < 50 kg would receive 100 mg)	Feb18 – Dec 19	Sri Lanka
ABBV-0483 drug's safety in healthy volunteers and assist in the selection of doses for future trials	1	Filariasis	ABBV-4083 (TylAMac™)		Dec 17 – 18	US

Table 1.2. Summary of clinical trials using anti-*Wolbachia* therapy on LF patients.

Drug	Dose/day, Duration	Major outcomes	Publication
Doxycycline	200 mg, 6 weeks	• Significant decrease in *Wolbachia* loads and microfilaraemia levels after 12 months.	(Hoerauf et al. 2003b)
Doxycycline	200 mg, 8 weeks	• Significant decrease in *Wolbachia* load, microfilaraemia, antigenemia and significant macrofilaricidal activity at 8-14 month read out	(Taylor et al. 2005)
Doxycycline	200 mg, 4 weeks	• Significant decrease in *Wolbachia* load at 4 months • Significantly lower microfilaraemia, antigenaemia and adult worm motility at 24 months. • 4 weeks regime a comparable macrofilaricidal treatment to 6 weeks	(Debrah et al. 2007)
Doxycycline +DEC + ALB	100 mg, 6 weeks	• Significant decrease in *Wolbachia* and microfilaraemia with DOX alone • Doxycycline reduced the incidence of adverse reactions	(Supali et al. 2008)

	+ 6 mg/kg + 400 mg, 1 day		
Doxycycline + ALB + IVM	200 mg, 3 weeks 400 mg, 1 day 10 mg, 1 day	• Significant decrease in *Wolbachia* load and microfilaraemia between 4 and 24 months. • Adult viability was not significantly different at 12 or 24 months	(Turner et al. 2006a)
Doxycycline	200 mg, 6 weeks	• Significant reduction in *Wolbachia* load, microfilaraemia, antigenemia and adult worm motility up to 24 months read out. • Significant decrease VEGF-C/sVEGFR-3 plasma levels with significantly lower mean stage of lymphedema after 12 months	(Debrah et al. 2006a)
Doxycycline	200 mg, 6 weeks	• Significant decrease in *Wolbachia* load, microfilaraemia and antigenemia • Significant hydrocele status improvement • Reduction in VEGF-A plasma levels	(Debrah et al. 2009)
Doxycycline + DEC	200 mg, 1 day 300 mg, 1 day	• The addition of doxycycline compared to DEC alone reduced the incidence of adverse reactions (45.5% compared to 58.85) • No severe reactions occurred in the doxycycline group compared to 3 of 25 subjects in the placebo group • The severity of adverse reactions was significantly lower in the doxycycline group (mean score 0.45) than in the placebo group (mean score 1.17)	(Sanprasert et al. 2010)
Doxycycline OR DOX+RIF	200 mg, 4 weeks OR 200 mg+10 mg/kg, 2 weeks	• 4 weeks DOX results in a significant decrease in *Wolbachia* load, microfilaraemia, adult worm motility and antigenaemia • 2 weeks DOX+RIF results in significant decrease in *Wolbachia* load and moderate adult worm motility. • 4 weeks doxycycline more superior than 2-week combination on all levels	(Debrah et al. 2011)
Doxycycline Amoxicillin	200 mg, 6 weeks 1000 mg, 6 weeks	• Significant decrease in severity of filarial lymphedema at 12 and 24 months compared to minimal improvement with amoxicillin	(Mand et al. 2012)
Doxycycline	200 mg, 30 days	• Doxycycline monotherapy results in significant decrease in microfilaraemia sustained at 1 year • Synergy between doxycycline and ALB in reduction of microfilaraemia when given in combination	(Gayen et al. 2013)
Doxycycline	200 mg 21 or 10 days	• Reduction in *Wolbachia* and microfilaraemia activity after 21 days but little significance with 10 days • Reduced scrotal lymph vessel diameter after 21 days treatment	(Mand et al. 2009)

Table 1.3 Summary of clinical trials using anti-*Wolbachia* therapy on onchocerciasis patients.

Drug	Dose/day, Duration	Major outcomes	Publications
Doxycycline	100 mg, 6 weeks	• Significant decrease in *Wolbachia*, adult worms viability and embryogenesis for at least 18 months	(Hoerauf et al. 2000a; 2001)
Doxycycline	100 mg, 6 weeks	• Significant decrease in *Wolbachia* load over a 6-month period • Inhibition of embryogenesis after 6 months with decline in mf after 11 months • No effect upon adult worm viability	(Hoerauf et al. 2003a)
Doxycycline	200 mg 2, 4 or 6 weeks	• Length of doxycycline treatment influences the reduction of mf in skin snips with significant reduction for 4 and 6 weeks at 18 months follow up	(Debrah et al. 2006b)
Rifampicin	10 mg/kg, 2 weeks OR 10 mg/kg, 4 weeks	• Significant decrease in *Wolbachia* load sustained for 18 months for both • Embryogenesis and mf production were reduced after 4 weeks treatment • No effect on adult worm viability • Less efficient than 6 weeks of DOX	(Specht et al. 2008)
Azithromycin (AZT)	6 weeks of 250 mg OR 1200 mg/week	• No significant effect on adult worm survival, embryogenesis or mf production/viability • No significant decrease of *Wolbachia* load at 6 months (250 mg/day only) • Significant difference in *Wolbachia* levels in female worms was observed at 12 months following 250 mg/day, but this was less pronounced than in previous doxycycline studies	(Hoerauf et al. 2008a)
Rifampicin AZT RIF + AZT	20 mg/kg, 5 days 12 mg/kg, 5 days 20+12 mg/kg, 5 days	• No significant depletion of *Wolbachia* load, adult worm survival or embryogenesis	(Richards et al. 2007)
Doxycycline	200 mg, 4 weeks OR 200 mg, 6 weeks	• Significant decrease in *Wolbachia* load, embryogenesis, mf production from 6 months and adult viability from 20 months sustained at 27 months • 6 week marginally more effective than a 4-week doxycycline regimen	(Hoerauf et al. 2008b)
Doxycycline	100 mg, 5 weeks	• Significant decrease in *Wolbachia* load, interruption of embryogenesis, mf production and adult worm viability at a 2 year follow up	(Hoerauf et al. 2009)
Doxycycline	200 mg, 6 weeks	• Significant reduction in *Wolbachia* load, adult worm viability, microfilaridermia and embryogenesis at 21-month read out • Well tolerated by patients with low to moderate co-infection with *Loa loa*	(Turner et al. 2010)
Doxycycline	100 mg, 6 weeks	• Significant reduction in *Wolbachia* load, embryogenesis, microfilaridermia and adult worm viability at a 20-month read out.	(Debrah et al. 2015)
Doxycycline Minocycline ALB DOX + ALB	200 mg, 4 or 3 weeks 200 mg, 3 weeks 800 mg , 3days 200 mg, 3w +800 mg, 3d	• *Wolbachia* load was significantly reduced at 6 months in all treatments compared to ALB alone with 4 weeks DOX having the greatest depletion • Embryogenesis is reduced by 4 weeks DOX and 3 weeks +ALB • Minocycline (3w) shows a trend for higher potency than DOX (3w)	(Klarmann-Schulz et al. 2017)

The anti-*Wolbachia* target of doxycycline treatment has multiple benefits including the key feature of permanent sterilisation leading to a sustained clearance of mf. Work by Landmann et al. (2011) linked this effect to extensive non-cell autonomous apoptosis following the depletion of *Wolbachia* leading to permanent sterilization. Another benefit of this treatment is the safe macrofilaricidal kinetics due to the slow kill of the worms and no risk of SAEs caused by the rapid death of mf (Slatko et al. 2010, 2014; Taylor et al. 2013, 2014). The final benefit of this treatment is through the reversal of lymphatic pathology in LF as well as the inflammatory pathology in onchocerciasis linked to worm death and release of *Wolbachia* (Debrah et al. 2006a; Mand et al. 2009; Tamarozzi et al. 2011).

In the context of the aim to achieve the elimination of LF and onchocerciasis, *Wolbachia* as the drug target provides promise, through its macrofilaricidal activity and ability to be utilised for both LF and onchocerciasis. This macrofilaricidal activity is discussed in Walker et al. (2015) meta-analysis and mathematical modelling of doxycycline clinical trial data. This work predicts that this curative treatment reduces the lifespan of *O. volvulus* female adult worms by 70-80%, from approximately 10 years to just 2-3 years. Curative anti-*Wolbachia* macrofilaricides would provide a valuable tool in the arsenal to achieving elimination of onchocerciasis and LF, in three main areas (Taylor et al. 2009; Taylor et al. 2010; Tamarozzi et al. 2011; Taylor et al. 2014; Walker et al. 2015; Basáñez et al. 2016). Firstly, it would provide a safe alternative treatment to current MDA strategies for both onchocerciasis and LF in areas co-endemic with loiasis. This safety profile relates to the lack of the *Wolbachia* target in these worms, thus eliminating the SAEs associated with microfilarcidal activity of current MDA treatments against *Loa loa*. Secondly, it could be used as a "mop up" strategy to shorten the protected tail of the "endgame" in areas where elimination is deemed achievable, but not yet completed. This could be of great benefit in areas where the 2020 elimination targets will not be reached, including hard-to-reach or hyperendemic areas. Thirdly, in areas of sub-optimal responders to IVM, it could be invaluable as a back-up treatment, especially for onchocerciasis which is limited to treatment with just IVM and the related drug moxidectin.

However, novel drugs are required without contraindications and with a shorter treatment regimen. Current literature in this field recommends the highest chance of success to achieve this, is through the establishment of collaborations which promote the dramatic

increase in large-scale drug library screening (Clark et al. 2013; Burrows et al. 2014; Panic et al. 2014; De Rycker et al. 2018). Many factors including the complexity of the biology and related cell-based assays, lack of validated targets and funding shortages involved in hit discovery for these filarial diseases (in common with many other NTDs) makes industrial scale programmes in this field extremely challenging (Johnston et al. 2014a; De Rycker et al. 2018).

1.5. The A·WOL drug discovery model cell line C6/36 (*w*AlbB)

At the beginning of the A·WOL Consortium, alongside anti-*Wolbachia* drug regime refinement field trials (Table 1.2 and Table 1.3), the second objective was to develop a high-throughput screening (HTS) assay. This HTS from either a nematode-*Wolbachia* assay or utilising the existing insect-*Wolbachia* assay would allow for the testing of large numbers of novel or re-purposed compounds.

Prior to the work by the A·WOL Consortium, in the late 1990s O'Neill et al. (1997) established and characterized the first mosquito cell line stability infected with *Wolbachia*, Aa23 cells. This cell line originated from eggs of a strain of *Aedes albopictus* naturally infected with *Wolbachia*. Fenollar et al. (2003a) later successfully inoculated C6/36 (*A. albopictus*) and human embryonic lung (HEL) cells with the *Wolbachia* from this Aa23 cell line (Fenollar et al. 2003a). Hermans et al. (2001) and Fenollar et al. (2003b) developed the Aa23 cells into a drug screening assay with, respectively, a Giemsa-light microscopy or immunofluorescent-antibody as well as quantitative PCR read-outs. These assays both identified the highest activity with doxycycline and rifampin. Some activity was observed for fluoroquinolones, but the β-lactams tested had no activity.

The newly infected cell line, C6/36 (*w*AlbB), became the model cell line used by the A·WOL Consortium (Turner et al. 2006b; Johnston et al. 2014b). Similar to the studies discussed above, the mosquito (*Aedes albopictus*) cell line, C6/36, was stably infected with a *Wolbachia* inoculum from Aa23 cells (Turner et al. 2006b). This cell line was used to develop a 9-day, 96-well plate format assay, which quantified the 16S rRNA gene copy number of intracellular *Wolbachia* bacteria. This assay, similar to the low throughput studies by Fenollar et al. (2003b), could be used to identify anti-*Wolbachia* active compounds. In addition, toxicity readouts to the host mosquito cell can be obtained by either a visual

analysis or using an ATP–luminescence-based cytotoxicity assay. This assay was transferred from LSTM to CombinatoRx™ Singapore where it was utilised to screen for anti-*Wolbachia* activity in the approved human drug-pharmacopoeia (2,664 compounds) (Johnston et al. 2014b). In order to access and screen larger diversity libraries in a reasonable timeframe, further development of this cell-based assay was required and is described in this thesis.

1.6. Project aims

This thesis aims to progress the identification of novel anti-*Wolbachia* compounds through the development of screening assays with higher capacity and throughput. Outputs from these larger scale screening campaigns can then be discussed.

The aims of this thesis can therefore be summarised as:

1. The development and validation of a High Content Screen using optimised C6/36 (*w*AlbB) cells.
2. The development and validation of an industrial scale anti-*Wolbachia* High-Throughput Screen (HTS).
3. The completion of an anti-*Wolbachia* industrial scale HTS campaign.

Chapter 2 : The development and validation of a high content anti-*Wolbachia* drug discovery screen

2.1. Abstract

This Chapter describes the development and validation of a 384-well format assay using a high content imaging system (Operetta®) in conjunction with optimised *Wolbachia* growth dynamics in the C6/36 cell line stably infected with *w*AlbB. This assay uses texture analysis of cells stained with the fluorescent nucleic acid stain SYTO®11 as a measure of bacterial load. The validation of this assay has provided the potential to dramatically increase the capacity of the A·WOL compound library screening programme 25-fold, which has opened up the opportunity for large diversity library screening against *Wolbachia*.

2.2. Introduction

2.2.1. Background

C6/36 (*w*AlbB) cells were adopted by the A·WOL Consortium as the basis of a primary screening assay for anti-*Wolbachia* drug discovery (introduced in Chapter 1.5). This screen identified potential drugs by quantifying the reduction in *Wolbachia* load compared to untreated cells (Johnston et al. 2014a, 2014b; Taylor et al. 2013, 2014; Slatko et al. 2010, 2014). Development of this screen used continuously cultured cells, which were sub-cultured 24 hours prior to incubation with compounds of interest for 9 days. *Wolbachia* levels were assessed using qPCR analysis (based on work by Makepeace et al. 2006) of the *Wolbachia* 16S rRNA single gene copy number, alongside visual toxicity analysis of the host C6/36 cells. The 16S results could be normalised to the cell number by 18S rRNA gene copy number analysed by qPCR (Makepeace et al. 2006; Turner et al. 2006b; Johnston et al. 2014a, 2014b).

Through the successful use of the *in vitro* cell screen against a 2,664 human pharmacopeia compound library from CombinatoRx™, the programme began to expand from small focused libraries to larger diversity compound libraries (Johnston et al. 2014a, 2014b; Slatko

et al. 2014). These larger libraries included a 10,000 compound library from BioFocus which took two full time employees (FTE) over one year to complete (Johnston et al. 2017). Along with the extensive screening time scale for this BioFocus library and an increasing number of libraries becoming available to the A·WOL programme, it became apparent a higher throughput *in vitro* screen was needed.

Improvements in technologies over the last 15 years have made high-throughput screening (HTS) of phenotypic microscopy assays possible through the improvements in fluorescence imaging techniques and the automation of microscopy image acquisition and analysis (Yarrow et al. 2003; Starkuviene and Pepperkok 2007; Zanella et al. 2010; De Rycker et al. 2013). This combination of automated microscopes and quantitative analysis of the acquired images has bridged the gap between HTS assays with a single/basic readout and low throughput detailed data-capture assays which require manual visual analysis. This combination coined the concept of a High Content Screen (HCS) which is an automated process of gaining both terabytes worth of data, followed by software based quantitative unbiased analysis (Starkuviene and Pepperkok 2007; Zanella et al. 2010). A high content imaging platform, Operetta® (PerkinElmer®) was investigated as a potential technology to enable the development of a higher throughput screen for the A·WOL drug discovery programme.

2.2.2. Aim of study

The aim of this study was to increase the capacity and throughput of the current A·WOL screening programme, by developing and validating a C6/36 (*w*AlbB) high content screen utilising the Operetta® platform.

2.3. Methods

2.3.1. Cell culture

This assay used a cell line previously created and used in the A·WOL Consortium's qPCR-based drug discovery assay. The C6/36 (*w*AlbB) cell line is a mosquito (*A. albopictus*) derived cell line, stably infected with native *Wolbachia pipientis* (*w*AlbB). To create this cell line the supernatant from cultured Aa23 cells (*A. albopictus*) naturally infected with the *Wolbachia pipientis* strain *w*AlbB was harvested and filtered to remove whole cells. This supernatant was used to inoculate C6/36 cells (ECACC No. 89051705) resulting in a stably *Wolbachia* infected cell line C6/36 (*w*AlbB) (O'Neill et al. 1997; Turner et al. 2006b). Cells were incubated at 26 ^{o}C and sub-passaged every 7 days using a 1 in 4 dilution in Leibovitz medium (Life Technologies™) supplemented with 20% foetal calf serum (FCS) (Fisher Scientific™), 2% tryptose phosphate broth (Sigma Aldrich®) and 1% non-essential amino acids (Sigma Aldrich®).

2.3.2. Anti-*Wolbachia* HCS assay set up

C6/36 (*w*AlbB) cells were sub-passaged 6-8 days before plating out at a density of 2,000 viable cells per well in a 384-well CellCarrier plate (PerkinElmer®), suspended in Leibovitz media (Life Technologies™) with the supplements described above. All compounds were dissolved in dimethyl sulfoxide (DMSO) (Sigma Aldrich®) with each compound added to a single well at a final concentration of 5 µM (resulting in <1% final DMSO concentration). Control samples per plate consisted of 12 wells of vehicle control (DMSO) and 6 wells of the following controls: 5 µM doxycycline (Sigma Aldrich®) (positive control - gold standard for *Wolbachia* reduction) and a sub-optimal 50 nM doxycycline concentration. Each well held a final volume of 100 µl, with the exception of the outer wells which contained 130 µl of phosphate buffered saline (PBS, Sigma Aldrich®) to reduce evaporation from the sample wells over the 7-day incubation period.

After 7 days of sterile incubation at 26 ^{o}C, 25 µl of staining media containing 60 µM of SYTO®11 nucleic acid stain (Life Technologies™) was added to each well. After a 15-minute incubation all media was removed from each well and replaced with fresh media (containing no SYTO®11). Using the Operetta® (PerkinElmer®) high content automated imaging system, 5 fields per well were imaged using a confocal x60 objective with the fluorescein filter

(excitation filter 460-490 nm, emission filter 500-550 nm). The associated Harmony® software (PerkinElmer®) was trained to first identify the cell nucleus and cytoplasm, followed by the 'Spot Edge Ridge' (SER) texture analysis which was used to score each intact cell on the complexity of the cytoplasm (Srinivasan and Shobha 2008).

2.3.3. Anti-*Wolbachia* HCS assay results analysis

Using the vehicle and positive controls, a threshold was set to indicate if each cell was classed as infected or uninfected. *Wolbachia* infected cells (vehicle control) have a complex cytoplasm texture (high SER Texture score), while *Wolbachia* uninfected cells (doxycycline treated positive control) have a uniform cytoplasm texture (low SER Texture score). From this analysis the following read outs were calculated per well: 'cell number', 'SER Texture score' and 'percentage of *Wolbachia* infected cells'. Z prime validation of each plate was calculated using the 'percentage of *Wolbachia* infected cells' value from the vehicle and positive controls (Zhang et al. 1999). Equation 1 illustrates the equation for calculating the Z prime in this assay. Vehicle controls have a high *Wolbachia* load and therefore a high percentage of cells classed as infected with *Wolbachia*. Positive control (doxycycline treated) cells have a low *Wolbachia* load and therefore a low percentage of *Wolbachia* infected cells (Figure 2.1). All compound sample wells were then analysed and normalised (along with the positive controls) against the vehicle (untreated) control to give a 'percentage reduction of *Wolbachia* infected cells'. Additionally, using the cell number analysis, any compounds with a host cell number less than 50% of the vehicle control were classed as toxic and could be retested at a reduced compound concentration. All compounds which were > 90% of the positive control's 'percentage reduction of *Wolbachia* infected cells' were classed as 'strong hits' (as they were similar to or greater than the 5 µM doxycycline positive control). Compounds which had infection rates between 50 and 90% of

$$\text{Z prime} = 1 - \frac{(3 \text{ x StDev negative control}) + (3 \text{ x StDev positive control})}{\text{mean positive control} - \text{mean negative control}}$$

Equation 1. Z prime equation reproduced from Zhang et al. 1999. This calculation is used to assess the quality of a high-throughput assay based on positive and negative controls. In this study doxycycline is used as the positive control due to its ability to reduce *Wolbachia* with DMSO as the vehicle/negative control.

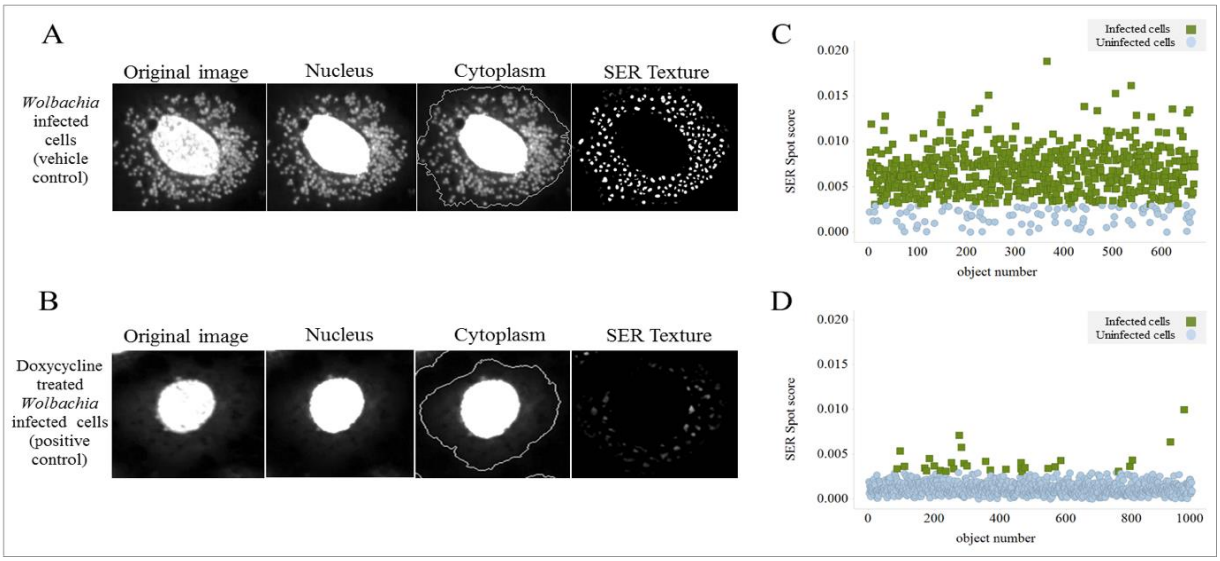

Figure 2.1. The A·WOL high content whole cell anti-*Wolbachia* screen. A) An example of a *Wolbachia* (small white dots) infected cell (C6/36(*w*AlbB)) imaged by the Operetta® and analysed by the Harmony® software to identify the nucleus, cytoplasm and assess the *Wolbachia* infection through 'Spot Edge Ridge' (SER) texture analysis of the cytoplasm. B) An example of a cell with no *Wolbachia* infection due to doxycycline treatment, analysed by Harmony® software's SER Texture analysis. C) A scatter plot of results from a sample well of C6/36(*w*AlbB) cells after a 7-day incubation with the vehicle control (DMSO). The SER Texture score (y axis) refers to the complexity of the cytoplasm texture. Each object number (x axis) refers to a single cell. The SER Texture threshold is set at 0.003, with all cells above this score being classed as infected (green squares). This well has 85% *Wolbachia* infected cells. D) A scatter plot from a sample well of C6/36(*w*AlbB) cells after a 7-day incubation with the positive control (doxycycline). This well has 3% *Wolbachia* infected cells.

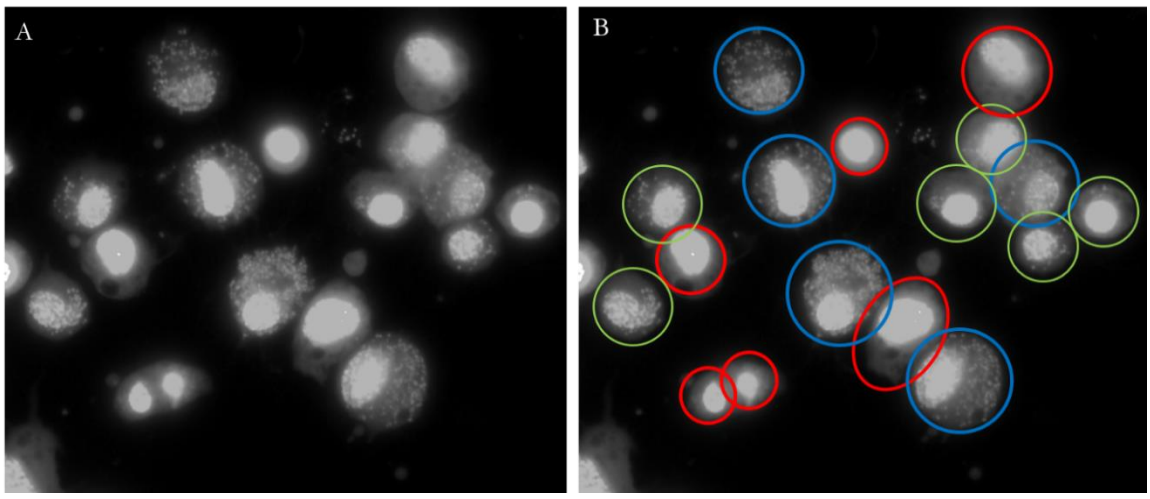

Figure 2.2. Example C6/36 (*w*AlbB) cell population with a heterogenous *Wolbachia* infection. Cells highlighted in blue have a high level of infection with *Wolbachia*, in green a low level of infection and in red the cells appear uninfected.

the positive control was classed as 'moderate hits' as they were similar to the sub-optimal (50 nM) doxycycline control. All hit compounds could then be reconfirmed in full dose response testing to define their potency.

2.4. Results

2.4.1. *Wolbachia* infected C6/36 (*w*AlbB) cell line dynamics

For image-based assays which use a per cell analysis, it is important to optimise the homogeneity of infection levels between cells. Initial analysis using the Operetta® highlighted that *Wolbachia* infected cells can exhibit variable bacterial loads from cell to cell, with some cells appearing to be uninfected (Figure 2.2). Such variation reduces the signal window, thus reducing the quality of any resulting assay and preventing assay validation (see assay validation section below). Therefore, the seeding density and media supplements were optimised to provide a robust method for producing cells with highly homogeneous *Wolbachia* loads. The main parameter that affected *Wolbachia* infection homogeneity was the percentage of FCS used in the culture media. Switching from the standard 5% FCS in the culture media to 20% typically increased the percentage of infected cells from 14-60% to above 70% across replicate wells (Figure 2.3). Overall, cells 6-8-day post passage, seeded at 2,000 viable cells/well of a 384-well plate, and maintained in media containing 20% FCS provided the optimised conditions. These seeding conditions were selected as they provided a confluent layer suitable for imaging. This allowed for imaging a large number of cells per field without compromising the image with overlapping or clumped cells.

2.4.2. Assay optimisation

Various settings were optimised on the Operetta® in order to increase the throughput of the assay. SYTO®11 green fluorescent nucleic acid stain was used to visualise both the *Wolbachia* and the host cell C6/36 (*w*AlbB) nuclei. The use of SYTO®11 as a live cell stain further enhances the simplicity of this method by reducing the number of steps involved in the staining process. A x60 objective was used for this assay as it gave the optimum cellular detail to assess the intracellular *Wolbachia* load whilst maximising the number of cells analysed per field/image. The final image from each field is a composite from 3 images

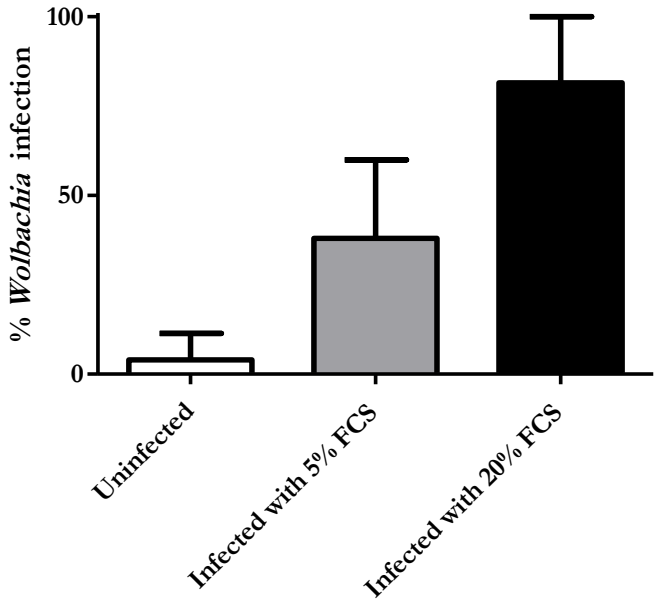

Figure 2.3. The impact of increasing the percentage of FCS in the culture medium on the *Wolbachia* infection of C6/36(*w*AlbB) cells. Each bar represents the mean for each cell population with the range presented by the error bars (95% confidence intervals).

taken at separate focal planes. This composite image proved robust in capturing the majority of cells in focus. The optimisation of the number of fields and number of planes were based on iterative Z prime analysis. Once the images were obtained the Harmony® software was optimised to identify the cell nuclei and cytoplasm (Figure 2.1A and B). Any cells which reside at the edge of the image (resulting in partial visibility of the cell cytoplasm) were excluded from the analysis. Texture analysis of the cytoplasm was then performed.

2.4.3. Harmony® texture analysis

Initial attempts to count the number of *Wolbachia* per cell was compromised as the density in cells maintained with 20% FCS culture media was too high to achieve sufficient accuracy through spot identification. Therefore, the *Wolbachia* infection was determined by the Texture analysis function available within the Harmony® software using 'Spot Edge Ridge' (SER) Texture analysis. This analysis used the cytoplasm (nucleus excluded) as the image region of interest. *Wolbachia* infected cells have a complex pattern to their cytoplasm which results in a high SER Texture score for each cell (Figure 2.1A and C). Conversely *Wolbachia* uninfected cells have a uniform non-complex cytoplasm texture resulting in a low SER

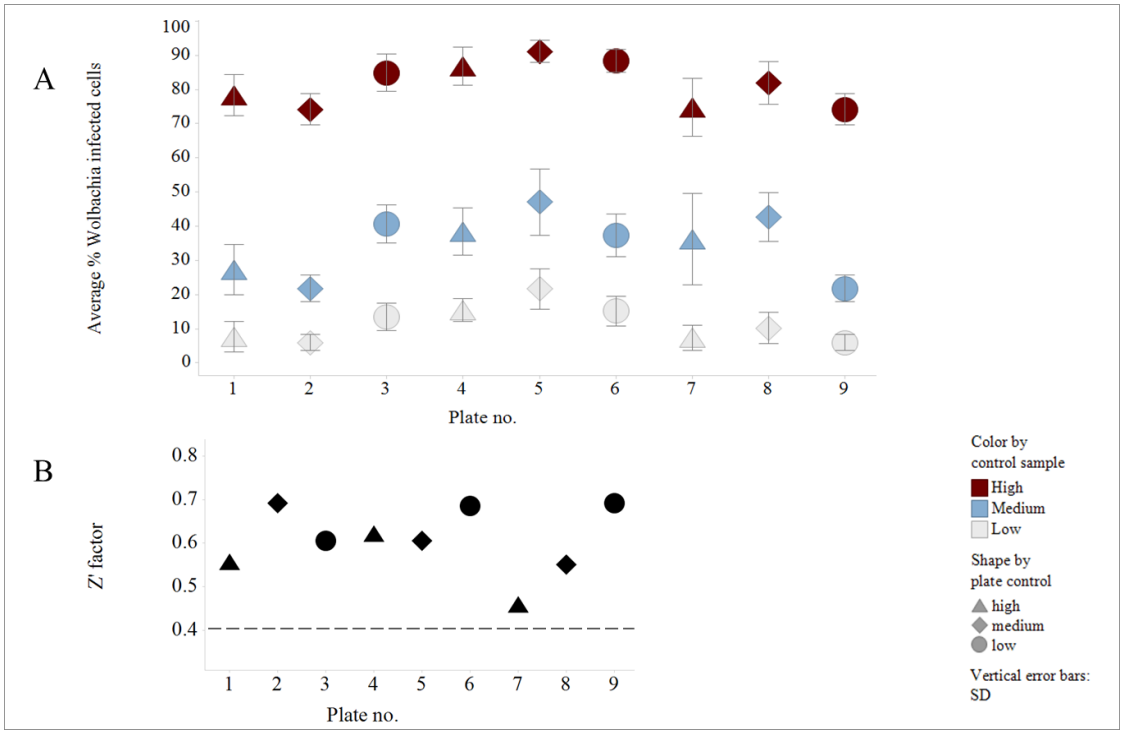

Figure 2.4. HCS assay validation data. A) The mean 'percentage of *Wolbachia* infected cells' with error bars (Standard Deviation) for each control sample, for 9 plates. High, medium and low *Wolbachia* level controls are produced through the incubation with either an optimum (low) and sub-optimum (medium) doxycycline concentration or DMSO vehicle (high). The different plates were set up with columns of the control samples (high, medium and low) in a repeating pattern. Each control plate starts at a different point in the pattern and the shape in the graph refers to the starting control row (triangle, diamond and circle respectively referring to the high, medium or low controls). These three control plates were set up on different days (plates 1-3 on day 1, plates 4-6 on day 2 and plates 7-9 on day 3). B) Z prime (Z') from each of the plates described previously, based on the high and low sample controls. All plates obtained Z' factor above 0.4 (dotted line) indicating a valid plate.

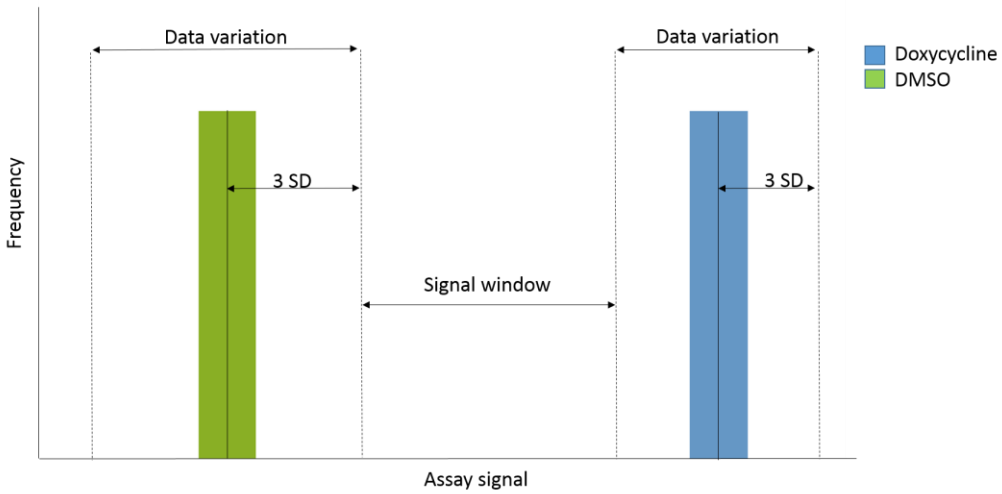

Figure 2.5. Illustration of the Z prime calculation used to validate the HCS assay. Z prime takes into account both the variation (3 x Standard Deviation (StDev)) within the data as well as the signal window by assessing positive (doxycycline) and negative (DMSO) control samples.

Texture score (Figure 2.1B and D). The difference between the SER Texture score of *Wolbachia* infected and uninfected cells was used to calculate a threshold value to classify the cells accordingly. Those above the threshold are defined as 'infected' whilst those below the threshold are defined as 'uninfected' (Figure 2.1C and D, threshold at 0.003). The software was programmed to calculate the 'percentage of *Wolbachia* infected cells' for each image based on these classifications. This resulted in 86% of cells (mean) classed as infected in the vehicle controls, whilst in the positive control (baseline reading) 15% of cells were classed as infected (Figure 2.4A, low and high controls). For each assay plate, vehicle control (*Wolbachia* infected) and doxycycline positive control (*Wolbachia* uninfected) samples were analysed first. The optimum threshold for each plate was then determined as the midpoint between the mean SER Texture scores for the vehicle and positive controls.

2.4.4. Assay validation

The vehicle control (*Wolbachia* infected) and positive control (doxycycline treated) were used to calculate the Z prime statistical parameter. The Z prime reflects both the variation within the control data and the signal window between these controls (Figure 2.5) (Zhang et al. 1999). Data with large variation in the control samples will pass the Z prime analysis as long as the signal window is also large. Conversely, an assay in which the signal window is small, can still pass the Z prime if the variation in the controls is also small. This Z prime analysis gives confidence that the data within an assay will give accurate hits due to distinctions within the data suggesting that a hit will be separate to the vehicle (DMSO in this case) control. Within the assay developed in this study, satisfactory Z prime factors were achieved (greater than 0.4) (Figure 2.4B). The assay was also validated by testing for edge or drift effects within each plate, as well as inter and intra-day variability. Three plates were prepared containing columns of cells with high (H - vehicle), medium (M- 50 nM sub-optimal dose of doxycycline) and low (L – 5 µM doxycycline) levels of *Wolbachia* infection. Each plate contained the same repeating column pattern H, M, L, however each plate started at a different point in the pattern (Iversen et al. 2004). Using this method across all three plates a single well position will gain a result for each treatment (Figure 2.6). This was then repeated on 3 different days. Consistent and robust results were obtained in this validation with all plates passing the Z prime (Figure 2.4), with little inter/intra day variation between the plates or drift/edge effects within each plate (Figure 2.4 and Figure 2.7).

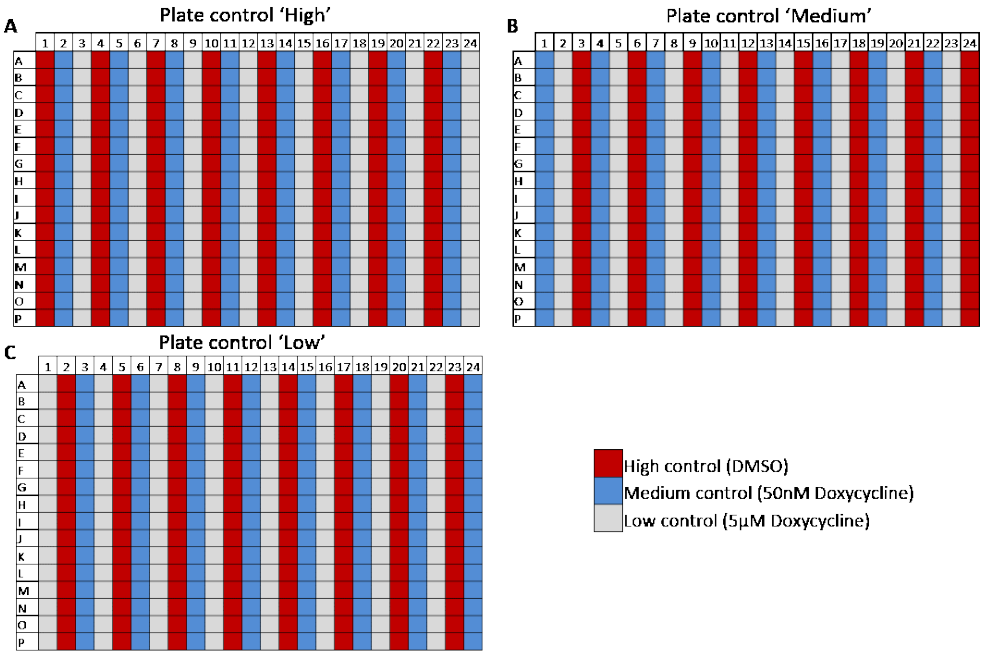

Figure 2.6. Diagram to represent the layouts of the validation plates to test for drift, edge effects, inter- and intra-day variation as well as Z prime analysis. The control plate type is determined by the control sample in column A.

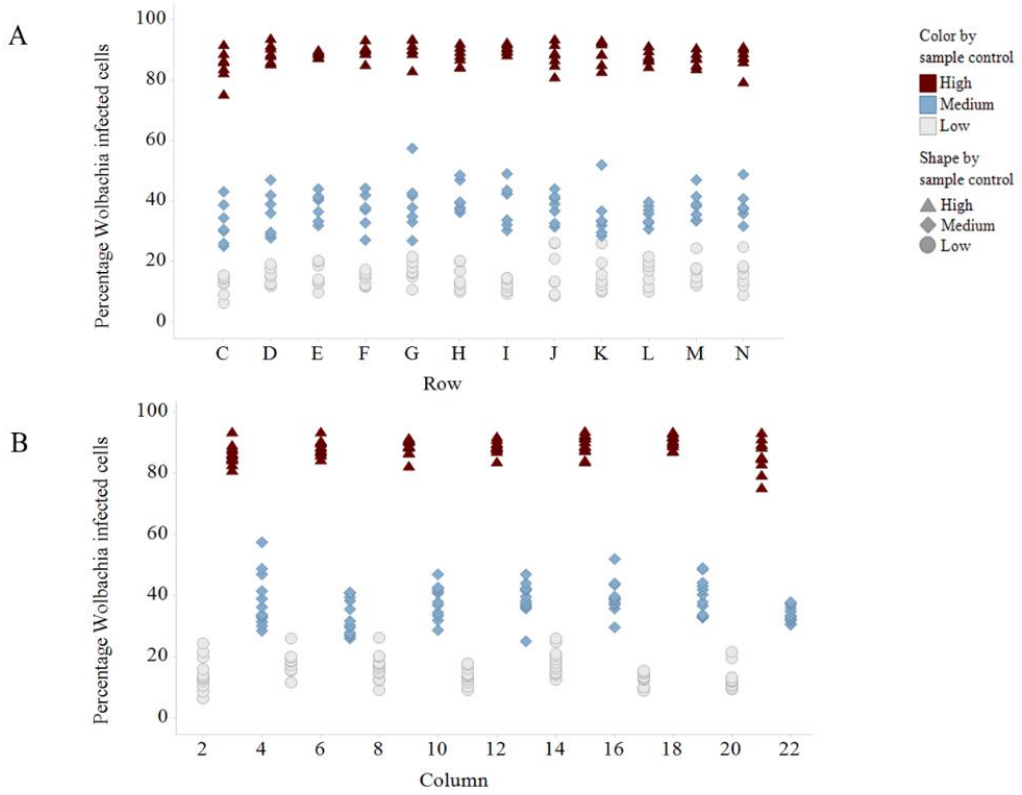

Figure 2.7. Drift and edge effects for the validation data. An example showing there is no drift across A) the rows (c to n) or B) the columns (2 to 22). Both Figures A and B demonstrate that there are no edge effects (outer columns 2 and 22 or outer rows c and n). For these Figures the colours and shapes refer to the control samples (high, medium and low *Wolbachia* level controls produced by the incubation with an optimum (low) and sub-optimum (medium) doxycycline concentration or vehicle (DMSO) control (high)).

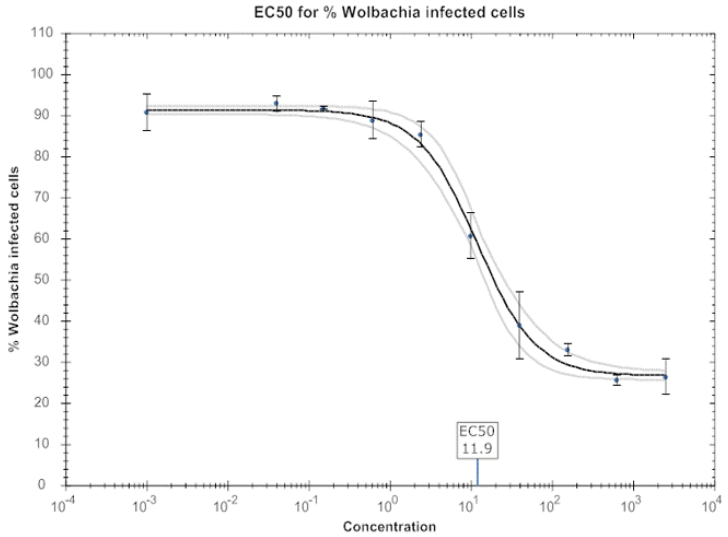

Figure 2.8. Dose response for doxycycline in the A·WOL HCS anti-*Wolbachia* screen. This is an example of a dose response curve generated by Harmony® software using doxycycline in the validated assay described in this study, resulting in an EC50 of 11.9 nM. Each point represents the mean with standard deviation error bars.

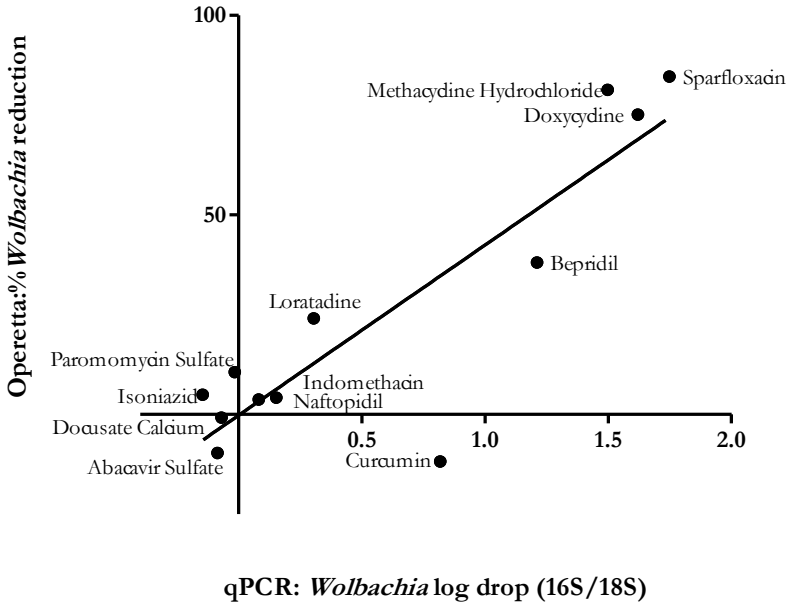

Figure 2.9. HCS screen vs qPCR screens. 12 compounds from the top priority list from A·WOL testing of the human pharmacopoeia (Johnston et al. 2014b) excluding those displaying toxicity (Pearson correlation (determination coefficient), $r^2 = 0.772$, $p = 0.0002$).

2.4.5. Hit dose responses

A significant benefit of this assay is that the A·WOL drug discovery programme now have the capabilities to produce dose response curves on hits. This allows for the calculation of EC50 (50% effective concentration) data, the concentration at which a drug gives half the maximal response. These curves are now routinely obtained in the A·WOL primary screen for smaller libraries and as a secondary screen for larger library hits. Doxycycline dose response curves are also run as a reference in these routine screens (Figure 2.8).

2.4.6. Toxicity

Toxicity was assessed in this assay by comparing the host cell number from compound samples to the vehicle control. This toxicity can result from either cell death or reduced cell replication due to exposure to a compound. In this assay a compound with a cell number less than 50% of the vehicle control cell number was classed as toxic.

2.4.7. Comparison between qPCR and Operetta® screening data

To further confirm validity of this assay a comparison was made to the qPCR-based assay. A selection of top priority hit compounds from the human pharmacopoeia screening (Johnston et al. 2014b) were set up in duplicate before being split for analysis by the two methods. This comparison shows a clear consistency between the two assays (Figure 2.9).

2.4.8. Validation of automation and reduced cost of SYTO®11

Once this assay had been developed and validated as described in this study, an automated robotic arm, allowing for 24/7 capabilities was incorporated into the process to overcome a 'bottle neck' in the screening process created by the imaging time on the Operetta® (3 hours). Therefore, the stability of the methods was examined to assess how long after staining could imaging within the Operetta® be achieved without detriment to the analysis. Figure 2.10 shows that there was no difference in the results of the same plate read on the Operetta® between 0 and 24 hours post staining (comparison between Figure 2.10 a to b and c to d). Further refinement included a reduction in the concentration of SYTO®11 with no detriment to the image quality or analysis.

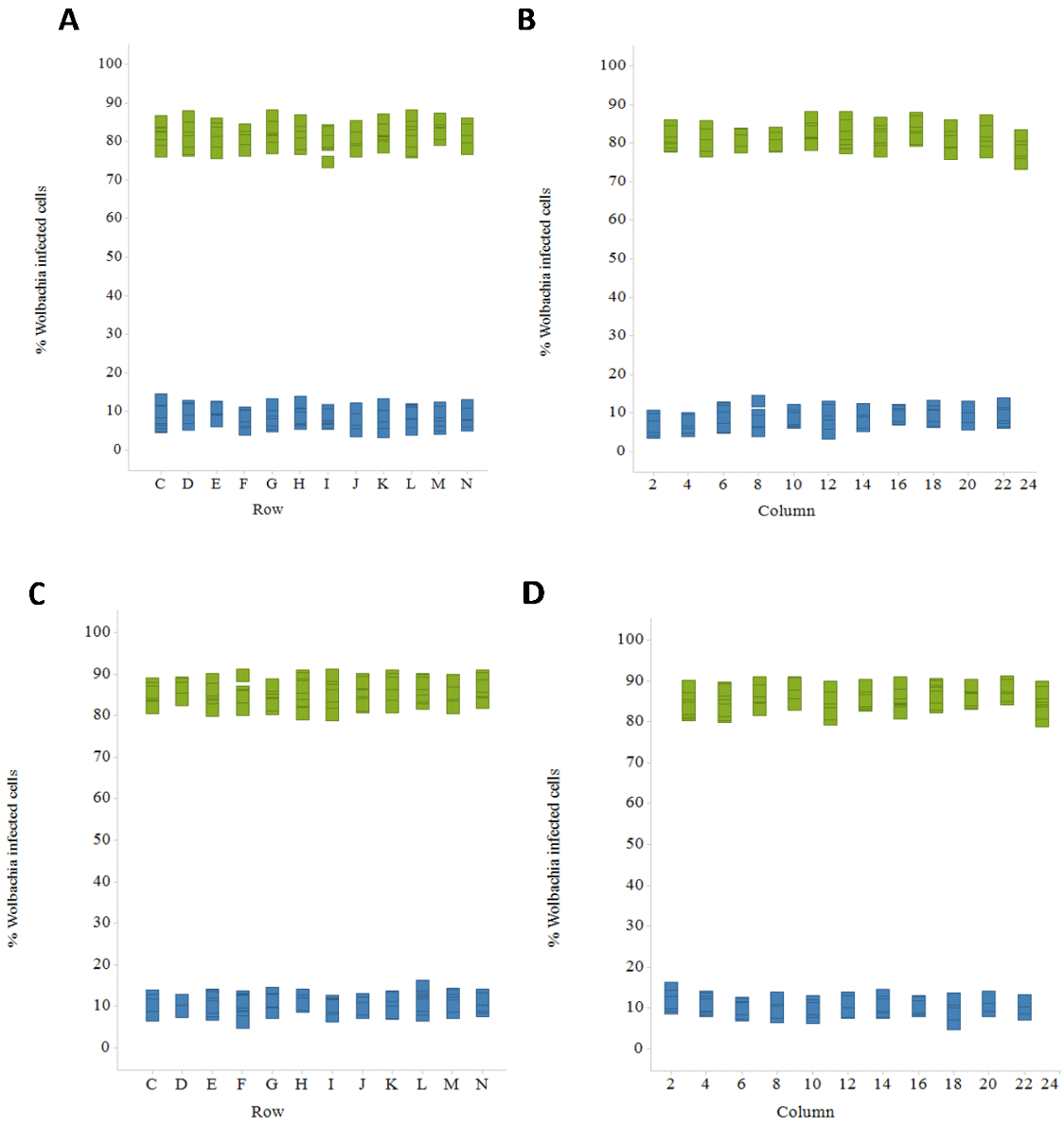

Figure 2.10. Validation of reducing the SYTO®11 concentration and stability over 24 hours. The reduction of the staining concentration maintains the assay window with no drift or edge effects in the A) by row graph and B) by column graph. This staining is also stable over time as can be seen by comparing the time 0 graphs (A and B) with the 24 hour post staining results in graphs C and D.

2.5. Discussion

Through optimising cell growth dynamics and using an image based detection with the Operetta® high content automated imaging system, this work has developed and validated a cell based screening assay with a higher throughput and capacity for the primary screening of anti-*Wolbachia* drugs. Improvements have also been made in evaluating cell toxicity using the Harmony® software. The miniaturisation from the 96-well qPCR format to a 384-well imaging format and the simplification of the staining method over a multi-step DNA quantification method has dramatically improved not only the throughput but also the screening cost per drug. All of these improvements have resulted in a 25-fold increase in throughput compared with the qPCR method, through which the A·WOL Consortium was able to screen approximately 1,000 compounds per month. Using this new HCS assay the A·WOL Consortium are able to screen over 25,000 compounds per month. This capacity alongside the ability to complete dose response analysis was instrumental in allowing the programme to initiate a medicinal chemistry 'hit to lead' and lead optimization development phase in the A·WOL II Macrofilaricide Drug Discovery programme (Taylor et al. 2014; Johnston et al. 2014a, 2017). Furthermore, this assay was transferable as evidenced by the AstraZeneca collaboration which is discussed in Chapter 3.

Increasing the FCS content in the incubation media has reduced the sensitivity of the C6/36 (*w*AlbB) cells to compound toxicity therefore reducing the number of hits discarded due to toxicity as well as reducing the number of re-tests required at a lower dose to confirm that the toxicity was not masking a potential hit.

An additional benefit of this screen is the improved data quality, as results are now obtained from an individual cellular level rather than a single whole well sample read out. This has allowed for direct monitoring of *Wolbachia* and host cell dynamics within a population, as demonstrated in the initial tests to compare *Wolbachia* levels in 5% and 20% FCS culture media. This was an extension on work by O'Neill et al. (1997) which stated that increasing the percentage of FCS can increase the intracellular *Wolbachia* load as well as the number of cells infected. The development of this HCS assay, which obtains data on an individual cellular level, can be utilised beyond drug discovery screening, for example to access morphological or molecular aspects relating to the *Wolbachia* infection of a cell. This validated cell-based HCS screen mirrors the move towards HCS of whole organisms or cell

based assays becoming more popular in both the pharmaceutical industry and academia, including the NTD field (Engel et al. 2010; Marcellino et al. 2012; Paveley et al. 2012; Cruz et al. 2013; De Rycker et al. 2013; Sykes and Avery 2013; Johnston et al. 2014a; Moon et al. 2014; Martin-Plaza and Chatelain 2015). This change is partly due to the high rate of attrition from early hits to robust lead compounds, as many of the molecular target based hits are not active at a whole cell level. Due to HCS phenotypic whole cell/organism screens being initiated at this whole cell rather than molecular level, this should increase the chance of obtaining robust lead compounds (Starkuviene and Pepperkok 2007; De Rycker et al. 2009; Zanella et al. 2010).

Improvements to the A·WOL primary screening assay has created the opportunity to increase the size and diversity of the A·WOL library screening activities to improve the anti-*Wolbachia* portfolio of drugs as safe macrofilaricidal therapies against filarial nematodes (Taylor et al. 2014). The value of this screen is further emphasised as there is good concordance in compounds presenting with anti-*Wolbachia* activity in this cell line translating to pre-clinical models and clinical trials (Johnston et al. 2014a). The confidence in these data resulted in the removal of the *ex vivo* screen from the screening funnel as part of the second A·WOL programme (Johnston et al. 2014a) (Figure 2.11). This was an important step in the A·WOL drug discovery funnel as it allowed for refinement through the removal of this *ex-vivo* worm screening, thus decreasing the timescale for progressing novel anti-*Wolbachia* hits.

Finally the capabilities of this assay to routinely supply EC50s has been instrumental in allowing for the initiation of a medicinal chemistry campaign and pharmacokinetic and pharmacodynamic (PKPD) prediction modelling for compounds across the A·WOL portfolio (Sharma et al. 2016; Aljayyoussi et al. 2017a; Johnston et al. 2017).

This study was published in the *Journal of Biomolecular Screening* (Clare et al. 2014).

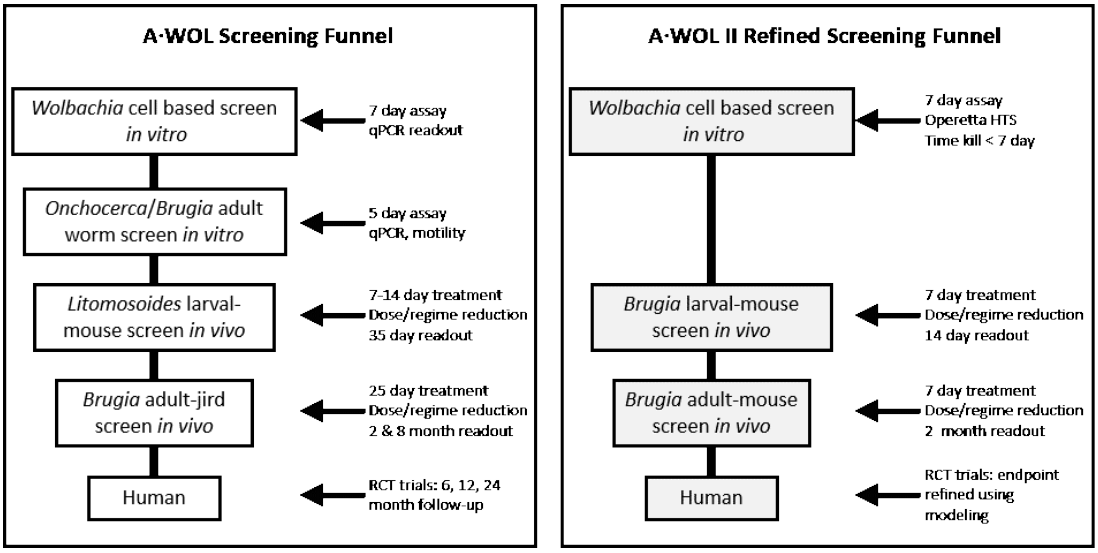

Figure 2.11. Refinement of the screening funnel from A·WOL to A·WOL II. Original funnel developed by A·WOL (A), and the refined funnel developed for A·WOL II (B). Figure taken from Johnston et al. 2014a with permission.

2.6. Summary

- Key to the development of a new high content screening assay was to enable a stable homogeneous and high *Wolbachia* infection within the host insect cell line.
- The analysis method was developed by utilising a nuclear staining protocol which was both affordable and required minimal steps to allow for multiple plates to be completed per assay.
- Validation of this assay through assessing edge effects, Z prime analysis and inter/intra-day variations has allowed for this robust assay to increase the screening capacity for the A·WOL drug discovery programme 25-fold.
- This assay has enabled dose response and toxicity analysis to be incorporated into the A·WOL screening funnel.

Chapter 3 : The development and validation of an industrial scale High-Throughput Screen (HTS) in a collaboration between A·WOL and AstraZeneca

3.1. Abstract

The C6/36 (*w*AlbB) high content screen was used as the basis to develop a highly automated assay suitable for industrial scale screening. This development included creating a cryobank of assay ready C6/36 (*w*AlbB) cells with a consistent *Wolbachia* load and an adaptation of the final read outs including a Hoechst staining of the host nuclei for toxicity and *wBm*PAL antibody staining for the *Wolbachia* analysis. Bespoke automated processes were created for the cell seeding into assay ready plates, staining protocol and plate reading, which allowed for the potential screening of 150 x 384-well plate batches. This assay was validated based on test compounds (AstraZeneca and A·WOL validation set) repeated on two occasions as well as stability for 7 days and quality control plate (DMSO and doxycycline) assessments. These data sources were also used to define the hit and toxicity criteria; greater than 80% reduction in *Wolbachia* with maximum toxicity of 60% loss in host cells. These test data predicted a hit rate of 1.28% in assays with a Z prime of greater than 0.7 suggesting screening of the full AstraZeneca library of 1.3 million compounds would be achievable and potentially produce over 16,000 hits.

3.2. Introduction

3.2.1. Background

Although A·WOL had made good progress with screening of large diversity libraries (Johnston et al. 2017), additional diverse chemical series were sought to broaden the portfolio of anti-*Wolbachia* compounds with different modes of action. The development of a high content anti-*Wolbachia* screen described in Chapter 2 paved the way to upscale the A·WOL drug discovery screening strategy to an industrial scale high-throughput screen (HTS). HTS screening has become the leading discovery tools in the pharma industry since the late 1980s through the ability to screen vast numbers of compounds in a diverse

chemical space to efficiently identify active compounds (Zhang et al. 1999; Hughes et al. 2011; Wigglesworth et al. 2015). In addition, cheminformatics can be used to analyse the results to build up structural activity relationships (SAR) within compounds of similar structures (clusters). These SARs are key to the development of a medicinal chemistry campaign. Gaining such information on multiple clusters rather than individual hits allows for the selection of the most promising clusters containing multiple good quality hits (Katsuno et al. 2015). Once clusters of interest are identified, target discovery can then be retrospectively applied to identify the mode of action (Burrows et al. 2014). Added to this, the completion of whole organism phenotypic HTS screening can further enhance good quality hits in comparison to molecular target based screening, therefore reducing the chance of attrition (Burrows et al. 2014; Katsuno et al. 2015).

HTS screening is clearly of benefit to the NTD field, in which out of the 850 new therapeutic products registered between 2000-2011 only 5 were indicated for NTDs, none of which were new chemical entities (NCE) (Martin-Plaza and Chatelain 2015; Hotez et al. 2016). To date only two industrial scale NTD HTS screens have been carried out, both against kinetoplastids. GlaxoSmithKline's 1.8 million diversity set has been screened against three kinetoplastids; *Leishmania donovani*, *Trypanosoma cruzi* and *Trypanosoma brucei* which cause leishmaniasis, Chagas disease and African trypanosomiasis (HAT) respectively (Pena 2015). The Genomics Institute of the Novartis Research Foundation (GNF) has screened 3 million compounds against the same parasites (Khare et al. 2016). Both of these screens were completed as part of open-access/source collaborations, which highlights the trend in pharma beginning to come on board with global health drug discovery as highlighted by key initiatives such as the London Declaration and the Global Health Innovative Technology Fund (GHIT), as well as the development of dedicated research sites e.g. GlaxoSmithKline's Drugs for the Developing World facility at Tres Cantos in Spain, the Novartis Institute for Tropical Diseases in Singapore, and the AstraZeneca's open innovation initiative (Burrows et al. 2014; Katsuno et al. 2015; Martin-Plaza and Chatelain 2015).

A·WOL and AstraZeneca initiated such an open access collaboration to attempt to create an anti-*Wolbachia* industrial scale HTS. In addition to giving access to their full 1.3 million compound library, AstraZeneca hosted my secondment with the Global High-Throughput Screening (HTS) Centre in Alderley Park. This full open access, allowing me to utilise a wide

range of automated equipment, and alongside guidance from the AstraZeneca HTS team, enabled the development of this assay.

3.2.2. Aim of the study

The aim of this study was to develop and validate an industrial scale anti-*Wolbachia* HTS screen capable of screening AstraZeneca's 1.3 million compound library to identify novel anti-*Wolbachia* compounds as potential new treatments for LF and onchocerciasis.

3.3. Methods

3.3.1. Cell culture

The C6/36 (*w*AlbB) cell line used in this screen has been described previously (Chapter 2.3.1). In brief this is a mosquito (*A. albopictus*) derived cell line, stably infected with *Wolbachia pipientis* (*w*AlbB). In this screen, the cells were cultured in Leibovitz medium (Life Technologies™) supplemented with 20% FCS (Fisher Scientific™), 2% tryptose phosphate broth (Sigma Aldrich®), 1% non-essential amino acids (Sigma Aldrich®) and 1% Penicillin-Streptomycin (Sigma Aldrich®) at 26 ^{o}C. This medium was optimised based on previous work discussed in Chapter 2 (Clare et al. 2014).

3.3.2. Large scale cryopreserved cell bank

C6/36 (*w*AlbB) cells were cultured at scale in nineteen T225 cm^2 flasks (VWR) to generate 6.16 x 10^9 cells after a 7-day incubation. To produce the cryopreserved cell bank, spent medium was removed and replaced with 20 ml of fresh cell culture medium. The cells were detached by scraping, combined and centrifuged. The pellet was re-suspended in cryopreservation medium (90% FCS (Fisher Scientific™) and 10% DMSO) to a density of 3 x 10^7 cell per ml. The cells were aliquoted with 1 ml per cryovial for cryopreservation using a Kryo 560-16 control rate freezer (Planer PLC). This resulted in a cryopreserved cell bank of 190 vials containing 3 x 10^7 cells in 1 ml per cryovial.

3.3.3. Large scale cryopreserved cell bank recovery and quality control

A single cryovial was recovered by defrosting at 37 ^{o}C for 45 seconds, followed by immediate re-suspension in 40 ml of cell culture media, resulting in a DMSO concentration of <0.25%. The cells were centrifuged and re-suspended in 45 ml of cell culture media in a

T225 cm^2 flask (VWR). After a 7-day incubation at 26 ^oC, the cells were first tested (quality control) for *Wolbachia* infection by scraping in the spent media and a set volume added to a 384-well black, clear bottom, tissue culture treated plate (781090, Greiner Bio-one). Once settled the cells were fixed for 20 minutes with formaldehyde (0.9% final concentration) supplemented with Hoechst 33342 (6 µg/ml final concentration, Life Technologies™). A PBS (Scientific Prep Laboratory, VWR Catalyst) wash was followed by incubation with SYTO®11 for 15mins (10 µM final concentration, Life Technologies™). After a final PBS wash the cells were analysed on the Operetta® (PerkinElmer®) to assess the percentage of cells infected with *Wolbachia*. Using a x60 confocal objective the nucleus was identified by the Hoechst staining, allowing for the cytoplasm (omitting the nucleus) to be located by the SYTO®11 staining. As previously reported in Chapter 2.4.3 and in Clare et al. (2014), the cytoplasm texture was analysed with *Wolbachia* infection signified by a more complex cytoplasm texture. Based on analysis of infected and uninfected cells, a threshold was set at a texture score of 0.0028, above which cells were classed as infected with *Wolbachia*. Cells with greater than 50% of the population infected with *Wolbachia* were classed as having a sufficient level of *Wolbachia* infection and therefore suitable for screening.

3.3.4. Compounds

Compounds sourced from the AstraZeneca library were plated from liquid 10 mM compounds in 100% DMSO stored in 1536 well stock plates. For single shot screening, 80 nl of this stock (via acoustic drop eject on the Echo® 550 liquid handler units, Labcyte®) was plated per well into a 384-well, clear bottom, assay plate (781090 Greiner Bio-one). Once diluted in 80 µl of cell suspension, this resulted in a final screening concentration of 10 µM. On-board controls were included per assay ready plate (ARP) in two central columns resulting in 16 wells of either 80 nl of 5 mM doxycycline (Sigma Aldrich®) or DMSO. Dose response ARPs were created for concordance testing of A·WOL compounds using the Echo® 550 liquid handler to create ARPs with a final dose range of 30 µM to 20 pM (13 point, 1 in 3 serial dilution dose response). These compounds were selected and sourced from LSTM at a stock of 10 mM.

Additionally, quality control (QC) plates were produced by the compound management group, as 'back ups' in case there were issues with the on-board controls. These plates include columns of 'maximum' (DMSO), 'minimum' (doxycycline 5 µM) and 'reference'

(doxycycline 50 nM) controls repeated across the plate.

3.3.5. *Wolbachia* specific primary antibody production

The antibody was made by Covance® as previously described (Turner et al. 2009), by immunising five specific pathogen-free rabbits with *Wolbachia* peptidoglycan associated lipoprotein from *B. malayi* (*wBm*PAL) produced and donated by New England BioLabs. The antisera was obtained and the anti-*wBm*PAL antibody purified by affinity column chromatography. From this we gained 350 ml of antibody which was titrated against various concentrations of the secondary antibody, Alexa Fluor® 680 Goat Anti-Rabbit IgG (A-21076, far red fluorescence, Life Technologies™).

3.3.6. Anti-*Wolbachia* assay set up

Compound plates were defrosted overnight before being organised to include two 'max' plates (maximum signal, no compounds or DMSO added) at the beginning of each run and 3 QC plates dispersed throughout the run. All barcodes were scanned and recorded, and the plates labelled in numerical order. On the morning of the assay set up, cells recovered from a cryovial 7 days previously were checked for confluence as well as Operetta® analysis (described in the methods Chapter 3.3.3. Large scale cryopreserved cell bank recovery and quality control). The cells were counted in triplicate on the Vi-Cell™ XR (Beckman Coulter). Within a sterile class II biosafety cabinet the cells were diluted to a density of 25,000 cells per ml and a sterile magnetic stirrer added for continual mixing of the cells whilst 80 µl was added per well using a Multidrop™ Combi (Thermo Scientific™) resulting in 2,000 cells per well. All plates were foil sealed using a PlateLoc® thermal plate sealer (Agilent) (2 seconds at 230 ^{o}C) and incubated for 7 days at 26 ^{o}C before characterisation. In addition to the assay plates, an extra max plate was created with a clear seal to monitor the cell growth over the 7 days without having to disturb any assay plates.

3.3.7. HTS anti-*Wolbachia* and cytotoxicity assay characterization

On day 7 post assay set up, the plates were re-loaded into the incubator (Liconic) on the BioCel 1800 automated system (Agilent Technologies) held at 26 ^{o}C. To enable this staining protocol the BioCel system was set up with; a plate carousel, 3 x robotic arms, 5 x Multidrop™ Combis (Thermo Scientific™), 2 x PW 384 plate washers (Tecan®), a PlateLoc® thermal plate sealer (Agilent) and an XPeel® automated plate seal remover (Brooks Life

Sciences). Using this automated system, the plates were fixed by adding 20 µl of 9% formaldehyde containing 3 µg/ml of Hoechst 33342 (Life Technologies™) directly into each well containing 80 µl of cell culture, for 20mins. The fixative was washed off with 80 µl of PBS (Scientific Prep Laboratory, VWR Catalyst) and the adherent cells permeabilised with 80 µl of PBS + 0.25% Triton-X 100 (Sigma Aldrich®) for 30mins, followed by another 80 µl PBS wash. The plates were blocked with 80 µl of PBS + 6% bovine serum albumin (BSA) (Sigma Aldrich®) for 40 minutes before removal and an overnight incubation in the *Wolbachia* specific anti-*wBm*PAL primary antibody (30 µl of 1 in 2000). After a 12-hour incubation, the primary antibody was removed with a 6-minute wash of 80 µl PBS + 0.05% polysorbate 20 (Sigma Aldrich®) before a 1-hour incubation in the secondary antibody (30 µl of 1 in 400), Alexa Fluor® 680 Goat Anti-Rabbit IgG (A-21076, far red fluorescence, Life Technologies™). Finally, the secondary antibody was removed with 2 x 80 µl washes (6 min PBS + 0.05% polysorbate 20) and left in 40 µl of PBS with the plates sealed with foil (170 ^{o}C for 1 second). Between each stage described above, the wells were emptied of liquid. All reagents except for the addition of Hoechst and the antibodies were made by Scientific Prep Laboratory, VWR Catalyst.

The fixed antibody stained plates were read on both an acumen® (TTP Labtech) (*Wolbachia* analysis) and an EnVision™ (PerkinElmer®) (Hoechst host cell toxicity analysis) encompassed in a HighRes Biosolutions automated system. The acumen® (TTP Labtech) was set using a 633 excitation laser (via a 633 Dichroic mirror) and *Wolbachia* fluorescence detected by a 655 long pass filter (727.5/72.5 filter). The acumen® explorer software (TTP Labtech) identified objects, based on separate areas of fluorescence which were subsequently gated for excessive area and fluorescence intensity. The total area of the filtered objects (assumed to be cytoplasm encapsulated *Wolbachia*) per well was calculated as the read out. This gave quantification of *Wolbachia* levels per well, in which compounds with anti-*Wolbachia* activity are represented by a small total area per well. As this small area of *Wolbachia* fluorescence would also occur if the compounds showed cell toxicity (low number of cells either with or without a *Wolbachia* infection) a cell toxicity read was included, to identify these false positives. To optimise throughput this toxicity read was carried out by a single fluorescence read out per well based on the intensity of Hoechst staining on an EnVision™ (PerkinElmer®). The EnVision™ was optimised using a bottom mirror with the excitation

filter 355/103 and emission filter 460/207, with 10 flashes per read. Per plate, the acumen® read was processed in approximately 20 minutes, whilst the EnVision™ read was obtained in 2 minutes. This total screening time of 22 minutes per plate, allowed for a full run of 150 plates to be read in 55 hours. To increase the throughput further, two acumen®s and an EnVision™ were utilised, allowing for the 150-plate batch to be read in 28 hours.

3.3.8. Validation of the HTS assay

For validation of this assay, the plates were set up and analysed as described in the methods Chapters 3.3.3. Large scale cryopreserved cell bank recovery and quality control and 3.3.4. Compounds using two sources of validation compounds. Firstly, the AstraZeneca validation set of 7,000 compounds was completed in single shot on two separate occasions with different cryopreserved cell populations and all reagents. On each occasion the compounds were in different layouts on the plates to avoid results being influenced by compound location (pick 1 vs pick 2).

Secondly a set of 20 compounds was selected from the A·WOL drug discovery programme with various activities for both *Wolbachia* inhibition and cell toxicity. This set of compounds, including A·WOL's gold standard compound doxycycline (Sigma Aldrich®), was run in dose response as described in Chapter 3.3.4. Compounds method above, creating IC50 (50% drug inhibitory concentration) data which were compared to the EC50s achieved in the HCS assay (Chapter 2 and Clare et al. 2014).

3.3.9. Data analysis

The software programme Genedata Screener (Genedata) was used for all data management and analysis. Readouts from both the acumen® (TTP Labtech) and EnVision™ (PerkinElmer®) were imported into Genedata Screener, in which data for toxicity (Hoechst read on the EnVision™) and *Wolbachia* inhibition (antibody fluorescence read on the acumen®) were normalised per plate. The toxicity reads were normalised based on the mean read from all compounds on each plate as it is assumed the toxicity level should be limited. This mean represents a 'max signal' (0% inhibition of the insect cell) as there is little cell toxicity. The *Wolbachia* reads were normalised based on the 'max signal' (DMSO controls) and 'min signal' (doxycycline 5 µM); these respectively represent 0% and 100% inhibition of *Wolbachia*. As a back-up to issues with on-board controls, 3 QC control plates were included

within each run, at the beginning, middle and end. These could then be used in place of the on-board controls to provide the maximum and minimum signal for normalisation.

The data were filtered to identify 'hits' (*Wolbachia* inhibitors) that present no toxicity to the cell line. To do this the normalised *Wolbachia* data were filtered to identify compounds with greater than 80% inhibition. Additionally, these active compounds were filtered for those with less than 60% inhibition to the cell line based on the normalised data, to eliminate toxic and therefore false positive compounds.

Additionally, all plates were monitored for Z prime and signal to background. These data could then be analysed on a per plate basis within each run but also across all runs in the completed screen.

3.4. Results

3.4.1. C6/36 (*w*AlbB) optimisation for HTS

Although this cell line has been used as part of the screening pipeline at LSTM, within this collaboration the aim was to produce populations with a highly consistent *Wolbachia* infection. Our experience in screening at LSTM shows that the *Wolbachia* levels when cells are continuously cultured can alter over extended time periods. For this reason, with the expertise at AstraZeneca, we produced and tested assay ready cryopreserved cells in an attempt to keep the *Wolbachia* level consistent. Through advice from the AstraZeneca staff, we first altered our cryopreservation media from 10% glycerol to 10% DMSO with 90% FCS. Previously we had inconsistent and slow recovery of our cells, yet with this media the cells would consistently recover within 7 days. Cells were bulked up and the *Wolbachia* levels monitored until we gained nineteen 225 cm^2 flasks containing in total 855 ml of media (standard flasks at LSTM: 75 cm^2 with 15 ml of media). This quantity was required to make a large scale cryopreserved bank of 190 vials containing 3 x 10^7 cells in 1 ml per cryovial. This cell concentration was determined alongside the optimised cryopreservation media, to allow a single cryovial to provide enough cells after 1-week recovery for a daily batch of 150 plates, whilst also maintaining the *Wolbachia* load.

After recovery and growth for one week, a quality control step was included by testing the *Wolbachia* infection level on the Operetta® before each population was used for screening.

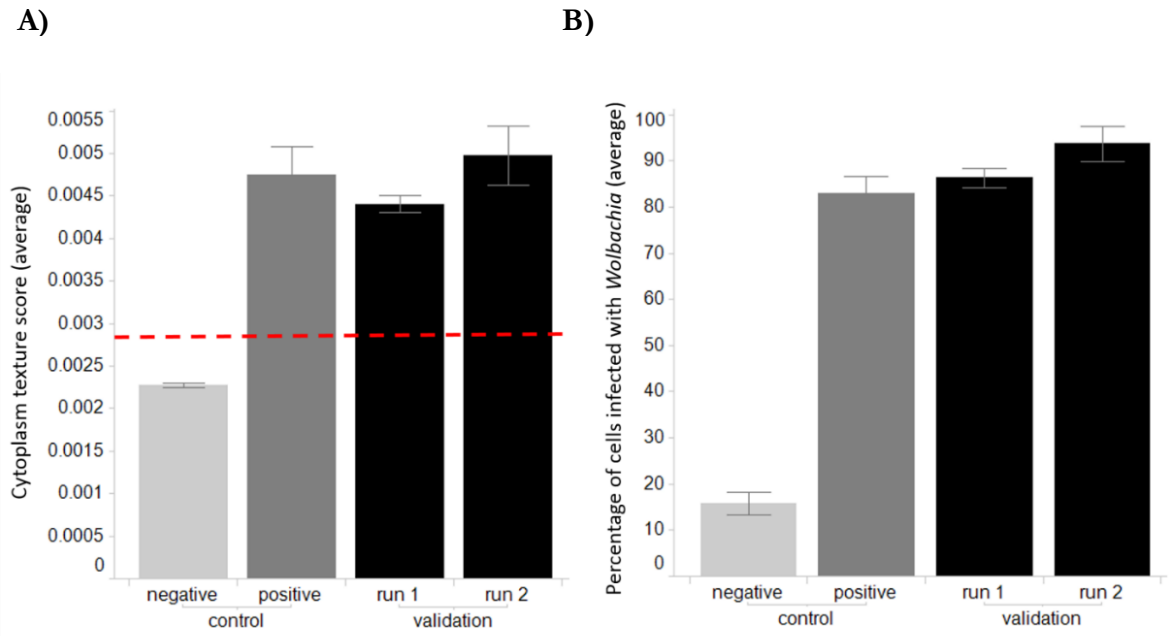

Figure 3.1. Validation of the cryopreserved cell bank. Control samples (with positive and negative *Wolbachia* infection) and QC results for the cells used in the validation of this assay, which were sourced from a single large scale cryopreserved cell batch. This would also be used for the full screen (means with StDev). A) Cytoplasm texture score, the red dotted line represents the threshold of the texture score above which cells are classed as infected B) The percentage of cells which are classed as infected based on the cytoplasm texture score. Comparison of the negative control with all *Wolbachia* infected samples (positive control, validation run 1 and 2) gives a Z prime of 0.67 and a signal to background of 5.6.

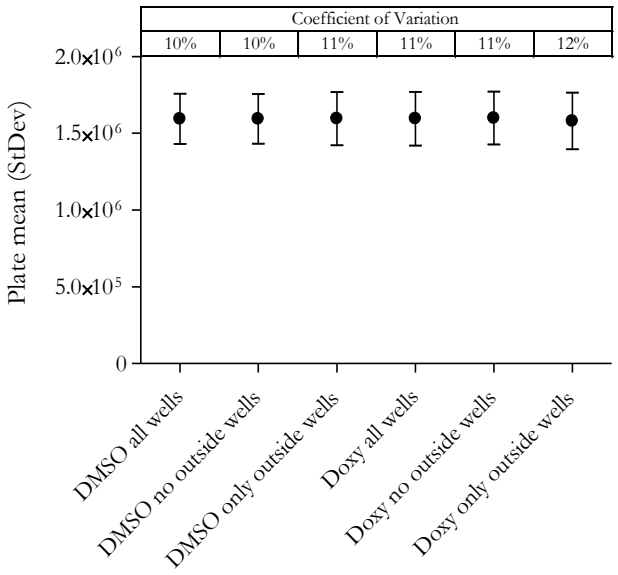

Figure 3.2. HTS edge effects validation. The edge effects on sealed Greiner plates seeded with 2,000 cells per well are minimal indicated by the consistent plate mean and standard deviation (StDev) with and without edge effects included and only a 1% increase in the CV on the outer wells compared to all internal wells.

This analysis was based on that previously described for the HCS assay (Chapter 2 and Clare et al. 2014) with the exception of formaldehyde and Hoechst addition as described for this HTS assay. The latter was used for nuclei identification. Figure 3.1 demonstrates the results from *Wolbachia* positive and negative controls (from continuously cultured populations with known *Wolbachia* levels). This was used to optimise the analysis methods in the Operetta® Harmony® software, including the decision for the threshold to be set at 0.0028, above which cells are classed as infected with *Wolbachia* (Figure 3.1A). Figure 3.1 demonstrates the consistency of these cryopreserved cells, as those used for the validation of this assay presented very similar cytoplasm texture score and percentage of cells infected with *Wolbachia*. This QC step would be included throughout the screen to monitor intra-cellular *Wolbachia* and to identify any changes in these levels over the course of the screen.

During the development of this assay we noticed variability in cell growth between different batches of FCS. Therefore, we would use a specific batch of FCS for the entire HTS. This along with the stability of the assay ready cryostocks and QC steps gives confidence that the cells will be robust and consistent, which is of high priority for a HTS campaign.

Finally the media was supplemented with 1% Penicillin-Streptomycin, which although not used as standard in the HCS assay has been used without interfering with *Wolbachia* levels (O'Neill et al. 1997; Hoerauf et al. 2000b; Foster et al. 2005). This was seen as important to avoid any failures in this intensive screen due to contamination during the staining protocol.

3.4.2. Plate characteristics optimisation

Greiner plates were selected over Corning plates after a cell density test determined superior growth and improved coefficient of variation (CV ~10% Figure 3.2). Cells were seeded into both plate types at either 1, 2 or 3 x 10^3 cells per well and incubated for 7 days (Figure 3.3) with both DMSO and doxycycline (striped across the plate). In the Greiner plates, the cell concentrations made little difference to the final cell numbers, except for when the plates were sealed. This heat foil seal provides the benefits of increased sterility and a reduced risk of spillage or leaching between wells and most importantly reduced evaporation minimising any edge effects. Figure 3.2 demonstrates this minimal edge effect in which the CV is only 1% higher when comparing outer wells to internal wells.

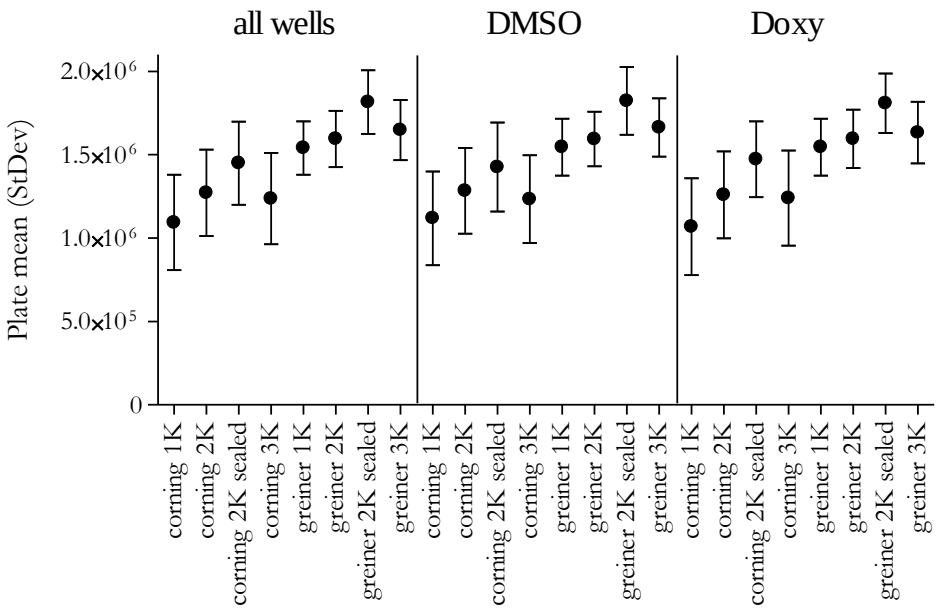

Figure 3.3. HTS seeding density optimisation. Cell growth measured by the acumen® analysis of Hoechst stained cells when the seeding density ranges from 1 to 3 x 10^3 cells per well in two 384-well plate types (Greiner or Corning). Data represent the means with StDev error bars.

3.4.3. Washing experiment

Through initial testing it was identified that the multiple plate washing steps as part of the staining process caused cells to be dislodged, resulting in the cell layer not being confluent. well (to stop the tip touching and physically dislodging the cell layer), liquid dispense/aspiration speed (sheer effect removing the cell layer by force – indicated by a U shape from the tip to the edge of the plate) and volume remaining in the well (aim to focus the sheer effect at the liquid rather than the cell layer). These settings were optimised to result in 7-10 µl of liquid being left in the well post aspiration and all aspiration/dispenses conducted at slow speed. These optimisations were tested by repeating wash steps with microscopy imaging between each step, for both a confluent cell layer and a layer with a physical scrape made in the cell layer (Figure 3.4). The results demonstrate the success of this optimisation as there was no significant loss to the cell layer after up to 14 wash steps. The success of this method can be further demonstrated in Figure 3.5C. This is a typical image from the acumen® displaying the confluent cell layer (Hoechst staining) after the completion of the validated assay described in this Chapter.

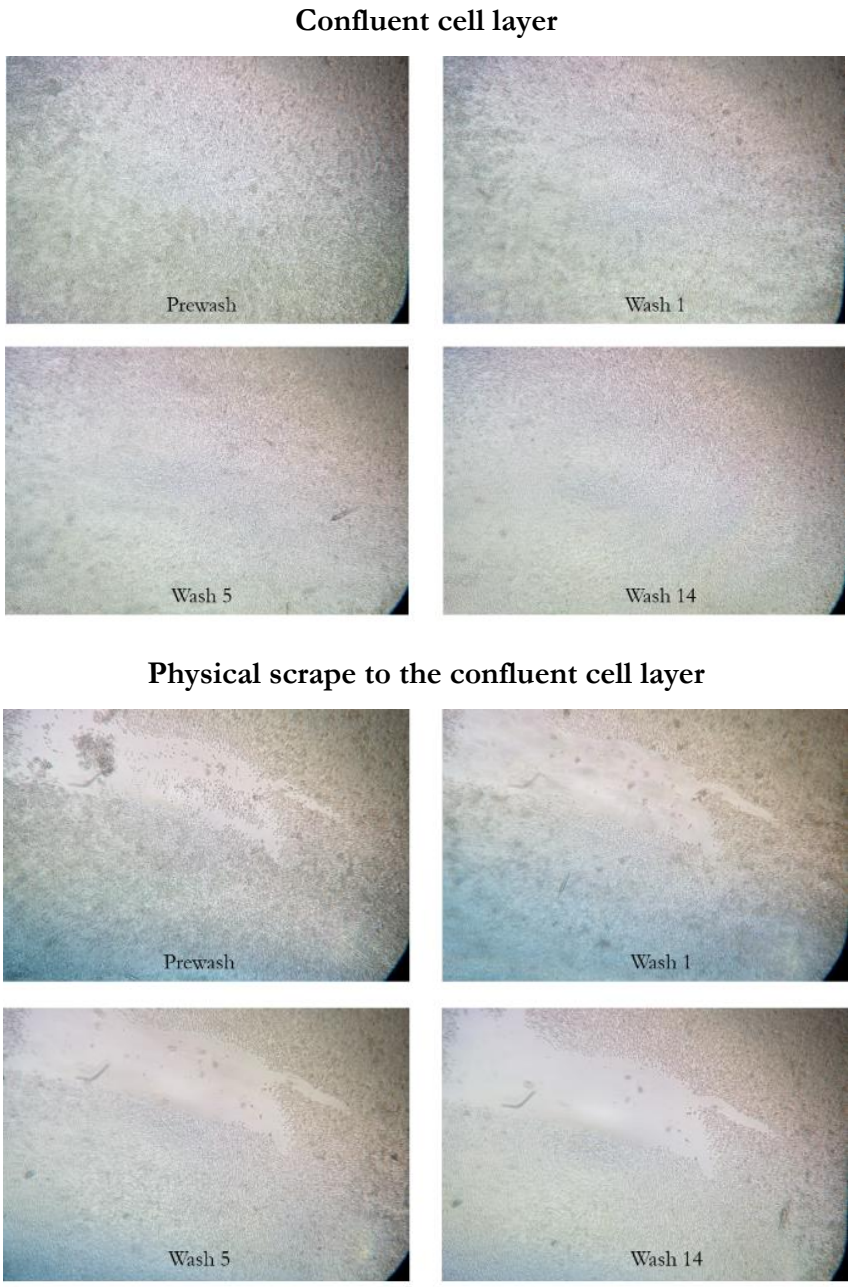

Figure 3.4. Validation of optimised wash settings. Optimised settings results in no significant loss in the cell layer on either a full confluent cell layer or one containing a physical scrape before the washing was initiated (pre-wash) after up to 14 washes.

3.4.4. Antibody method optimisation

The first step in developing the read out for this assay was to attempt a direct transfer of the HCS assay described in Chapter 2 which utilised a single staining step with SYTO®11 (a DNA stain) to image both the cell nucleus and *Wolbachia* (chapter 2 and Clare et al. 2014). However, this method when tested on higher throughput robotics (acumen® and EnVision™) than the Operetta®, presented too much background from the cell nucleus to

identify differences in *Wolbachia* levels, even when Hoechst was included to identify the nucleus. For this reason, we moved to a differential antibody staining technique.

During the development of the antibody staining protocol we achieved successful staining for both anti-*wBm*PAL (*Wolbachia* specific) and anti-FtsZ (generic bacteria) primary antibodies. We progressed with the anti-*wBm*PAL over anti-FtsZ antibody based on cost; 15-fold difference in estimates of £15 to £221 per plate.

Both Alexa Fluor® 488 (green fluorescence) and Alexa Fluor® 680 (far red fluorescence) (Life Technologies™) conjugated secondary antibodies were tested as part of this assay development. The decision to use a red-shifted fluorochrome in detection of the *Wolbachia* was taken in order to ensure maximum separation from the Hoechst emission spectra (461 nm). It also avoided the observed green autofluorescence of the C6/36 (*w*AlbB) cells. In addition it has been reported previously that many cyclic compounds are inherently fluorescent in the blue/green range of the spectrum (Thorne et al. 2010). Experience of imaging based screens tested against diverse compound libraries within AstraZeneca has shown that higher wavelength fluorochromes can generate a more robust assay, that is less prone to compound artefacts such as crystallisation (personal communication from Clark, Roger).

A matrix test of various concentrations of both primary and secondary antibody was used to optimise the antibody concentrations where possible (Figure 3.5). Figure 3.5A demonstrates that 1 in 2000 dilution of the primary antibody combined with 1 in 400 of the secondary antibody was optimal for the screen as it gave both the best Z prime and signal to background window. Additional to this, selecting the lower concentrations provided a significant cost saving. The original estimate of £15 per plate for the primary antibody was based on a 1 in 500 dilution, thus reducing the estimated cost of this antibody to less than £4 per plate.

Additional optimisation steps for the *wBm*PAL antibody included reducing the wash regimens and combining steps where possible. Although multiple combinations were tested (permeabilization+block, primary+secondary antibodies) as well as eliminating steps (permeabilization) the only improvement was the combination of Hoechst staining and fixation with formaldehyde. The most significant change to this protocol was altering the

A)

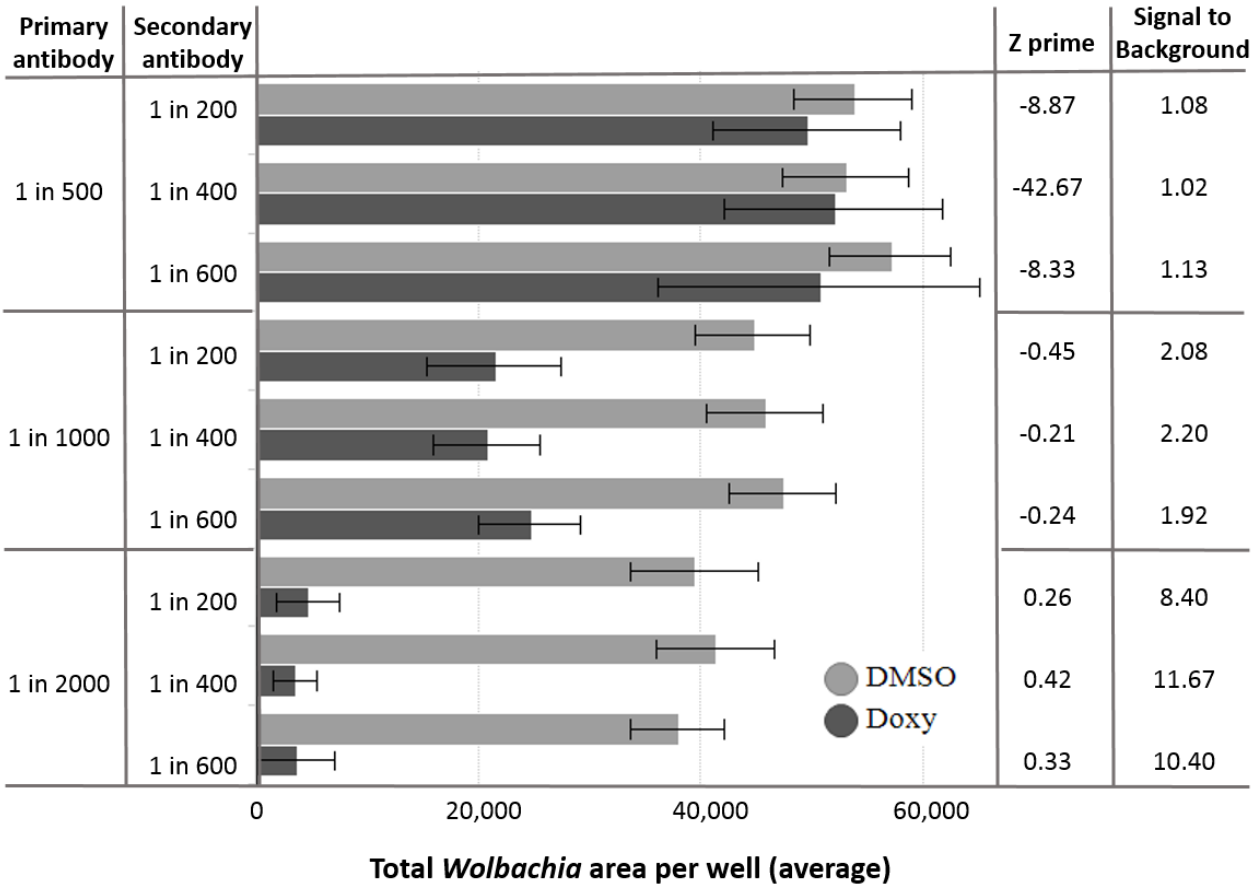

B) Operetta® image of nucleus /Hoechst and Alexa Fluor® 680 *Wolbachia*

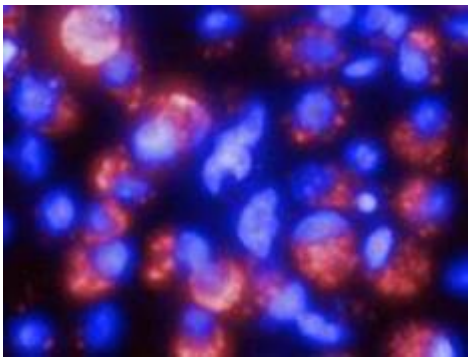

C) acumen® image of nucleus/Hoechst

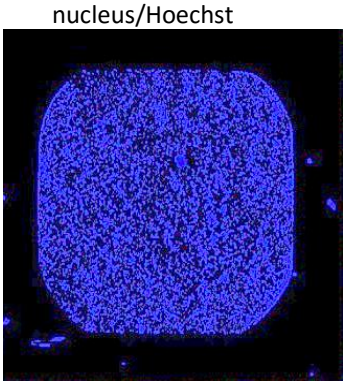

D) acumen® image of *Wolbachia*/Alexa Fluor® 680

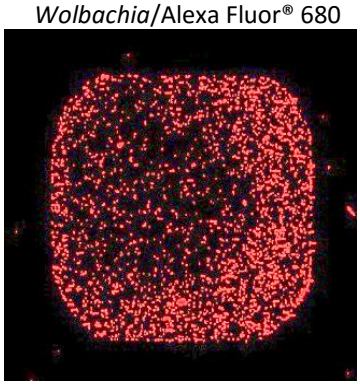

Figure 3.5. Antibody staining optimisation A) *Wolbachia* total area read on the acumen® for matrix titration of primary and secondary antibody concentrations. The data represent the means with StDev error bars. The columns on the right include analysis of the titrations based on comparing the results from DMSO (*Wolbachia* positive) and doxycycline 5 µM (*Wolbachia* negative control) treatment. B) Images from the Operetta® of C6/36 (*w*AlbB) cells stained with Hoechst to identify the nucleus (blue) and antibody staining (primary antibody against *wBm*PAL with Alexa Fluor® 680 secondary antibody) to identify the *Wolbachia* (red). C) C6/36 (*w*AlbB) cells stained with Hoechst and imaged on the acumen®. D) C6/36 (*w*AlbB) cells with *Wolbachia* specific antibody fluorescing in far red.

primary antibody incubation from 4 °C to room temperature overnight. This lower temperature would have further increased the complexity of the automated process as a second incubator would have been needed which was unlikely to be possible due to the amount of equipment already required in the BioCel system.

3.4.5. Optimisation of plate imaging

Early in the assay development, the acumen® was recommended by AstraZeneca for the end-point acquisition due to the speed of the system and data storage efficiency.

C6/36 (*w*AlbB) cells treated with either DMSO or doxycycline and stained with *wBm*PAL primary antibody and Alexa Fluor® 680 (far red) secondary antibody were initially imaged on the Operetta® alongside scanning on the acumen® in order to create a highly resolved image to guide the optimisation on the acumen®. This combined approach quickly allowed for characteristics of *Wolbachia* (including clumps) to be defined on the Operetta® and related gating applied to the acumen®. This was crucial for the development of this assay as the acumen® is not configured with high enough resolution as a compromise to obtaining a whole well image with a fast acquisition time (20 minutes per plate). This approach allowed background/artefacts (e.g. fluorescent contaminants) to be removed from the analysis which would otherwise easily compromise this read out. The Operetta® imaging determined that the largest *Wolbachia* clusters were around 100 µm x 40 µm; therefore, an upper gate was set on the acumen® for maximum object area of 4,000 μm^2 (Figure 3.6). The final read out for *Wolbachia* analysis was total area per well. Although this same method could be applied to the host cell toxicity readout out through Hoechst staining analysis, this would incur an additional 20 minute read time per plate. Due to this time penalty, work was carried out to assess a total well fluorescence read out due to the consistency of the cell growth, achieved through the optimisation of the cell culturing methods. This successful read out on the EnVision™ plate reader resulted in an analysis of the whole plate in just 2 minutes. The analysis of both *Wolbachia* levels and cell toxicity was achieved in just 22 minutes compared to a comparative analysis taking approximately 3 hours on a high resolution system such as the Operetta®.

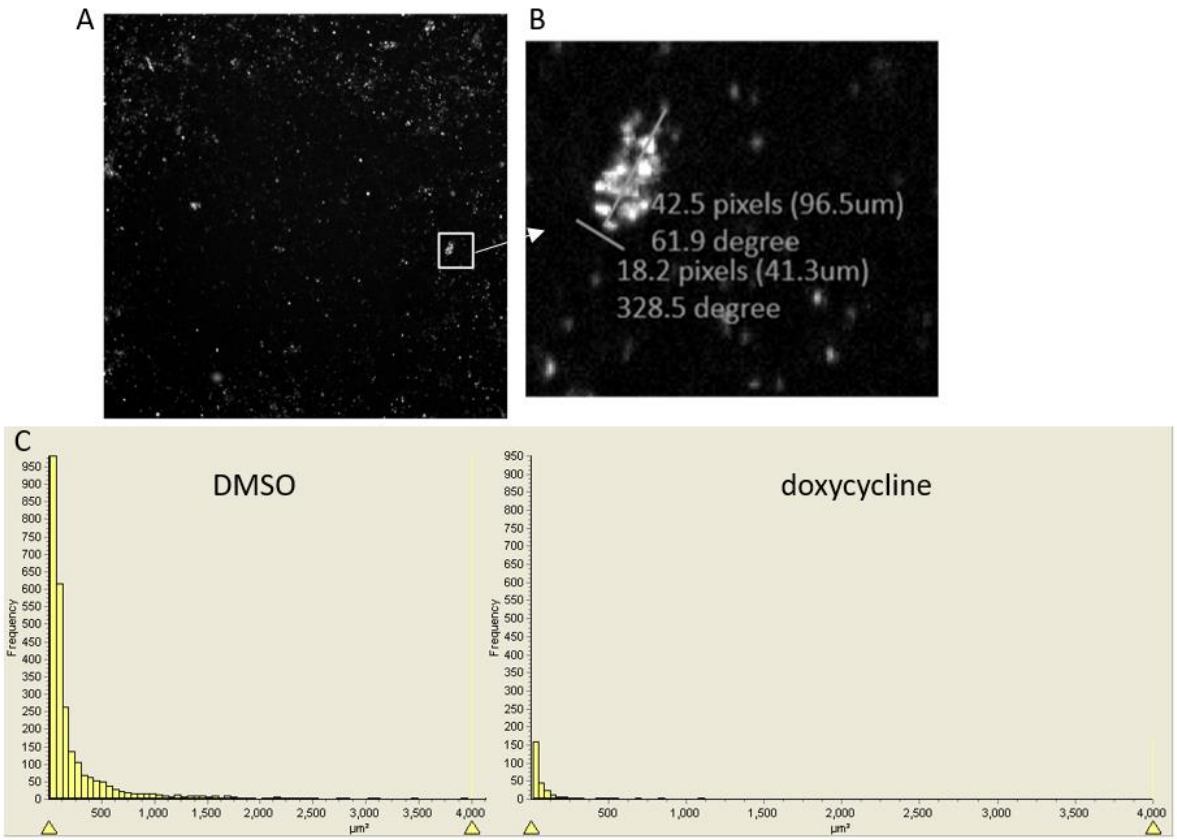

Figure 3.6. Optimisation of the acumen® *Wolbachia* analysis. A) Operetta® image (4x Objective) of a 384-well plate containing C6/36 (*w*AlbB) cells infected with *Wolbachia* stained with primary antibody against *wBm*PAL with Alexa Fluor® 680 secondary antibody. White box denotes *Wolbachia* clump. B) Zoomed view of *Wolbachia* clump (white box in A) with measuring lines. C) acumen® histogram of object (*Wolbachia*) frequencies by area gated at a maximum of 4,000 µm² for both DMSO and doxycycline controls, the latter clearly demonstrating reduced frequency.

3.4.6. BioCel automated staining protocol optimisation

Test compounds from AstraZeneca's core screening collection were prepared by the Sample Management group at AstraZeneca with the optimised staining protocol (as described in 3.3.6. Anti-*Wolbachia* assay set up). This protocol was transferred onto the BioCel system for a fully automated assay build. The system was configured by AstraZeneca staff. Several rounds of optimisation were undertaken to establish the correct timing for plate entry onto the platform (otherwise known as 'pacing time' or 'tick time').

The complexity of the overall assay procedure can be seen in Figure 3.7, encompassing four stages:

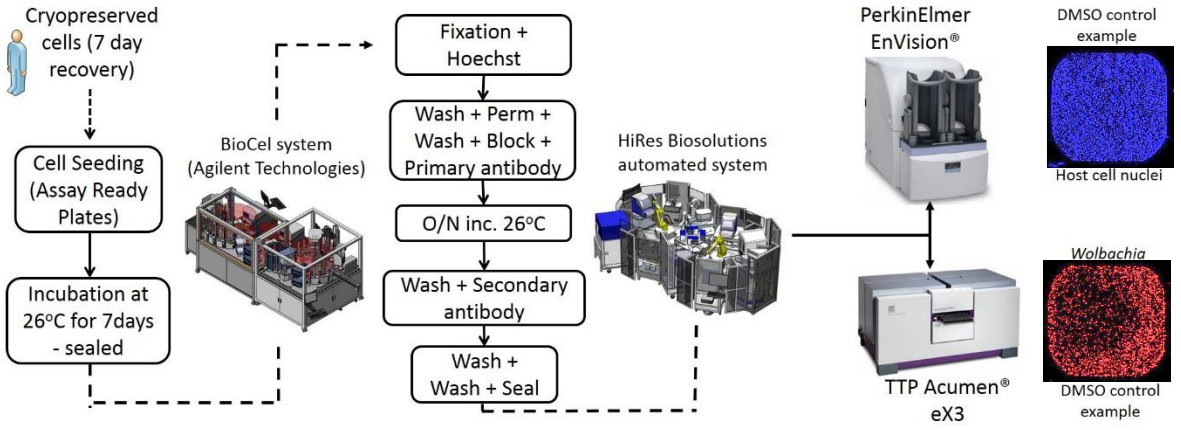

Figure 3.7. The full 3 week protocol for the industrial scale anti-*Wolbachia* HTS. The diagrams demonstrate cell recovery for 1 week. Following this in week 2 cells were plated onto assay ready plates which were then incubated through week 2. In the final week, plates were processed through a fully automated protocol on the BioCel system to allow for fixation, Hoechst staining of the host cell nuclei (toxicity read) and *Wolbachia* specific antibody staining. Once stained, the plates were moved onto a second automated system (HighRes Biosolutions) to read each plate for host cell toxicity (EnVision™) and anti-*Wolbachia* activity (acumen®).

1. Manual 1 week recovery of cryopreserved cells in T225 cm^2 flasks, followed by addition on day 7 into ARPs using a Multidrop™ Combi (Thermo Scientific™) inside a class II biosafety cabinet, to minimise contamination.
2. On day 14, after 7 days incubation with compounds, formaldehyde fixation, Hoechst staining and primary antibody staining of test plates was conducted on the BioCel system.
3. On day 15, after a 12 hour incubation of the primary antibody on the first plate, the second part of the BioCel protocol was initiated to carry out secondary antibody staining, washing and re-sealing of the test plates.
4. From day 15 to 17 (dependent on the batch size), the plates were scanned to determine the *Wolbachia* area end-point on the acumen® units (this read being split over two HighRes Biosolutions automation platforms feeding individual acumen® units) and reading of the Hoechst end-point on the Envision™ integrated into one of the HighRes Biosolutions platforms.

Due to the complexity of the automated method and the fact that assay runs were interleaved (to progress through the compound collection in a timely fashion) it was important to consider error recovery strategies. The automated part of the protocol was

configured so that a limited number of assay plates were released onto the robotic system at any one time through a 'phased-release' (effectively forming a series of mini-batches) to mitigate against potential large-scale loss of test plates due to unforeseen automation crashes. Assay plates remained relatively stable if left for extended periods in PBS during the protocol, however deterioration in assay quality was observed if fixative or permeabilisation steps extended beyond the optimised time. Due to these reasons if crashes occurred plates held at PBS stages were processed whereas those in other phases would be discarded.

3.4.7. Assay validation

3.4.7.1. AstraZeneca Validation set plates

In order to validate the assay, we first utilised the standard validation process the HTS department at AstraZeneca employ. This involved testing a 'validation set' of compounds which are representatives of the full library collection. The results obtained from this are used in four key ways.

Firstly, this validation can assess the consistency and stability of the developed assay. For this assay, this was assessed through screening the 'validation set' of compounds on two separate occasions (using different reagents and cryo vials) and on each occasion a single compound was plated into a different well location (to avoid results being impacted by the position on a plate). These two tests are classed as pick 1 (occasion 1) and pick 2 (occasion 2). Figure 3.8A demonstrates the consistency obtained between these two picks for the *Wolbachia* read out (total *Wolbachia* area in μm^2 per well) with the majority of data being within 10% of y = x. Similarly, Figure 3.8B demonstrates the consistency in toxicity read out of total area per well of the host cell nuclei (Hoechst staining). There is more variation in the results for non-toxic compounds, which is not surprising over a 7-day assay, but the compounds which are toxic are repeatable.

An alternative graphical assessment of the data was carried out using a Bland-Altman plot (Bland and Altman 1986), Figure 3.8C. This is a quantitative method to look at the differences between two sets of data, rather than the relationship between them e.g. correlations. Figure 3.8C displays the *Wolbachia* read out for pick 1 minus pick 2, with the overall mean difference lying very close to 0% difference (1.38%). This suggests little difference between the picks overall. This is further emphasised by 1 standard deviation of

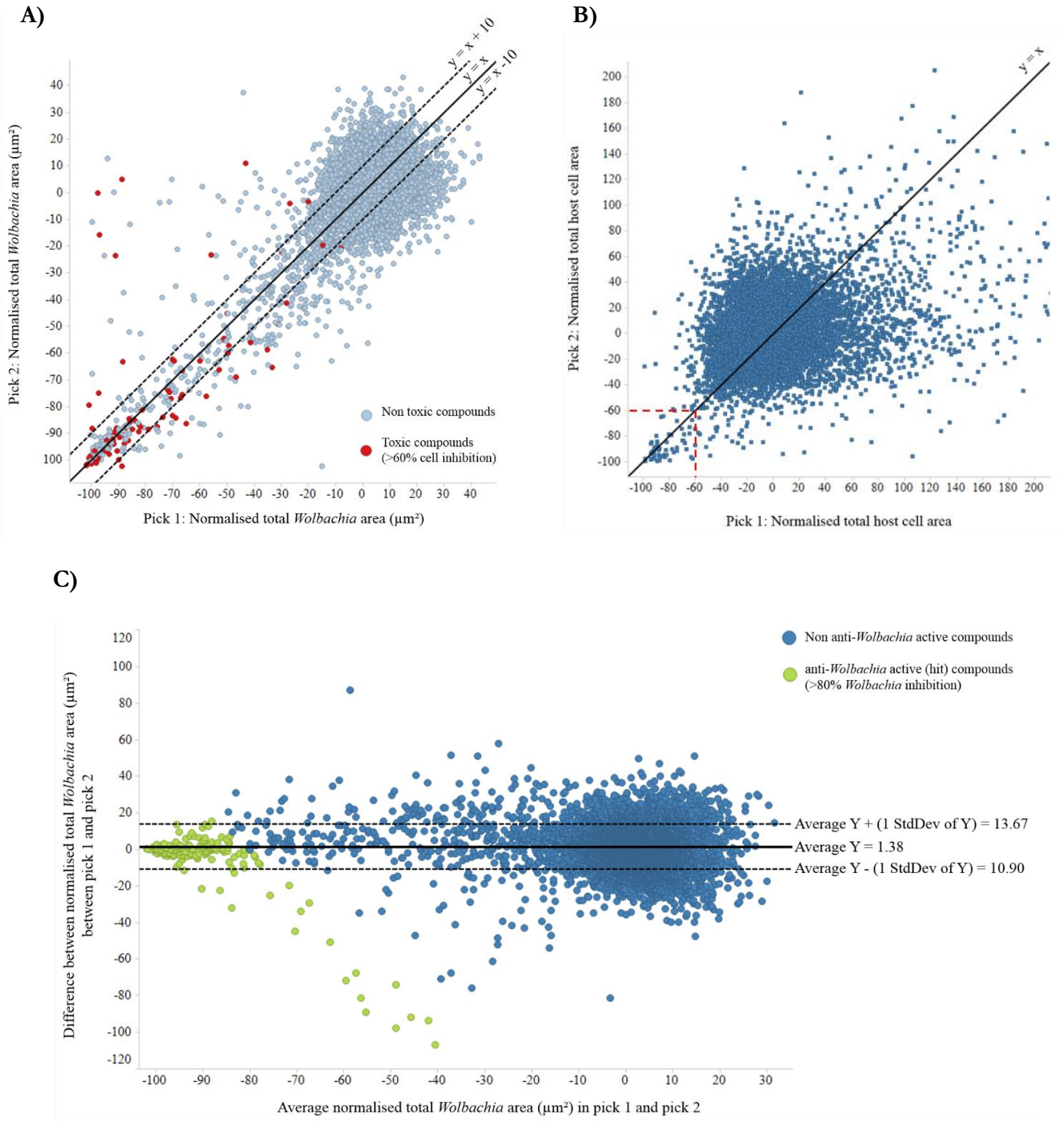

Figure 3.8. HTS assay validation A) Correlation of anti-*Wolbachia* activity between pick 1 and pick 2, were anti-*Wolbachia* 'hit' activity is demonstrated by less than -80% of the normalised results (> 80% inhibition of *Wolbachia*). Toxic compounds in red, are defined by less than -60% of the normalised result (> 60% inhibition of host cell). B) Correlation of toxicity to the host cell line in pick 1 versus pick 2, showing clear correlation in toxicity defined as less than -60% of the normalised results (>60% inhibition) C) Bland-Altman plot presenting good similarity in anti-*Wolbachia* activity between pick 1 and pick 2, with the mean difference lying close to 0% difference (1.38%) and 1x StDev at less than 14% from 0.

Table 3.1. Summary data for the QC plates from the validation screen. The 'Max' and 'Min' controls refer to DMSO and 5 μM doxycycline respectively. The mean readout refers to the total *Wolbachia* area per well (μM).

	Min		Max			Signal
QC Plate	Mean	CV	Mean	CV	Z prime	window
1	48890	18%	901356	7%	0.74	12.8
2	65249	18%	917427	6%	0.78	16.2

this mean lying at less than +/-14% difference. Although the vast majority of the results differ by less than 60% between the two picks, there are some strong outliers. One compound has much higher activity in pick 2 (indicated by the >80% difference), yet was not a hit in either. Conversely, 14 compounds have a highly negative difference (<-60%) and are therefore more active in pick 1. Of these, 5 were hits in pick 1 but not pick 2. These differences could be due to a variety of reasons including, errors in the assay set up (missing or incorrect compound concentration), staining issues (incorrect additions) or assay read (artefacts or contamination). However, overall the number of anomalies (<0.2%) is minimal, especially when considering only a single result is obtained for each compound per pick, in order to maximise throughput for a HTS.

Secondly, this data set can be utilised to set up analysis parameters and protocols, based on the sensitivity of the assay, for the full screen. Using this validation set, an anti-*Wolbachia* active (hit) compound was quantified as having greater than 80% inhibition from the DMSO control within each plate (less than -80% of normalised total *Wolbachia* area) (Figure 3.8B). Toxic compounds were determined as those having greater than 60% inhibition of the host cells (Hoechst) (Figure 3.8C).

Thirdly, using QC plates alongside the validation plates (as described in the methods Chapter 3.3.4. Compounds) provides evidence of the robust nature of this screen as the mean Z prime is 0.76 with a good signal window of 14.5 (Table 3.1). Furthermore, the confidence intervals around the 'Min' (18%) and 'Max' (6.5%) are extremely encouraging when considering this is a 7-day biological assay.

Finally, once the assay was approved to be suitable for a HTS screen this data set was used

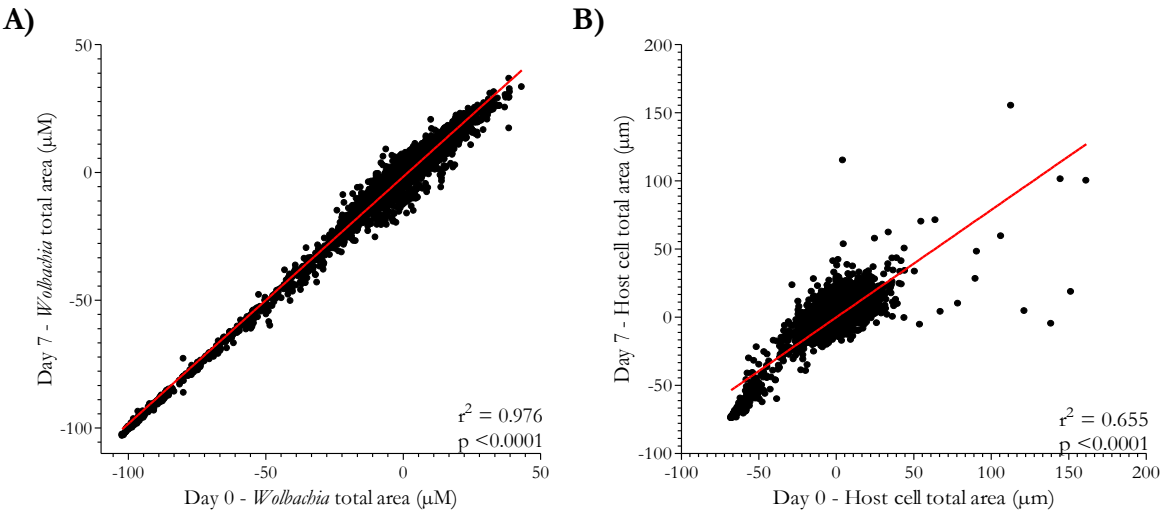

Figure 3.9. Validation compounds read on day 0 and 7 days post initial read A) anti-*Wolbachia* activity read out using the acumen®. B) host cell toxicity read out using the acumen®

to give an indication of the hit rate and toxicity level we are likely to obtain from the full library screen. Our validation set indicated an anti-*Wolbachia* hit rate of 1.80% (127 hits out of 7,038 compounds) including toxic compounds. However, when toxics are removed because they are likely to be false positives and will be eliminated from the final screen (see Figure 3.8A), the anti-*Wolbachia* hit rate was 1.28% (90 non-toxic hits out of 7,038). The toxicity rate for the 'validation set' compounds was 0.80% (56 toxics out of 7,038 compounds).

3.4.7.2. Stability over 7 days at 4 °C

With each plate taking 22 minutes to read on both the acumen® (*Wolbachia* analysis) and EnVision™ (toxicity analysis) and a planned batch size of 150 plates per day, a single run would take 28 hours to read when two acumen®s are available. To carry out multiple runs per week (ideally 4) and to allow for down time, the plates would be required to be stable over a longer period of time without any loss of fluorescent signal for either the antibody (*Wolbachia* read out) or Hoechst (host cell toxicity read out) staining. For this reason, we re-scanned the validation set of compounds 7 days after initial scanning (stored at 4°C). Figure 3.9A and B demonstrates strong correlation in the read outs ($p < 0.0001$, r^2 0.976 and 0.655 respectively), although there was more variation in the toxicity read out.

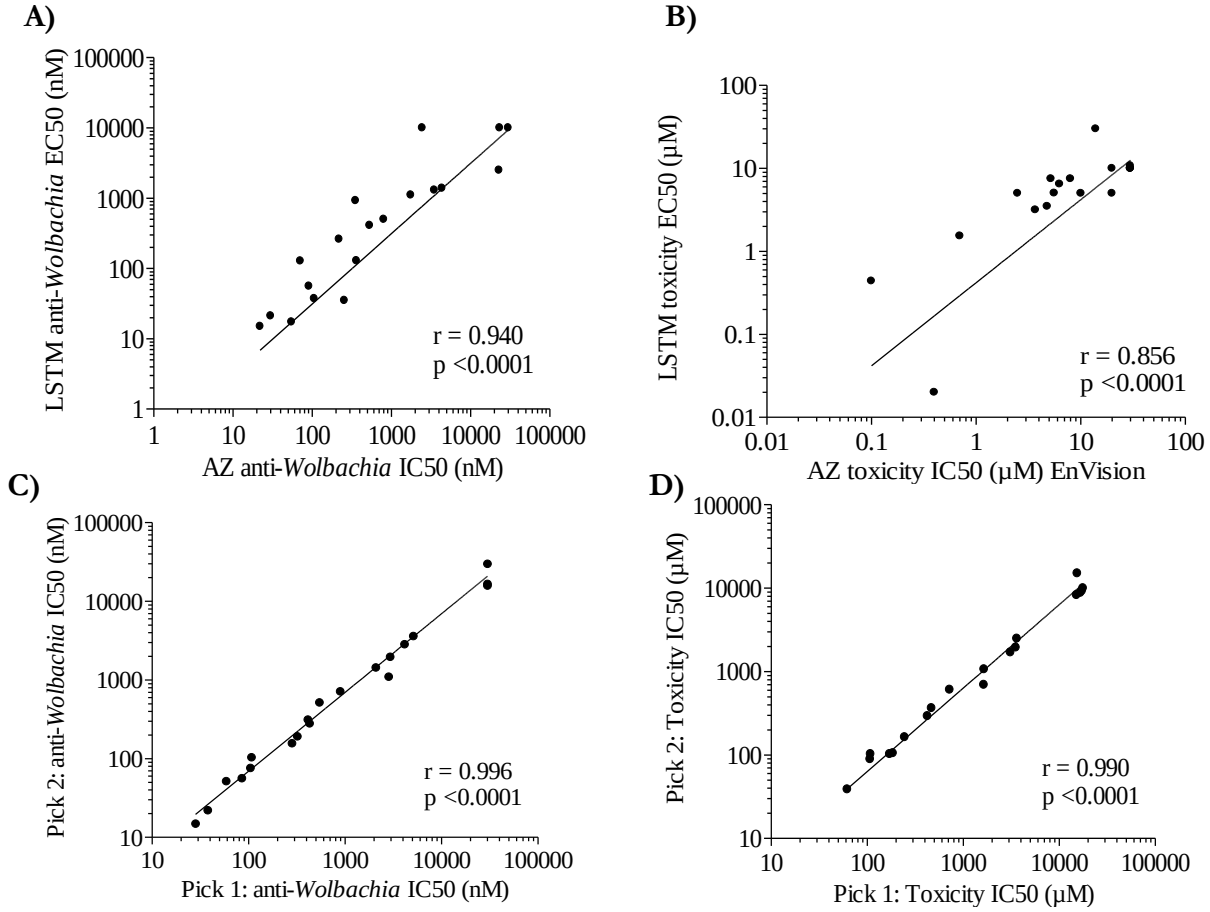

Figure 3.10. Concordance testing using 20 compounds from the A·WOL drug discovery programme, chosen for a variety of anti-*Wolbachia* potency and toxicity to the host cell line. A) anti-*Wolbachia* IC50s in LSTM vs AstraZeneca screens. B) toxicity IC50s in LSTM vs AstraZeneca screens. C) anti-*Wolbachia* IC50s for pick 1 vs pick 2 in the AstraZeneca screen. D) toxicity IC50s in pick 1 vs pick 2 in the AstraZeneca screen.

3.4.7.3. A·WOL validation set plates

In order to further validate this assay, a selection of compounds which have been tested within the A·WOL drug discovery programme where screened using this assay. These compounds were chosen to represent a range of anti-*Wolbachia* activity and host cell toxicity. Doxycycline was included in this collection as it is the gold standard compound in the A·WOL screens at LSTM. Figure 3.10A shows a strong correlation in anti-*Wolbachia* IC50s between the AstraZeneca and LSTM HCS assays ($r = 0.9405$ and $p < 0.0001$). Doxycycline shows consistent IC50s of 17.8 nM at AstraZeneca (mean, n=14 from 2 separate runs) and 16 nM at LSTM (median from 396 assays). The same correlation is seen for toxicity IC50s between the AstraZeneca versus LSTM HCS screen (Figure 3.10B, $r = 0.856$, $p<0.0001$). Furthermore to validate robust IC50s between runs within the AstraZeneca screen, Figure 3.10C and D demonstrate the high correlation between IC50s for anti-*Wolbachia* activity and toxicity for pick 1 versus pick 2 for the LSTM validation set ($r > 0.99$, $p < 0.0001$).

3.5. Discussion

The easiest route to initiate the development of an industrial scale A·WOL screen would be to simply upscale the HCS assay from the Operetta®. However, it soon became apparent that this assay was not suitable for upscaling, due to the long-read time per plate (3 hours). Miniaturisation of this assay to a 1536 well plate was attempted and although equipment was available to set up the plates, the wash steps were not achievable. Work therefore focused on the use of alternative plate readers, however it soon became clear that the benefit in the HCS dual SYTO®11 staining of both the *Wolbachia* and cell nucleus meant the latter masked any difference in the *Wolbachia* loads. Differential staining therefore appeared to be the best route. Antibody staining using the primary antibody *wBm*PAL was selected and tested with a secondary antibody with a far red fluorochrome to maximise the separation from the blue wavelength of Hoechst which was used to stain the host cell as a toxicity read out. The original method for this antibody staining was optimised to eliminate a 4°C step to allow the whole process to be carried out at room temperature. Although this process was simplified by this temperature change and reduced wash steps, it was still a complex process with 12 steps in this stage, especially when transferred to the automated BioCel system. Work was attempted to combine steps in this protocol which would have been beneficial to reduce the complexity, however, time constraints meant a decision was made to go forward with the protocol as it was. These time constraints were due to the large amount of work and time that was required in creating a consistent cell population. Although in the overall protocol this appears a small part, the creation of a large scale cryobank of cells with a sufficient *Wolbachia* load, resulted in a consistent read out between screening days, which will be vital to the success of this assay for repeated screening. Variability in the *Wolbachia* levels (as discussed in Chapter 2.4.1 and 3.4.1) for a variety of insect derived *Wolbachia* strains have been documented in many cell lines, both within and between cell populations (O'Neill et al. 1997; Dobson et al. 2002; Fenollar et al. 2003a; Frentiu et al. 2010; Venard et al. 2011; Serbus et al. 2012). Attempts have been made to increase and stabilise these *Wolbachia* infection levels by altering the cell culture protocol e.g. cell lines and media contents (Dobson et al. 2002; Fallon et al. 2008; Frentiu et al. 2010). Within Aa23 and JW18 cell lines, the maintenance of a *Wolbachia* infection over long time frames (years rather than months) has been linked to the provision of metabolic substrates

from their natural host. This includes *Wolbachia*'s requirement for amino acids from their host, as they lack the ability to synthesize key amino acids (Fallon and Witthuhn 2009; White et al. 2017). Conversely, cells such as TW-280, which cannot maintain a *Wolbachia* infection lack this ability to accommodate *Wolbachia* metabolically (Fallon and Witthuhn 2009). Genome-wide RNAi screening in the *Drosophila* cell line JW18 agree with this requirement for an amino acid source via ubiquitin-related pathways, as well as host lipid metabolism, phospholipase, sterol uptake and esterification and, mitochondrial metabolism (White et al. 2017; Grobler et al. 2018). This suggests that the C6/36 (*w*AlbB) cell line used in this thesis can accommodate *Wolbachia* metabolically, allowing for the maintenance of *Wolbachia* at an acceptable level for screening purposes. Although it has been shown that *Wolbachia* levels can be increased and infected cells can be recovered from cryopreservation (Dobson et al. 2002; Clare et al. 2014; Chapter 2), the use of a cryopreserved stock to stabilise the variation seen in *Wolbachia* levels was an important step in validating the suitability of this cell line to HTS drug discovery screening. The achievement of a robust cell population through the cryopreservation methods discussed in this Chapter, justified increasing the complexity of the assay as their consistency allowed for the simplicity and robust final readout of just two measures: total area per well of *Wolbachia* and host cell total fluorescence. These readouts were originally optimised for the acumen® which was selected due to its higher throughput than the Operetta® but with more detail than a single well fluorescent read out. The latter single fluorescent read out was attempted for the *Wolbachia* readout, but the variation was too high. However, once the robust cell population in combination with optimised growth conditions in the assay plates was achieved, the host cell number became consistent enough to obtain a single fluorescent read out to identify a significant reduction in cell number to indicate toxicity (>60% loss), thus the EnVision™ read out was selected. This was a crucial step in reducing the screening time per plate from 40 minutes solely using the acumen® (20 minutes per read for *Wolbachia* and host cell) compared to just 22 minutes using the acumen® for the *Wolbachia* (20 minutes) and EnVision™ for the cell number (host cell).

The validation stages described provided confidence that this assay would be able to achieve screening at an industrial scale, both in timescales and in its robust nature which would reduce assay failures. The latter was crucial as we had a limited time period to use

the AstraZeneca facilities, so the aim would be to maximise the number of compounds screened by minimising the need for repeats. In addition, the predicted hit rate of 1.28% gave us confidence in the value of carrying out this screen, as there appears to be the potential to identify novel compounds with anti-*Wolbachia* activity. Although A·WOL has made good progress in identifying novel compounds, the opportunity to explore new chemical diversity and potentially expand the A·WOL portfolio was a valuable prospect.

Furthermore, if the predictions are correct, i.e. the identification of 16,000 hits, this would allow for the input of triaging up front to focus down on compounds which have a higher chance of success to proceed though the A·WOL drug discovery pipeline.

The tight integration of my secondment embedding me within the HTS department at AstraZeneca for the duration of the screen optimisation, validation and ultimate execution, was imperative to the success of this project. This allowed for the easy flow of knowledge between A·WOL and AstraZeneca and consistent progress in the development of this work in the tight timescales.

AstraZeneca concluded that the validated assay was the one of the most complex assays developed in their unit, with a predicted time scale of 3 months to complete the full compound collection.

This study was accepted (February 2019) for publication in *SLAS Discovery* (Clare et al. 2019b).

3.6. Summary

- A collaboration between A·WOL and AstraZeneca has successfully adapted the C6/36 (*w*AlbB) high content assay to a multistage screen capable of testing the entire 1.3 million compounds in AstraZeneca's collection within months.
- This adaptation has developed from a simple dual DNA stain assay to a multistage highly automated differential staining method (*Wolbachia* specific antibody and Hoechst host DNA staining).
- The assay has been validated against quality control plates (DMSO vs the A·WOL 'gold standard' doxycycline), AstraZeneca's set of validation compounds (representatives of the whole library) and a spread of A·WOL compounds (selected based on a range of anti-*Wolbachia* activity and host cell toxicity).
- All validations indicate this assay should be robust enough to complete screening of the full 1.3 million compound library, especially when considering the creation of a large scale cryopreserved cell bank which should provide highly consistent *Wolbachia* levels across all screening events.
- The AstraZeneca validation set suggests that there could be a hit rate of 1.28%, presenting a high chance of strong hits to be identified out of the approximately 16,000 hits.

Chapter 4 : Screening of the full 1.3 million AstraZeneca compound library

4.1. Abstract

Through collaboration with AstraZeneca, our validated HTS assay was successfully deployed against 1,298,152 compounds from the AstraZeneca library. Following this primary screen, we identified 20,255 hit compounds. Cheminformatics were utilised to prioritise 6,324 compounds for secondary dose response screening. Within this secondary screen 77% of compounds maintained good activity (IC50 <10 µM), from which 58 clusters were selected based on an overall manual assessment of anti-*Wolbachia* activity, mammalian cell toxicity, measured compound purity, cluster size, and chemical structure. These clusters were assessed in a larval worm (mf) *in vitro* assay resulting in 5 clusters with similar EC50s to doxycycline and other A·WOL lead compounds after exposure for 6 days. However, when scrutinised further in a *Wolbachia* time kill assay in mf with compounds exposed to mf for 2 days, the *Wolbachia* reduction is maintained (66-85%) for all these compounds in comparison to doxycycline which reduces to 53%. Furthermore, when tested after 24 hour of drug exposure all but one cluster maintains >50% reduction in *Wolbachia* compared to doxycycline at 9%. These results show that we have identified compounds with a significantly faster rate of kill and therefore likely to have a different mode of action to current lead A·WOL compounds.

4.2. Introduction

4.2.1. Background

The validation of an industrial scale anti-*Wolbachia* HTS assay described in Chapter 3 provides the opportunity to screen larger libraries in a greatly reduced timeframe. Prior to the development of this HTS assay, the A·WOL programme had screened ~150,000 compounds using either the qPCR or HCS assays, resulting in 12 series of interest. Based on the validation of the screen, it was predicted that this assay could be used to screen the full AstraZeneca library of 1.3 million compounds, within just 2 months utilising 4 full time employees (FTE).

AstraZeneca's library incorporates compounds with desirable physiochemical properties including a mean cLogP of 2.9 (a predictor of good absorption due to high hydrophilicities) and molecular weight of 367. Lower molecular weights such as these tend to be good starting points for lead generation (Wigglesworth et al. 2015). This corporate library is likely to be composed of diverse compounds synthesized through various projects over the company's lifetime relating to their disease focuses of: cardiovascular and metabolism, oncology, respiratory, inflammation and autoimmunity, neuroscience and infection and vaccines. Compounds may also include those purchased from external vendors or compounds that were obtained through mergers and acquisitions (Nissink et al. 2014).

In addition to this library we also had access to a 500,000 compound library at LSTM from the Medicines for Malaria Venture (MMV). Screening of both of these libraries could create a dramatic increase in the number of hit compounds for A·WOL, potentially in novel chemical space.

4.2.2. Aim of the study

The aim of this study is to use the validated industrial scale screen discussed in Chapter 3 to screen the full library of ~1.3 million compounds at AstraZeneca's Global High-Throughput Centre and a 500,000-compound library from MMV.

4.3. Methods

4.3.1. Cell culture

The C6/36 (*w*AlbB) cell line used in this screen was described in Chapter 2.3.1 and 3.3.1. In brief these cells were mosquito derived and stably infected with *Wolbachia pipientis* (*w*AlbB). This screen exclusively used cells from the large-scale cryopreserved batch of these cells also described in Chapter 3.3.2 and 3.3.3. All cells in this screen were recovered and utilised through the following method. On day 0, a single 1 ml cryovial containing 3 x 10^7 cell per ml was removed from -180°C storage and transported on dry ice to the tissue culture lab. The cells were then partially defrosted for 45 seconds in a 37 ^oC water bath, before adding to 40 ml of room temperature culture media (Leibovitz medium (Life Technologies™), 20% FCS (Fisher Scientific™), 2% tryptose phosphate broth (Sigma Aldrich®), 1% non-essential amino acids (Sigma Aldrich®) and 1% Penicillin-Streptomycin (Sigma

Aldrich®)) within a sterile laminar flow cabinet. This volume of culture media diluted the DMSO from the cryopreserved media to less than 0.25% to avoid toxicity to the cell line. The defrosted cells were centrifuged at 1,000 rpm for 5 minutes and the cell pellet fully re-suspended in 45 ml of fresh culture media. This cell suspension was added to a T225 cm^2 flasks (VWR) resulting in a final cell concentration of approximately 6.7 x 10^5 cell per ml (1.3 x 10^5 per cm^2 if all adhered). This close-lidded flask was labelled with the date of recovery and day for use following a 7-day incubation at 26 ^oC.

4.3.2. Compound management (primary and secondary)

All compounds were prepared by the compound management team who provided the compounds in assay ready plates (ARPs) (781090, Greiner Bio-one) as described in Chapter 3.3.4. In brief, for the primary screen this resulted in 80 nl of 10 mM compound in 100% DMSO dispensed via acoustic drop eject on Echo® 550 liquid handler units (Labcyte®), resulting in a final screening concentration of 10 µM. The ARP layout included the two central columns containing on-board controls (16 wells of either 80 nl of 5 mM doxycycline (Sigma Aldrich®) or 80 nl of 100% DMSO). The remaining wells contained a single compound from the library, resulting in single shot screening of 352 compounds per plate.

The secondary IC50 ARPs were prepared in a similar way apart from the plate layout including the on-board controls dispersed throughout the plate rather than in the central columns. The remaining wells contained 36 compounds in a dose range from 30 µM to 1.5 µM (10 point, 1 in 3 serial dilution) in a serpentine pattern from left to right across the plate.

Additionally, quality control (QC) ARPs were produced by the compound management group, as ‘back ups’ in case there were issues with the on-board controls. These plates include columns of ‘Max’ (DMSO), ‘Min’ (doxycycline 5 µM) and ‘Reference’ (doxycycline 50 nM) controls repeated across the plate.

The original 384-well MMV compound source plates required re-formatting to be compatible with the automation available at AstraZeneca. Using the baseplate automated system (The Automation Partnership (Cambridge) Ltd), 4 x 384-well source plates were combined into a 1536-well daughter plate. The latter were subsequently used to create ARPs as described for the AstraZeneca library above.

4.3.3. Assay set up (same for primary and secondary)

The assay set up was as described in Chapter 3.3.6. The ARPs were defrosted at room temperature either the night before or morning of the assay set up. Each batch of ARP were organised and labelled with: plate number (e.g. 1 to 150), date and assay number. Plates 1 and 2 in each batch were blank 'max' plates (maximum signal, no compounds or DMSO added). QC plates were positioned at the beginning (plate 3), middle (around 67) and end of each batch covering each cell suspension used (66 ARPs per 2 L of cell suspension). Once in order, the barcodes were all scanned, recorded and checked.

The cell check quality control step was carried out on the specified flask (7 days since cell recovery); this included a visual assessment of media colour and adherent cell confluence, followed by Operetta® based image analysis (see Chapter 3.3.3). If the screener was satisfied with the cell and *Wolbachia* growth, the cells were scraped thoroughly in the spent media, counted in triplicate on the Vi-Cell™ XR (Beckman Coulter) and diluted to a density of 25,000 cells per ml in fresh media. The cell dilutions were made up in 2 L batches, enough for 66 plates. In order to keep the cells in suspension during the plating process, these cell dilutions were made up just before use and a sterile flea was added to each bottle for continual mixing on a magnetic stirrer. The cells were plated out manually using a Multidrop™ Combi (Thermo Scientific™) which had been sterilised and checked for accurate dispensing. The cell suspension was primed through all tubes to make sure there was no air in the tubing before 80 µl was added per well at high speed, resulting in 2,000 cells per well and a sterile lid added to the plate. The tips were continually monitored for blockages or bubbles which would alter the volume added per well. If either were found, they would be cleaned and fixed before continuing and a record made if this had altered any volumes. A visual check was carried out for the first plate from each cell suspension bottle as a second check that cells were successfully being added. Each plate was manually foil sealed using a PlateLoc® thermal plate sealer (Agilent) (2 seconds at 230 ^{o}C) and the sterile lid replaced. Both the foil seal and plate numbers were visually checked before housing in plate racks and incubated for 7 days at 26 ^{o}C. In addition to the assay plates, an extra plate was created with cells from each cell suspension bottle with a clear seal to monitor the cell growth without having to disturb any assay plates. Each assay (usually 4 per week) was housed in a different incubator, the outside of which was labelled with the assay number and date. Throughout

this process if any errors or issues were identified this was clearly labelled and included in the electronic write up of the data sheet.

4.3.4. Anti-*Wolbachia* and cytotoxicity assay results characterization

As described in more detail in Chapter 3.3.7, on day 14 (7 days after ARP cell seeding), the plates were re-loaded into the incubator (Liconic) on the BioCel 1800 automated system (Agilent Technologies) (26 ^{o}C). The BioCel system was set up with; a plate carousel, 3 x robotic arms, 5 x Multidrop™ Combis (Thermo Scientific™), 2 x PW 384 plate washers (Tecan®), a PlateLoc® thermal plate sealer (Agilent) and an XPeel® automated plate seal remover (Brooks Life Sciences). Using this automated system, the plates were: fixed and DNA stained (Hoechst, Life Technologies™), PBS (Scientific Prep Laboratory, VWR Catalyst) washed, permeabilised, PBS washed and blocked (PBS + 6% BSA (Sigma Aldrich®)) followed by an overnight incubation in the *Wolbachia* specific anti-*wBm*PAL primary antibody (30ul of 1 in 2000). This primary antibody was removed (6-minute wash with PBS + 0.05% polysorbate 20) before a 1-hour incubation in the secondary antibody (30 µl of 1 in 400), Alexa Fluor® 680 Goat Anti-Rabbit IgG (A-21076, far red fluorescence, Life Technologies™). Finally, the secondary antibody was removed (2 x 6-minute PBS + 0.05% polysorbate 20 washes) and left in 40 µl of PBS with the plates sealed with foil. Between each stage described above, the wells were emptied of liquid. All reagents were made by the Scientific Prep Laboratory, VWR Catalyst, with the exception of the addition of Hoechst and the antibodies immediately prior to the initiation of the run.

The fixed antibody stained plates were read on both an acumen® (TTP Labtech) (*Wolbachia* analysis) and an EnVision™ (PerkinElmer®) (Hoechst host cell toxicity analysis) encompassed in two HighRes Biosolutions automated systems. One system encompassed both an acumen® and EnVision™, the latter of which could also be used manually. The second HighRes Biosolutions system incorporated the second acumen® which was fed by a plate stacker and robotic arm. The final read outs were: the total *Wolbachia* area per well (acumen®) and host cell fluorescence intensity per well (EnVision™). Per plate, the acumen® read was processed in approximately 20 minutes, whilst the EnVision™ read was obtained in 2 minutes. The total screening time of 22 minutes per plate, using two acumen®s and an EnVision™ (automated and manual), allowed for the 150-plate batch to be read in 28 hours. Plates not being read immediately were stored at 4°C until required, at which time they

were brought back to room temperature for 1 hour before being loaded onto the reader platforms.

4.3.5. Data analysis

As described in Chapter 3.3.9 GeneData Screener software (Genedata) was used for all data management and analysis and run by the AstraZeneca staff involved with this screen. The readouts from both the acumen® (TTP Labtech) and EnVision™ (PerkinElmer®) were imported into GeneData Screener, in which data for toxicity (Hoechst read on the EnVision™) and *Wolbachia* inhibition (antibody fluorescence read on the acumen®) were normalised per plate. The toxicity reads were normalised based on the mean read from all compounds on each plate as it is assumed the toxicity level should be minimal. This mean represents a 'Max signal' (0% inhibition of the insect cell). The *Wolbachia* reads were normalised based on the 'Max signal' (DMSO controls) and 'Min signal' (doxycycline 5 µM); these respectively represent 0% and 100% inhibition of *Wolbachia*. If there was an issue with the on-board controls the three QC control plates included within each run were used for normalisation.

The data were filtered to identify 'hits' that had no toxicity to the cell line. To do this the normalised *Wolbachia* data were filtered to identify compounds with greater than 80% reduction. These active compounds were subsequently filtered to remove those with toxicity to the cell line, to eliminate false positive compounds. Toxic compounds were classed as having greater than 60% inhibition of the normalised cell density.

All plates were monitored for Z prime and signal to background. These data were then available for analysis on a per plate basis within each run but also across all runs in the completed screen.

For the secondary screen analysis curve fitting was also carried out within GeneData Screener by AstraZeneca with the output of IC50s for both the anti-*Wolbachia* activity and host cell toxicity.

The MMV library analysis was completed by A·WOL staff manually from the output Excel worksheets from the acumen® (*Wolbachia* analysis) and EnVision™ (host cell toxicity). A visual QC step was included covering: QC plate signal window confirmation, mean *Wolbachia* signal for the 'Max' wells should be close to 600,000 μm^2 and the mean toxicity

read should be 4,000,000. An Excel Macro script (created by Andrew Cassidy) was then used to move the raw Excel sheets into template worksheets set up to normalise the test compounds to the mean Max controls per plate. Hits were then identified using the same criteria as the AstraZeneca library screen: greater than 80% *Wolbachia* reduction and less than 60% cell toxicity. QC plates were used to monitor the performance of the screen through analysis of the 'Max' and 'Min' controls, Z prime and signal to background data.

4.3.6. Primary screen triaging

Chemists from both A·WOL and AstraZeneca triaged the 20,000 hit compounds from the primary screen down to ~6,000 compounds, as this was the maximum capacity for the secondary screening. This triaging was based on the information from AstraZeneca's databases and prior chemistry experience from the A·WOL programme. Compounds were excluded if they were known antibacterial structures or had previously been identified by A·WOL, as well as those known by AstraZeneca to have unwanted characteristics, for example genotoxic or reactive metabolite substructures. After these exclusions, the remaining compounds were prioritised by the chemistry team based on a balance of the following measures: LogD, solubility, molecular weight, human microsomal data, rat hepatocyte data and chemotype diversity. This is more extensively described in Clare et al. 2019a.

4.3.7. Secondary screen triaging – including mammalian toxicity

Mammalian cell toxicity information was provided by AstraZeneca on these compounds, through simultaneous screening of the selected compounds through a mammalian toxicity assay as well as the anti-*Wolbachia* dose response HTS screen. The mammalian screen was performed by AstraZeneca staff using the THP-1 cell line (ATCC® TIB-202) in RPMI 1640 medium supplemented with 10% FCS and 2 mM L-glutamine. The cells were maintained at 37°C with 95% humidity in 5% CO_2 in a shaking incubator. They were passaged every 2-3 days to ensure confluency did not exceed 1.5 x 10^6 cells/ml. This counter screen was tested in a 10-point dose response range with a top dose of 100 µM followed by a 1 in 2 dilution.

Following the completion of the IC50 screening in the C6/36 (*w*AlbB) insect cell line, as well as assessment of mammalian toxicity, 58 clusters with at least three compounds each were prioritised by both A·WOL and AstraZeneca chemists. The selection of these clusters was

based on an overall manual assessment of anti-*Wolbachia* activity, mammalian toxicity, measured compound purity, cluster size, and chemical structure (more extensively described in Clare et al. 2019a). From these prioritised clusters the two most potent compounds with sufficient remaining stocks were provided for screening in the tertiary microfilarial assay (larval worm *in vitro* assay) described in Chapter 4.3.8 below.

4.3.8. Tertiary screening

Two representatives from each of the prioritised clusters were screened at LSTM in a *B. malayi* microfilarial (mf) assay at a final concentration of 5 µM. Screening in this worm assay confirmed activity against the target nematode *Wolbachia* and the necessary characteristics to penetrate nematode tissues.

The mf were obtained by peritoneal lavage of gerbils (*Meriones unguiculatus*) harbouring a patent infection of *B. malayi* as described in Griffiths et al. (2010). Mf were purified using a PD-10 desalting column (Fisher Scientific™), centrifuged (1200 rpm for 5 minutes at room temperature) then re-suspended in complete media consisting of RPMI (Invitrogen™) supplemented with 10% FCS (Fisher Scientific™), 1% Penicillin Streptomycin (Life Technologies™) and 1% Amphotericin B (Life Technologies™). After determining the concentration of mf, the stock solution was diluted in complete media to ensure a final concentration of 8,000 mf/well of a 96-well plate (CytoOne) (100 µl per well). Compounds to be tested (10 mM stock in 100% DMSO (Sigma Aldrich®)) were diluted in complete media and 100 µl was added to the appropriate wells of the 96-well plate containing the mf, giving a final concentration of 5 µM. Five replicates were used for each compound and each plate contained doxycycline (5 µM, Sigma Aldrich®) and DMSO controls. The assay plates were incubated at 37 ^{o}C for 6 days in 5% CO_2, after which a visual assessment of motility was performed and the wells scored from 0 to 4 using the methods described by Rao and Weil 2002 (where 0 = immotile and 4 = highly motile). The DNA of each individual sample was extracted using the QIAmp DNA Mini Kit (Qiagen) before quantitative PCR was performed to obtain the ratio of *Wolbachia* Surface Protein (*wsp*) copy number to Glutathione S-Transferase (*gst*) copy number both originating from *B. malayi* based on modified methods from McGarry et al. (2004). For the *gst* qPCR, each reaction mixture included 1 µl of parasite DNA, 1.2 µl of each primer (see appendix for detail), 0.4 µl $MgCl_2$ (Sigma Aldrich®), 6.2 µl nuclease free H_2O (Ambion™) and 10 µl of SYBR® Green (Qiagen). The reaction mixtures

were heated at 95 ^{o}C for 15 minutes, then subjected to 40 cycles of 94 ^{o}C for 15 seconds, 57 ^{o}C for 30 seconds, and 72 ^{o}C for 30 seconds, with a final extension at 60 ^{o}C for 0.5 seconds followed by 1 minute at 97 ^{o}C. The *wsp* qPCR reaction mixture included 2 µl of parasite DNA, 1.4 µl of each primer, 0.8 µl $MgCl_2$ (Sigma Aldrich®), 4.4 µl nuclease free H_2O (Ambion™) and 10 µl of SYBR® Green (Qiagen). The reaction mixtures were heated at 95 ^{o}C for 15 minutes, then subjected to 40 cycles of 94 ^{o}C for 15 seconds, 60 ^{o}C for 30 seconds, and 72 ^{o}C for 30 seconds, with a final extension at 60 ^{o}C for 0.5 seconds followed by 1 minute at 97 ^{o}C. PCR cycles were performed on a C1000 thermal cycler CFX384 Real-Time System (Bio-Rad).

The *wsp*:*gst* ratio data allowed for normalisation of the *Wolbachia* level to the mf biomass for each well. The change in *wsp*:*gst* for each compound compared to the DMSO control was calculated before normalisation to the doxycycline reduction of *wsp*:*gst* for the particular plate concerned, to allow for inter-assay comparison.

Wolbachia time kill assays in mf were completed using the same method with the exception of a wash step on the required day. This was completed through transferring the samples into a deep well plate and diluting the samples in culture media (no compounds). The plate was then centrifuged at 1,000 rpm for 5 minutes before moving the pellet to a fresh plate and repeating the process 5 times. On the final wash 200 µl including the pellet was moved back to a fresh culture plate and returned to the incubator for the remainder of the assay.

4.4. Results

4.4.1. Primary screen consistency of the assay

Using the cryopreservation method, developed for the purpose of this screening campaign, we gained very consistent cell recovery (Figure 4.1). From each cryovial containing 3 x 10^7 C6/36 (*w*AlbB) cells recovered into 45 ml of media (0.7 x 10^6/ml) we gained a confluent cell layer from all flasks across the full 30 run screen. This resulted in a mean of 8.4 x 10^6/ml cells (StDev 1 x 10^6/ml) with a very small efficient of variation (CV 12%). This recovery rate suggests a doubling time of approximately 48 hours which matches work previously carried out at LSTM. More importantly the *Wolbachia* infection level is also constantly maintained across this screening campaign. All cryo recovered cell populations in this campaign had

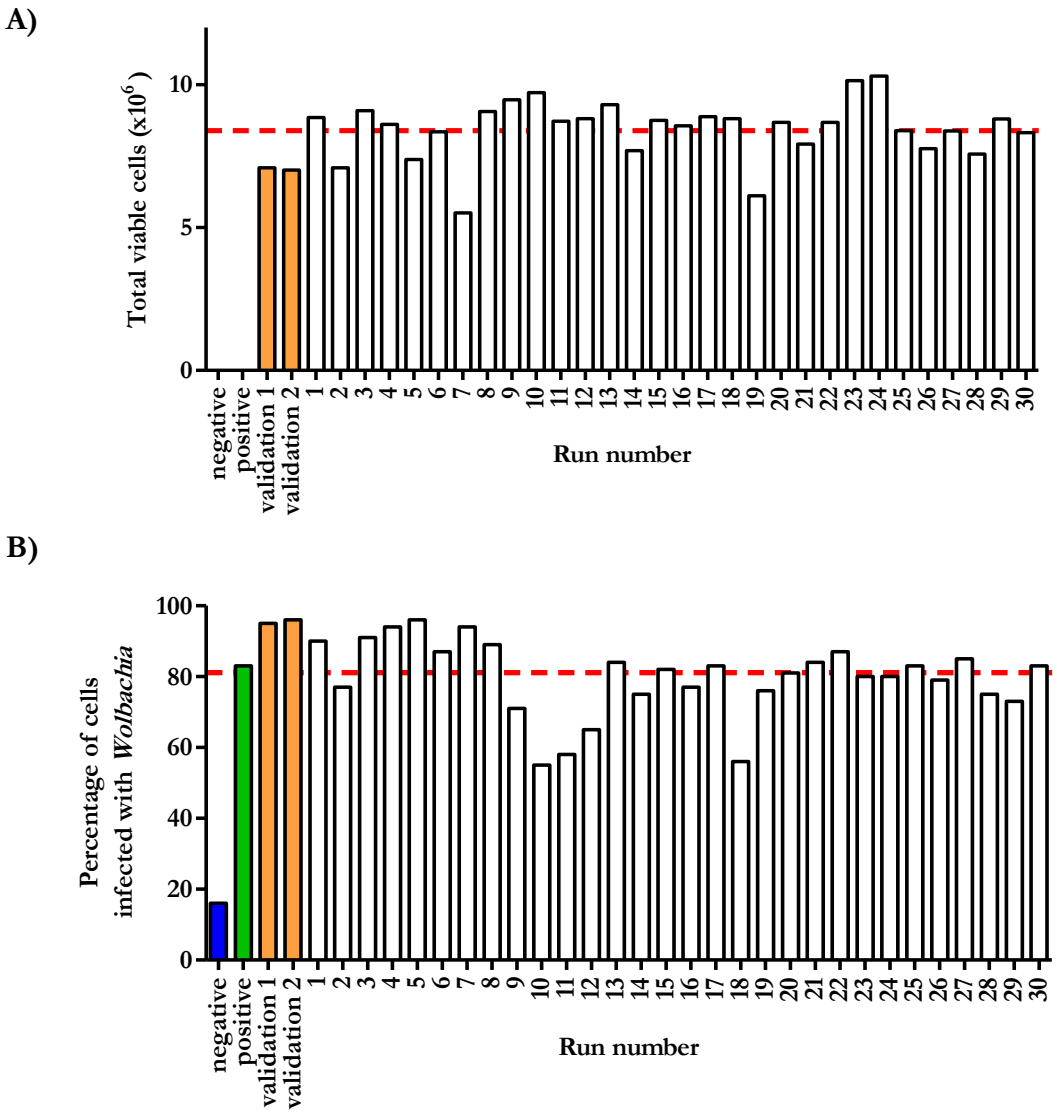

Figure 4.1. Consistency of the assay ready cryopreserved C6/36 (*w*AlbB) cells across the HTS campaign. A | Bar chart of the cell recovery after 1 week. Each bar represents viable cell growth from a single cryo vial (0.7 x 10^6/ml in a total of 45 ml) used in each assay run, with the mean indicated by the dashed red line (8.4 x 10^6/ml, StDev 1.0 x 10^6/ml). B | Bar chart of the *Wolbachia* infection within the recovered cells. Using Operetta® QC analysis the texture score is used to analyse the percentage number of cells classed as having a *Wolbachia* infection (mean indicated by the dashed red line, 81.1%, StDev 10.8%).

greater than 50% of the cells infected with *Wolbachia* (mean of 81%, StDev 10.8, CV 13%). Throughout this screening campaign all cell recoveries passed the QC resulting in no delays in the screening schedule (Figure 4.1). The cells produced consistent results within the assay (Figure 4.2). The Z prime across the whole screen was consistent, with means of 0.59 and 0.62 and CV of 23% and 32% on the two acumen® machines respectively. The signal to background ratios (assay window) were also consistent with a mean of 27.5 and 22.5% and CV of 24% and 17%.

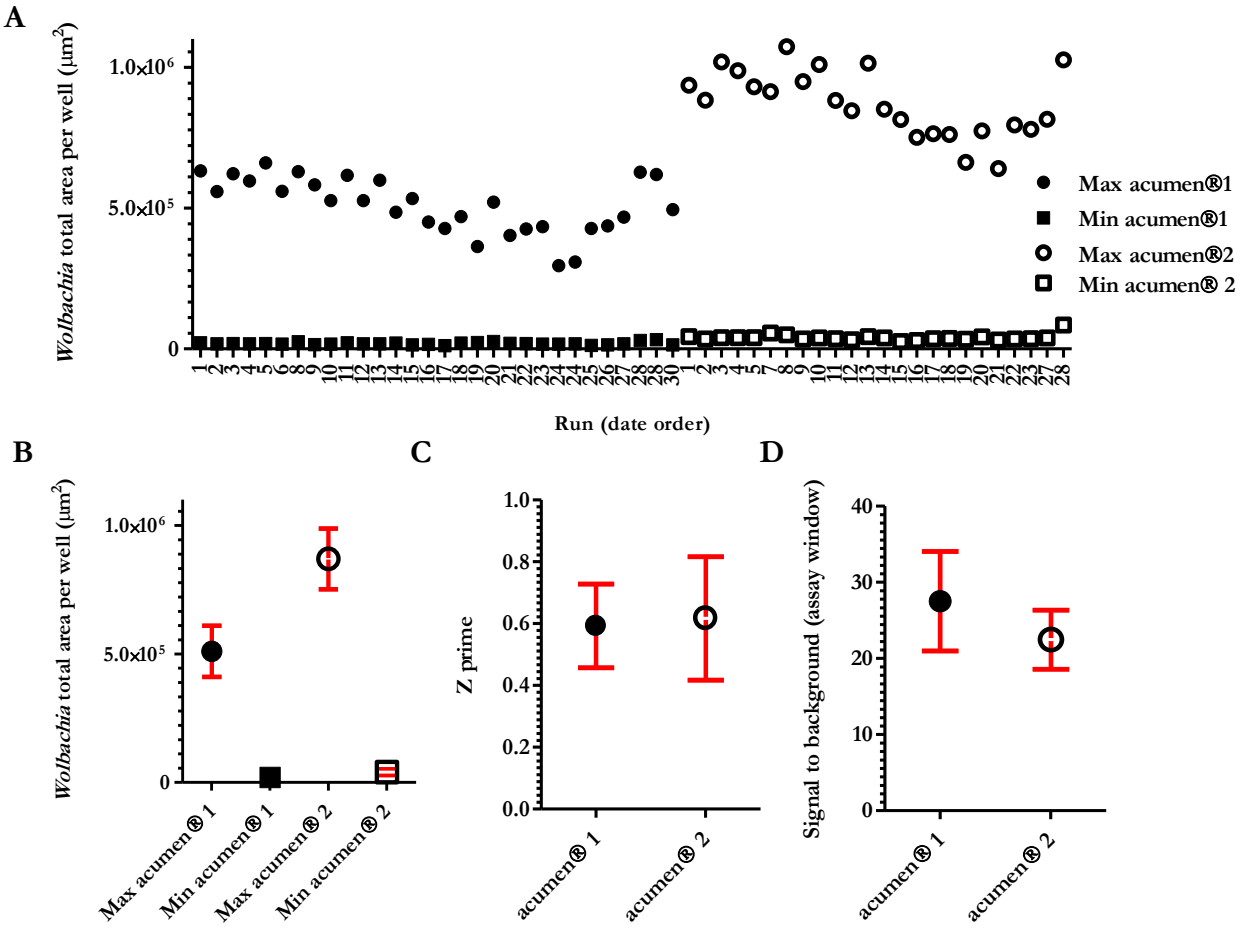

Figure 4.2. Screening statistics over the two-month primary HTS campaign. A| Scatter plot analysis for control samples. Each data point represents 1 run on one of two acumen®s for both the mean Max (vehicle control) and Min (doxycycline control) signals. **B| Mean signal, C| Mean Z prime analysis and D| Mean Signal to Background data, between the two acumen® systems across the whole screening campaign.** Z prime (black) is consistently greater than 0.4, while the signal to background is routinely above 20 throughout the screen. All error bars represent StDev.

Table 4.1. Binned data from the secondary dose response HTS at AstraZeneca.

	Mammalian toxicity IC50 (µM)	*Wolbachia* IC50 (µM)	Number of compounds	Number of pure compounds (>85%) (including compounds with no purity data)	Additional compounds with unknown purity data
Bin 1	> 0	< 10	4,863		
Bin 2	> 30	< 10	3,647	2600	951
Bin 3	> 30	< 1	776	579	176
Bin 4	> 30	< 0.1	162	123	36
Bin 5	> 30	< 0.01	32	25	6

4.4.2. Primary screen time scales for completion

This screen was completed over 2 months (October – December 2014) in which time 3,744 x 384-well compound plates were screened (in addition to 40 x validation and 76 x QC plates). This resulted in the testing of 1,298,152 compounds in singleton. From this screen 105 plates required re-testing, all of which was due to robotic or human errors.

4.4.3. Primary screen hits and toxicity

From the ~1.3 million compounds tested 2.36% were classed as active based on their total *Wolbachia* area read being greater than 80% reduction (>30,000 compounds) (Figure 4.3). Once compounds which were toxic to the host cell line (greater than 60% reduction) were removed this resulted in a hit rate of 1.56% providing us with 20,255 compound hits.

4.4.4. Secondary EC50 screen

The 20,255 hits from the primary screen were triaged down to 6,324 compounds for secondary dose response screening. This triaging was initiated by the removal of unfavourable chemistry known to hinder successful druggable compounds. In addition, in order to focus on novel chemotypes, known antibacterials and structures previously worked on by A·WOL were excluded. The final compounds were then selected based on a balance of molecular weight, predicted logD, solubility, intrinsic clearance (models for human microsomes and rat hepatocytes) and chemotype diversity.

Dose response screens were performed on these 6,324 compounds as 10-point curves, 2-fold dilutions from a starting concentration of 30 µM. Curve fitting was completed by AstraZeneca staff using their GeneData Screener software for both *Wolbachia* and the mammalian cell (toxicity) IC50 screened in parallel (Figure 4.4). For the *Wolbachia* IC50s only 23% of compounds were classed as not active (1,115 compounds with IC50>10 µM and 371 for which curves could not be fitted). From the remaining compounds 60% (3,787) had minimal activity (1-10 µM IC50), 843 compounds (13%) with good activity (0.1-1 µM) and 208 (3%) had strong activity (<0.1 µM). The latter is within the range of that seen for doxycycline and other known A·WOL hits.

Out of the total compounds 84% (5,332 compounds with IC50 >10 µM) were not classed as toxic to the mammalian cells (over 5,000 of which actually had IC50s above 30 µM). From the remaining, 952 compounds (15%) had some toxicity (1-10 µM) and less than 1% had

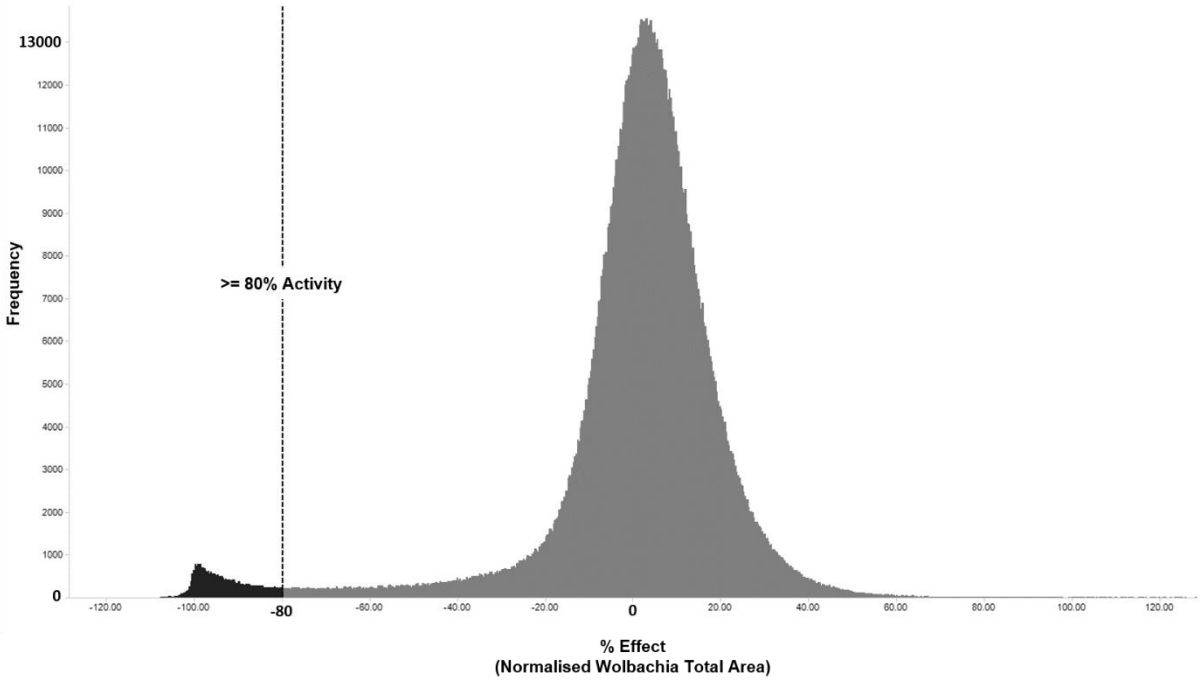

Figure 4.3. Frequency plot of primary HTS results across the 1.3 million compounds. The dotted line shows the cut-off used in the screen to select 'hits' (>=80% activity as measured by total *Wolbachia* area). The distribution can be seen centred around zero with a tail leading out towards the left (active compounds). The proportion of compounds falling beyond the cut-off line shown is 2.36% of the total compounds tested. This Figure was created by AstraZeneca.

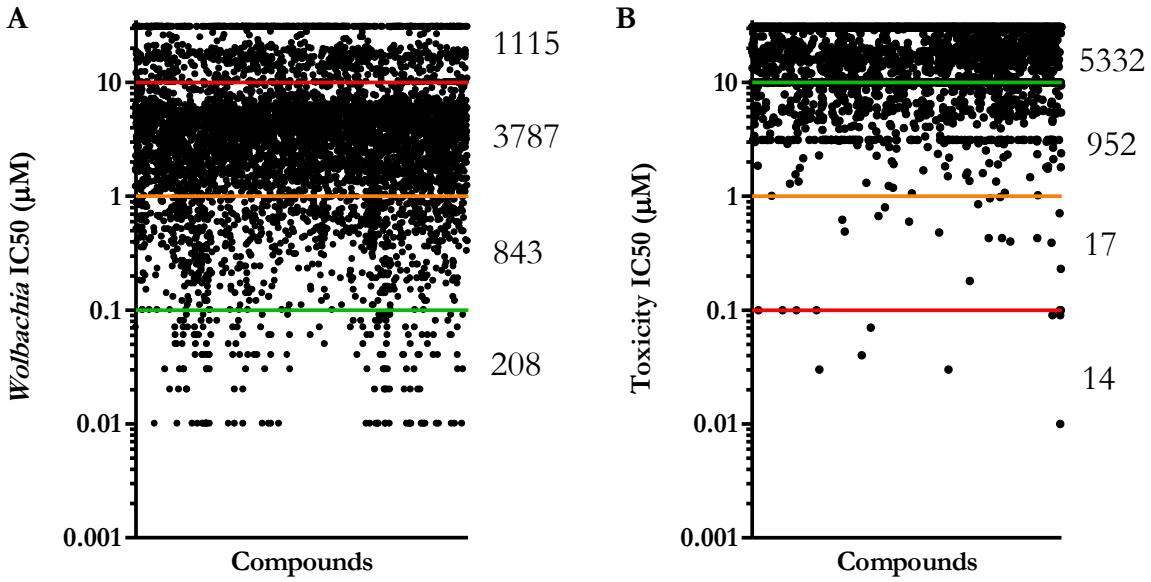

Figure 4.4. Overview of the secondary screen for both the anti-*Wolbachia* activity and mammalian cell toxicity. A| Scatterplot of the anti-*Wolbachia* activity for all compounds. Activity is related to highly active (green line <100 nM IC50), good activity (orange line <1 μM IC50) and inactive above the red line. **B| Scatter plot of the mammalian cell toxicity for the same compounds.** Compounds with less than 100 nM IC50 are highly toxic compared to no toxicity for those above 10 μM (green line).

medium (17 compounds, 0.1-1 µM) or high (14 compounds, <0.1 µM) toxicity (Figure 4.4). Following this work, mass confirmation and purity data were obtained by liquid chromatography mass spectrometry (LCMS) and combined with the above data to place the compounds into 'bins' to aid prioritisation (Table 4.1). Of the 5,960 compounds that were available to be analysed via LCMS, 5816 (97.6%) had their mass confirmed. Of those compounds with their mass confirmed, 372 (6.4%) had a purity <85%. Based on the binned data, we gained 579 pure compounds with no mammalian toxicity (>30 µM) but anti-*Wolbachia* IC50s less than 1 µM. Futhermore, 25 of these compounds were more active than doxycycline (IC50s <10 nM).

4.4.5. Secondary EC50 screen triaging

During the process of analysing our hits including 'binning' the data, a spin out company from AstraZeneca (Entasis Therapeutics) took the ownership of over 1,000 of the hit compounds, which included many of our highly active hits. This resulted in depleting our available hits from the ~6,000 down to ~4,900. The remaining ~4,900 compounds were clustered based on their chemical structures. Once complete, any clusters with less than three compounds were removed. The remaining clusters were prioritised based on a manual overall assessment of anti-*Wolbachia* activity, mammalian toxicity, cluster size and chemical structure as well as measured compound purity. This work was completed in collaboration between A·WOL and AstraZeneca chemists and resulted in 58 prioritised clusters containing 3-19 representatives covering in total 360 compounds. Two representatives from each cluster were provided by AstraZeneca for confirmation testing in the HCS Operetta® C6/36 (*w*AlbB) assay. The overall consistency between the two cell assays performed at two different laboratories is highly consistent ($p<0.0001$) (Figure 4.5). Therefore, to further prioritise these compounds as well as confirming anti-*Wolbachia* activity in nematodes a tertiary screen was developed to test these compounds in a larval worm assay (mf).

4.4.6. Tertiary screening – *in vitro* mf assay

All 115 representative compounds from the 58 clusters (2 per cluster with the exception of 1 cluster having a single representative) were tested at 5 µM in the mf screen (Figure 4.6). From this we obtained a 16.5% hit rate relating to strong hits for 19 compounds (>80%

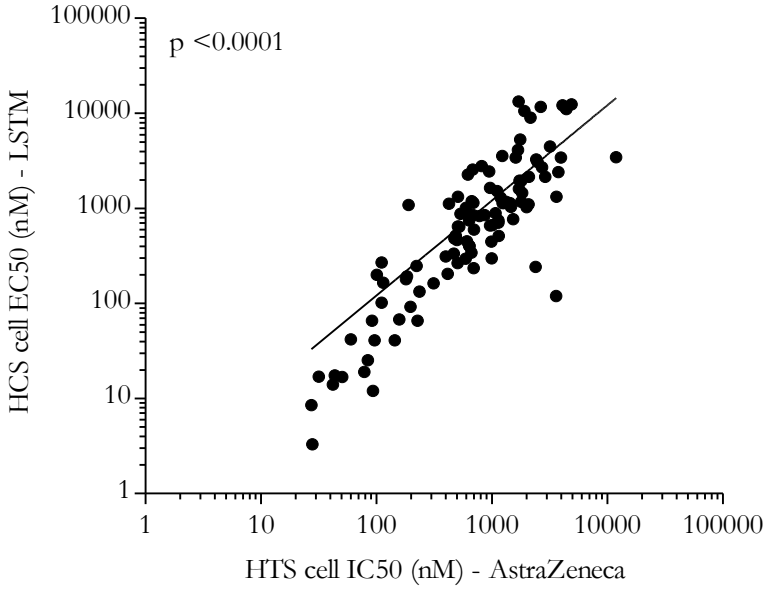

Figure 4.5. Scatter plot demonstrating the correlation between the HTS completed at AstraZeneca and the same compounds tested in the HCS at LSTM.

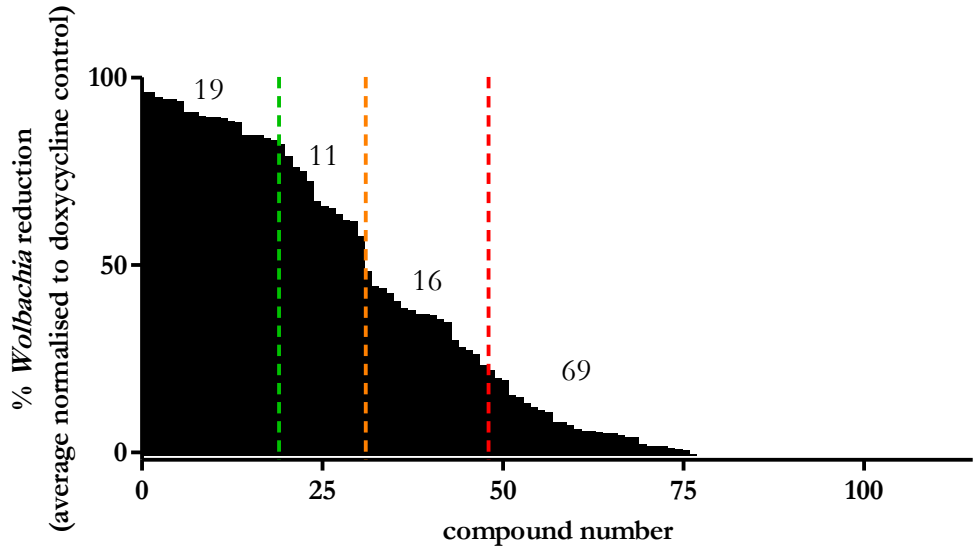

Figure 4.6. Overview of the 5 µM mf tertiary screen. All compounds to the left of the green vertical line have strong anti-*Wolbachia* activity (>80%). Compounds with reasonable activity (80-50%) fall between the green and orange lines. Compounds with minimal activity (50-25%) fall between the orange and red lines. All compounds to the right of the red line (25% *Wolbachia* reduction) are classed as not active. The total numbers of compounds per activity class are indicated above the bars.

reduction in *Wolbachia* compared to the doxycycline control). In addition, there were 11 compounds with good activity (9.5% with activity between 50-80% *Wolbachia* reduction) and 16 compounds with some activity (14% with activity between 25-50% *Wolbachia* reduction). Although 40% of compounds presented with at least some activity, the remaining 69 compounds (60%) were not classed as active (less than 25% *Wolbachia* reduction) which failed to replicate the activity observed in the cell line (>80% *Wolbachia* reduction at 10 µM and EC50s less than 5 µM).

Of all compounds screened, only 6 compounds (5%) presented with toxicity directly to the mf. Of these, 4 compounds had reduced motility (score of 2) and 2 compounds immobilised the mf (score of 0). None of this toxicity was observed for compounds with anti-*Wolbachia* activity with the exception of one compound. The latter compound SN1088844157, from cluster 22 had a motility score of 0 in duplicate assays, with *Wolbachia* reductions of 81 an 83%. Due to the direct anti-nematode activity observed this compound was not progressed.

The anti-*Wolbachia* active compounds were re-tested at 1 µM resulting in only 5 compounds from 3 clusters having no activity (<25% *Wolbachia* reduction normalised to doxycycline) (Figure 4.7). One compound/cluster had minimal activity (31% *Wolbachia* reduction). However, both representative compounds in two clusters had good activity (63-74% *Wolbachia* reduction). Most importantly, 7 compounds across 5 clusters were still

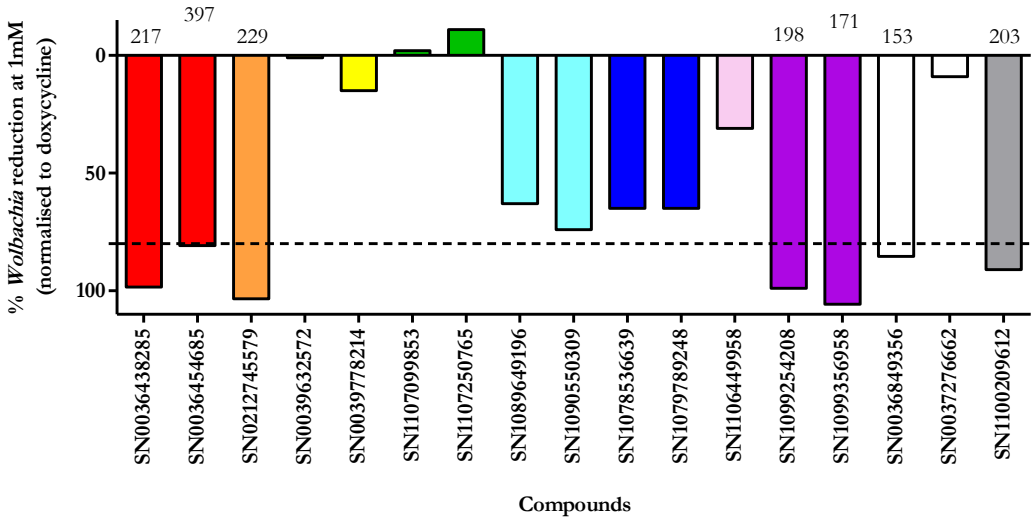

Figure 4.7. Mf screening at 1 µM for the most active clusters. Compounds with activity greater than 80% *Wolbachia* reduction (normalised to doxycycline) at 1 µM were tested in dose response and their EC50s (nM) are presented in text above each bar. The colours relate to the clusters: 30 red, 33 orange, 42 yellow, 53 green, 64 cyan, 139 blue, 142 pink, 150 purple, 242 white and 671 grey.

highly active at this lower dose (>80% *Wolbachia* reduction). These 7 compounds were tested at further doses of 200 and 4 nM to gain EC50s (Figure 4.7). All bar one compound had activity around 200 nM (range from 153 to 229 nM) which is similar to the activity we see for doxycycline (117 nM) and the A·WOL lead series (Template 1, AWZ 1066S: 227 nM (Hong et al. 2019)). However, they are not in the same activity range as the A·WOL lead candidate TylAMac™ (0.584 nM) (Taylor et al. 2019).

4.4.7. Oxazolidinones

4.4.7.1. Oxazolidinone secondary screening - High Content Cell Screen at LSTM

When the triaging stage was initiated, we revisited the known antibiotics which had been filtered out. It was found that there were no tetracyclines in the AstraZeneca library. However, there were: quinolones (53 hits), phenicols (9 hits), azaquinolones (12 hits), coumarols (1 active), mulins (1 active) and oxazolidinones (392 hits). The latter class with such high hit rate warranted a more detailed assessment. A compound from this class, linezolid, had been screened early in the A·WOL programme and presented with high cell toxicity, which is an issue widely experienced with this class of compounds (Bozdogan and Appelbaum 2004; Balasubramanian et al. 2014).

Cheminformatics was used to investigate the 392 anti-*Wolbachia* active oxazolidinones based on physicochemical properties and anti-*Wolbachia* activity in the single shot screen. In addition, compounds with known mammalian toxicity in AstraZeneca's historical screening were removed. This triaging resulted in the selection of 214 compounds, covering 19 out of the 21 sub-clusters these compounds had been characterised by. Compound management at AstraZeneca created ARPs of these compounds in a dose response range (30 µM to 1.5 µM in a 10-point curve) which were then tested at LSTM in the HCS assay. From this screen only 4 compounds presented with no activity at any doses (<50% of the doxycycline control). However, only 17 compounds presented with activity above >90% of doxycycline and were therefore suitable for EC50 analysis (ranging from 63 to 740 nM). The remaining majority of this class had medium activity (<90% >50% of the doxycycline control at any dose). Furthermore, the levels of toxicity were acceptable with 51 compounds presenting with no toxicity at any doses and from the remaining 161 compounds the toxicity was only at the higher concentrations (1-10 µM).

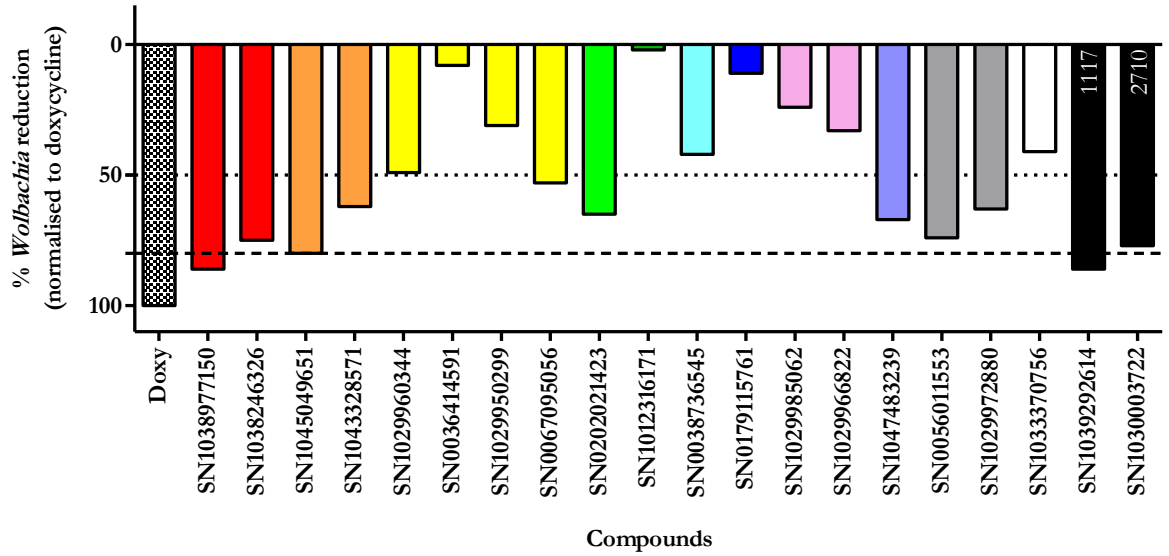

Figure 4.8. Tertiary mf *in vitro* screening of the 20 representatives from sub-clusters of the oxazolidinone class. There is a range in activity between the sub-clusters but strong activity (below the dashed line) in sub-clusters 1 (red), 2 (orange) and 12 (black) as well as clusters 4 (green), 9 (purple) and 10 (grey) to a lesser extent. Sub-clusters are coloured by: 1 red, 2 orange, 3 yellow, 4 green, 5 cyan, 6 blue, 8 pink, 9 purple, 10 grey, 11 white and 12 black. EC50s from powders supplied by AstraZeneca for sub-cluster 12 are written in text within the bar (nM).

4.4.7.2. Oxazolidinone tertiary screening - in vitro mf assay

Based on further cheminformatic analysis, 20 compounds were selected. This was based on ranking informed by the anti-*Wolbachia* activity in the HCS assay and predicted Drug Metabolism and Pharmacokinetics (DMPK) data from AstraZeneca (solubility, rat hepatocyte and human microsomal clearance). These 20 compounds (covering 11 out of the 19 originally selected sub-clusters) were tested in the mf assay at the standard 5 µM with no toxicity observed. Out of these 11 sub-clusters, only two compounds obtained >80% *Wolbachia* reduction when normalised to doxycycline (standard definition of a strong hit). These two compounds were within sub-clusters 1 and 12. The partner compound in these clusters both presented with >75% *Wolbachia* reduction (Figure 4.8). It is worth noting that these sub-clusters have respectively an additional 29 and 6 compounds in the AstraZeneca collection. A further 3 sub-clusters (2, 8 and 9) had activity between 50% to 80% *Wolbachia* reduction (classed as moderate activity) for both representatives. The remaining sub-clusters had low activity. Oxazolidinone sub-cluster 12 was selected as one of the final compounds released by AstraZeneca (discussed further in the next section) for further

Table 4.2. Overview of screening data for the lead compounds.

Cluster	Sample ID	HTS cell IC50 (nM)	HCS cell EC50 (nM)	mf EC50 (nM)	mf EC50 (nM) powder	
64	SN1089649196	228	68	-	2227	More active against cells than mf
	SN1090550309*	145	41	-	219	Consistent across all screens
30	SN0036438285	111	269	217	296	
242	SN0036849356	185	192	153	161	
139	SN1079789248	158	68	-	293	
	SN1078536639	594	296	-	271	Consistent within LSTM screens
671	SN1100209612	2391	242	203	164	
33	SN0212745579	684	2559	229	447	More active against mf than cells
150	SN1099254208	511	645	198	223	
	SN1099356958*	968	662	171	183	

A·WOL analysis. A powder stock was used to test this sub-cluster in dose response in the mf screen. The resulting EC50s were in the µM range (SN1030003722: 2.7 µM and SN1039292614: 1.1 µM), with only the top 5 µM dose producing moderate activity (52 and 67% *Wolbachia* reduction normalised to doxycycline). For this reason, the oxazolidinone cluster was deprioritised.

4.4.8. Structures and DMPK data on the lead clusters

Following the mf testing, AstraZeneca released 10 structures along with powders for confirmation mf testing. Table 4.2 shows this confirmation testing was successful, with the EC50s remaining around 200 nM. All but one compound are within 80 nM of the original EC50. The one exception still has a reasonable EC50 of 447 nM compared to the original EC50 of 229 nM. Table 4.2 also displays the comparison between the cell and mf screens. Cluster 30/242 (combined due to chemical similarity) and 139 show consistency across the different assays, as does cluster 671 except for the AstraZeneca secondary cell screen. However, of interest, clusters 33 and 150 are more active in the mf assay over the cell-based assays.

Table 4.3. Structures and DMPK properties of the lead compounds. The five axes in the radar plots represent: mf EC50 values (nM) (mf), rat hepatocytes clearance (µl min^{-1} 1 x 10^6 $cells^{-1}$) (Rat Heps), human microsome clearance (µl min^{-1} mg^{-1}) (Hum Mics), LogD7.4 (LogD) and log value of aqueous solubility in pH7.4 PBS buffer (µM) (LogS). The central blue shaded area within each radar plot, indicates acceptable DMPK properties for each of the five axes listed. The red (first compound in the cluster) or blue (second compound in the cluster) lines indicate the measured data for each compound. Comparison of the measured data to the acceptable DMPK properties (blue shaded area) can be used aid hit selection, as well as identifying areas which need to be addressed for the progression of the compound. * re-synthesised by A·WOL.

Cluster	Compound	Structure	Radar plot properties
30/ 242	SN0036849356	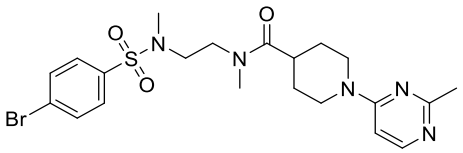	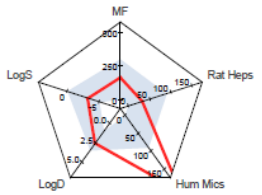
	SN0036438285	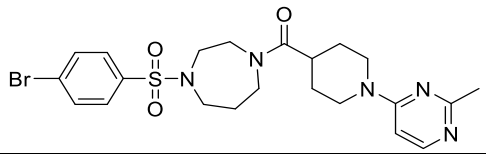	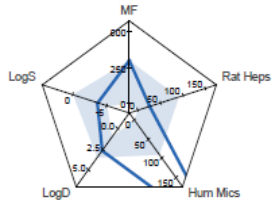
671	SN1088675911	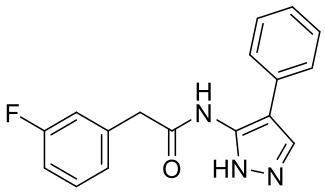	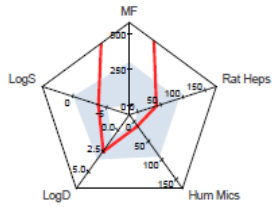
	SN1100209612	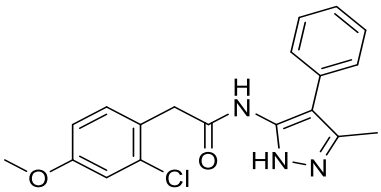	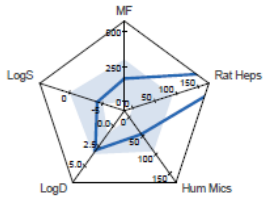
150	SN1099356958	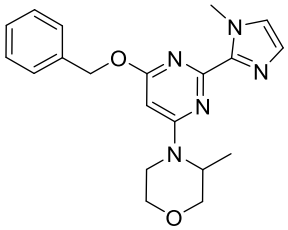	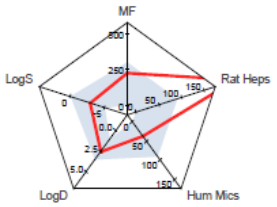
	SN1099254208	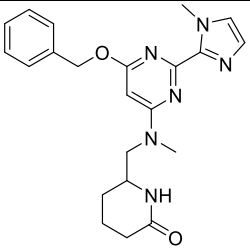	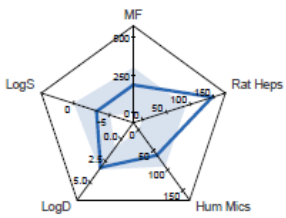

139	SN1078536639	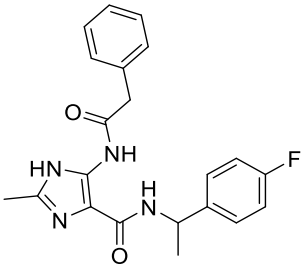	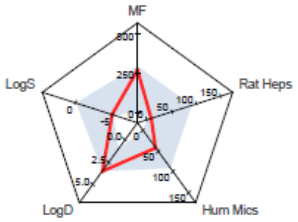
	SN1079789248	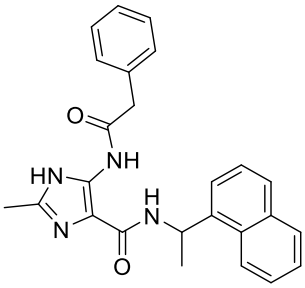	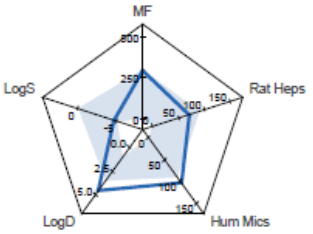
33	SN0212745579	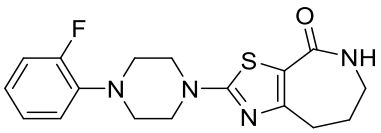	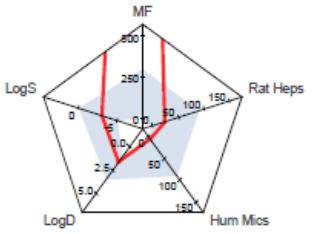
	SN0212747792	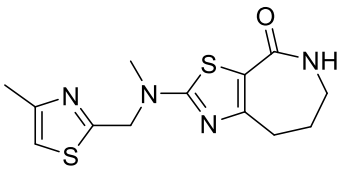	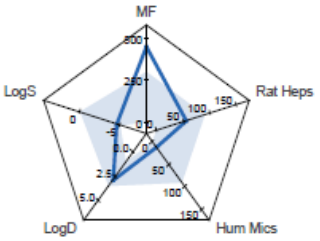
64	SN1089649196	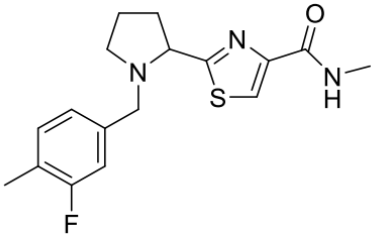	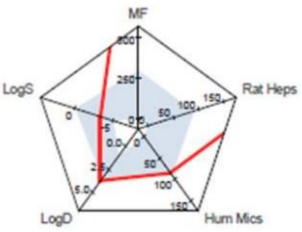
	SN1090550309	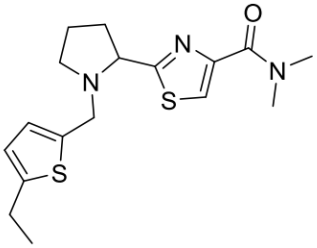	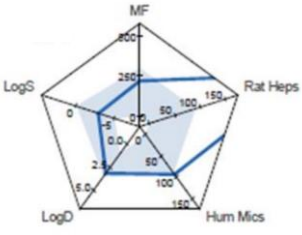

In addition, experimental DMPK including: rat hepatocyte clearance (Rat Heps), human microsome clearance (Hum Mics), LogD7.4 (LogD) and solubility (LogS) were outsourced. Alongside the 10 chemical structures, Table 4.3 displays radar plots which include the associated DMPK data and mf EC50s. The blue shaded area in the centre of the radar plot indicates acceptable DMPK properties for hit selection. Compounds from cluster 139 have very promising DMPK properties. The remaining clusters all have just one feature which would require optimising as part of an SAR chemistry programme to begin to develop these compounds towards lead compounds and potentially candidates.

4.4.9. *Wolbachia* time kill assay data in mf

To scrutinise these compounds further we carried out a time course assessment to reveal any difference in activity between these compounds compared to our existing A·WOL lead compounds. Figure 4.9 confirmed that all these compounds reach strong activity after 6 days but this is actually achieved by day 4. Similarly, when looking at shorter time points

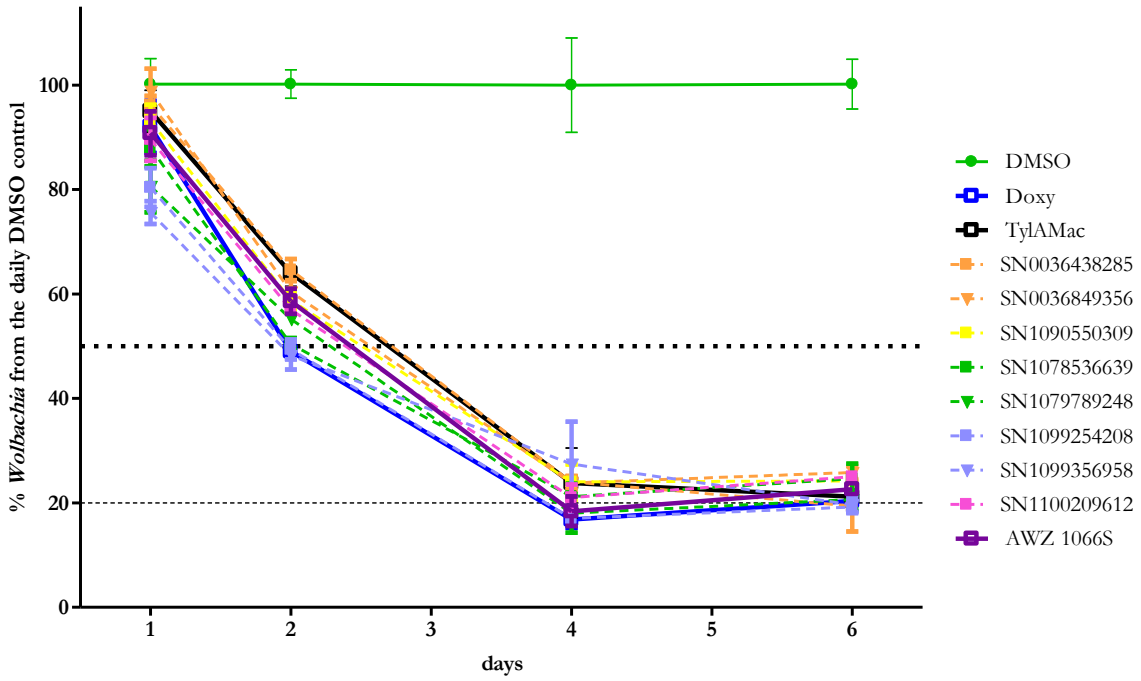

Figure 4.9. Time course for lead compounds in the mf assay. Compounds from clusters: 30/242 (orange), 64 (yellow), 139 (green), 150 (lilac) and 671 (pink) alongside A·WOL lead compounds doxycycline (blue), TylAMac™ (black) and AWZ 1066S (purple). Data represent the means with StDev error bars. The dotted horizontal line indicates the 50% reduction from the DMSO control. The dashed horizontal line indicates greater than 80% *Wolbachia* reduction from the DMSO control below this line (20% of the DMSO control).

there was little discrimination after 1 and 2 days of drug incubation with poor activity for all compounds (respective range: 0-25% and 35-50% *Wolbachia* reduction).

To further discriminate compounds, wash out experiments at earlier time points were assessed. Figure 4.10 shows that there is little activity seen after 4 hours for any compounds. However, after a 12 hour exposure clusters 30/242 and 139 are beginning to show activity superior to doxycycline but matching that of TylAMac™ (Taylor et al. 2019) and A·WOL's back-up candidate AWZ 1066S (Hong et al. 2019). Contrary to this, at day 1 clusters 30/242, 139 plus 64 and 671 match the good activity (50-80% *Wolbachia* reduction) of AWZ 1066S, superior to TylAMac™. Washing on day 2 further emphasises this pattern with all our compounds displaying strong activity close to 80% *Wolbachia* reduction across two repeat assays superior to AWZ 1066S (single assay repeat). In addition, when registered antibacterials known to have strong anti-*Wolbachia* activity are assessed with this two day wash out, none of them reach such strong activity (Table 4.4: 34-64% *Wolbachia* reduction). The 7 compounds within 5 clusters discovered as part of this screening campaign are, therefore, believed to be the fastest killing compounds the A·WOL programme has identified. No direct acting activity on the mf was observed for any of the compounds tested in this *Wolbachia* time kill screen.

Table 4.4. *Wolbachia* time kill assay in mf with compound wash out on day 2. These data represent the leading registered antibacterials with activity against *Wolbachia*. However, the activity is mediocre when tested in this assay. Low activity indicated in orange boxes (<50%) and mediocre activity in yellow boxes (50-80%).

Inhibitory activity	Target	Antibiotic	Mean % *Wolbachia* reduction normalised to DMSO	StDev	n
Protein synthesis	30S ribosomal subunit	doxycycline	48.5	7	3
		minocycline	34.1		
	Presumed 50S ribosomal subunit	TylAMac™	63.7	11	3
	Elongation factor G	fusidic acid	58.7	13	2
	DNA-directed RNA polymerase	rifampicin	38.8		1
DNA replication and repair	DNA gyrase	moxifloxacin	51.5		1

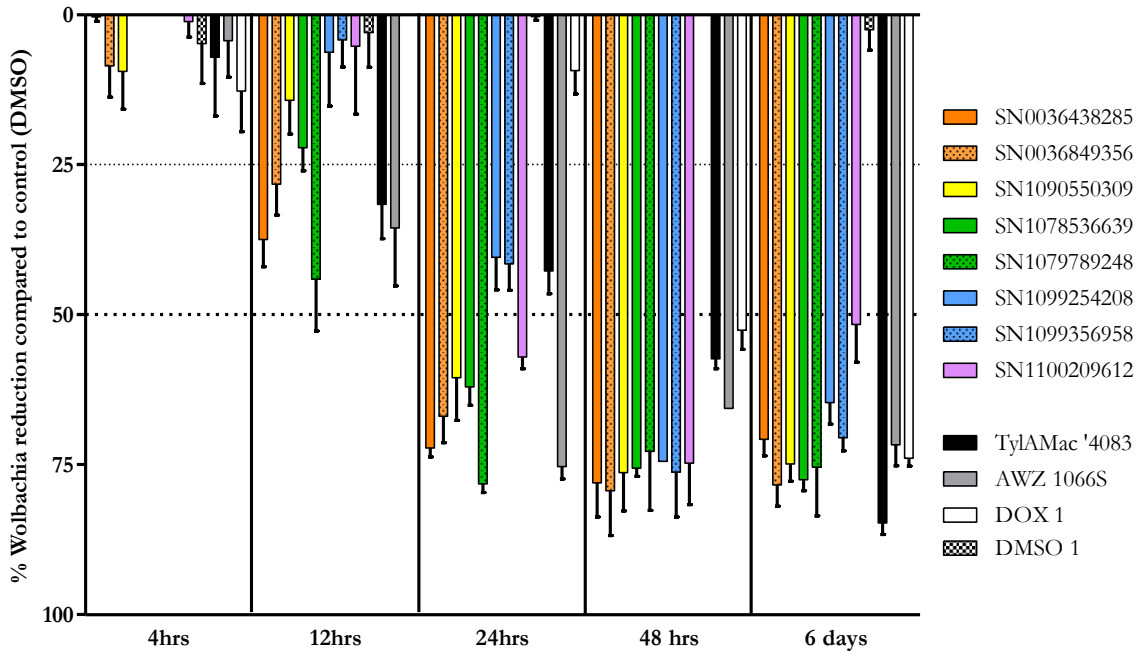

Figure 4.10. *Wolbachia* time kill assays in mf washed at 4, 12, 24 and 48 hours alongside the standard 6-day assay. The first three-time points are from the same assay with 48-hour and 6-day data presented as means from two separate assays (means with StDev error bars). The clusters are represented by colours: 30/242 (orange), 64 (yellow), 139 (green), 150 (blue) and 671 (purple) alongside A·WOL lead compounds doxycycline (white), TylAMac™ (black) and AWZ 1066S (grey).

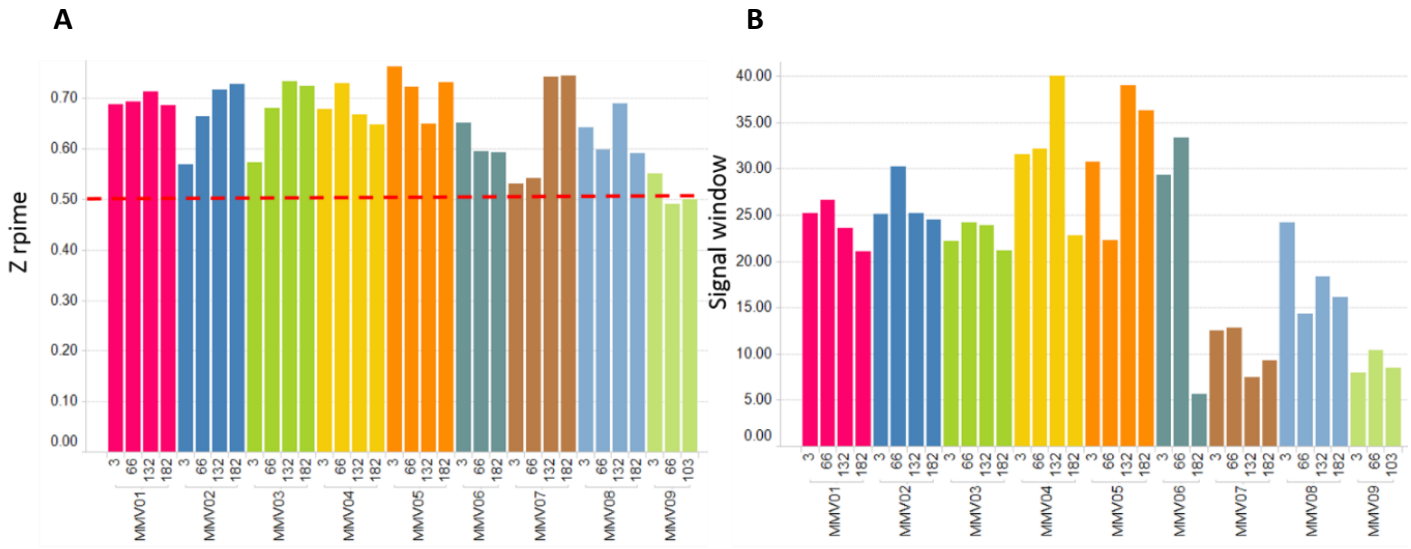

Figure 4.11. Performance analysis of the MMV HTS screen at AstraZeneca. A| Z prime analysis. All assays displayed good Z primes (> 0.45, the red dashed line indicated 0.5). **B|Signal window**. The signal window are reasonably strong for all assays (>5). The assay number is indicated in the x axis (MMV01-009, separated by colours), with each bar representing a QC plate result. The QC plate number (3, 66, 132, 182) indicates the position/plate number in the 182-plate batch (with the except of 103 plate batch size for MMV09).

4.4.10. MMV library screening

In addition to the screening of the AstraZeneca library we were given the opportunity to screen the remaining compounds from a 500,000-compound library from the Medicine for Malaria Venture (MMV) started using our previous screening strategy. After transferring this library and re-formatting the plates to create an assay ready format with the aid of AstraZeneca's compound management group, we were able to successfully complete this screen within just one month. Similar to the HTS library, we obtained good cell recoveries throughout the 9 assay runs (182 x 384-well batches), with *Wolbachia* levels above 50% of cells being infected. Throughout the screen we maintained good Z primes (>0.45) and signal window greater than 5, satisfying that we were confident in the results obtained (Figure 4.11).

The screening of this library had been initiated at LSTM on prioritised plates utilising the HCS cell assay. These plates had been prioritised based on iterative cheminformatic analysis with the aim of testing compounds which are different from that previously tested within the A·WOL programme. This method screened 51,725 compounds at 5 µM over 18 months with a primary hit rate of 0.44% (231 compounds). The remaining ~495,000 compounds screened at 10 µM within AstraZeneca resulted in 1,071 hits (0.22%). This 2-fold reduction in hit rate within the larger screening at AstraZeneca suggests a lot of the hits were identified by priority testing especially when considering the testing dose was double that of the HCS screen. In addition, the hit criterion for the HCS is much more stringent (>90% *Wolbachia* reduction) than the HTS assay (>80% *Wolbachia* reduction).

Following confirmation testing of the 231 hits from the HCS assay, 71 compounds maintained activity (31% confirmation rate), resulting in a reduction in the overall hit rate to 0.14% (~10-fold less than the AstraZeneca 1.3 million compound library). For the HTS assay, confirmation testing was not carried out due to the logistical challenge of manually sourcing hits from the original plates. Therefore, priority testing was used to select 80 compounds of interest to test in the HCS assay, of which only 5 maintained activity (confirmation rate of 6%). This is further evidence that the primary hit rate in the HTS is an over estimation compared to the HCS assay due to the lower testing dose and more stringent hit criteria.

4.5. Discussion

The successful completion of this screening campaign covering 1.3 million compounds was achieved due to the robust development and validation of this assay. The assay ready cryopreserved (ARC) method resulted in a stable cell and *Wolbachia* recovery, as well as highly consistent proliferation within the 7-day assay period for all 30 runs over a two-month period. This stability was repeated in the 1-month screening of the MMV library as well as the follow up dose response secondary screen of the AstraZeneca library hits. This stability is not only valuable to avoid assay failures, but also maintains consistency between assay runs, aiding the comparison across screens. This is important as work at LSTM has found that the *Wolbachia* level within cells can shift the EC50 results. The stability of this ARC method was reflected in the robust assay statistics with all assays presenting with a mean Z prime above 0.6 and signal to background greater than 20.

Across the AstraZeneca screen, no assays failed due to cell based rational with the low plate failure rate of 3% being due to either robotics or human errors. When considering the complexity of this assay including 2 weeks of cell proliferation, this demonstrates the robust development and validation of this assay.

The quality of the initial hit rate of >30,000 compounds was improved through the removal of 1/3 of the hits due to host cell toxicity. This showed the value of including the cell host toxicity read out, which although incurred time (2 minutes per plate) and cost penalties (Hoechst reagent) removed ~10,000 hits which were likely to be false positives. These false positives would have had a much greater time and cost penalty further down the pipeline line if they had not been removed at this primary screening stage. This final hit rate of 1.56% was just above the 1.28% hit rate predicted as part of the validation of the screen.

A further saving in attrition was the triaging early in the campaign to take forward only novel (no known antibacterials or structures previously worked on by A·WOL) compounds with good drug like properties. This cheminformatics analysis so early on in the process maximized the potential to identify diverse hits, as well as, steering the selection towards promising compounds for the initiation of a medicinal chemistry programme.

Following the secondary cell screen, a high hit rate was maintained, with 579 of these being pure (by LCMS) and not toxic to mammalian cells (IC50 >30 µM), but with anti-*Wolbachia*

activity at less than 1 µM concentration. One major set back was the loss of ~1000 (18%) of our active compounds to Entasis Therapeutics, a newly formed AstraZeneca spin-off company. The hits we lost access to may have been extremely interesting, especially when considering they were selected by a company who are working on next generation antibacterial therapies.

The further assessment of an mf screen was an important criterion to assess the hits in a more biologically relevant system. *B. malayi* whole worm screens applicable to drug discovery have been developed through automated analysis of motility (Marcellino et al. 2012; Storey et al. 2014; Lu et al. 2018). However, motility assessment does not indicate anti-*Wolbachia* activity, as the latter does not cause direct activity to the worm in the short term.

Although the cell line screening model is an extremely useful tool for hit identification at a medium to high throughput (which is not possible with mf), the further validation of these hits in the mf assays is of great value to reduce attrition. Firstly, it confirms activity against the nematode *Wolbachia* which is representative of that in the human parasite (*wBm* strain in *B. malayi*), rather than insect derived (*w*AlbB). Secondly, testing within a whole worm rather than the insect cell line eliminates compounds with indirect insect cell activity or barriers to drug penetration into the nematode. These disparities between the assays highlight the value of the tertiary mf screen to avoid attrition latter in the drug discovery pipeline with progression to more complex and time consuming *in vivo* studies. Work to date within the A·WOL Consortium displays a strong correlation between this mf *in vitro* assay and *in vivo* animal model testing. Therefore, even before the time kill data are considered, these compounds are extremely promising lead hits as they have good anti-*Wolbachia* activity which is predicted to correlate with *in vivo* models. In addition, the employment of cheminformatics has prioritised good chemical starting points as these hits are: pure, promising chemical structures, in cluster sizes greater than 3 and without toxicity in the mammalian cell counter-screen.

The final screen utilising a *Wolbachia* time kill assay revealed the most progressive data on these top 5 chemotypes. Activity after 2 days drug exposure is unprecedented with the exception of the A·WOL back-up lead candidate, AWZ 1066S (Hong et al. 2019). Therefore, the finding that one compound potentially has superior activity to AWZ 1066S after not only

24 hours but as early as 12 hours, suggests that we have found the fastest acting anti-*Wolbachia* compound identified to date. If this translates down the drug screening pipeline, it could result in a drug with a shortened treatment period than the A·WOL target product profile (TPP) of less than 7 days. Finally based on the cheminformatic analysis this fast-acting activity is shared by 5 distinct series, dramatically increasing the chemical diversity of the A·WOL drug portfolio.

These compounds have also been tested at LSTM against tuberculosis (TB), malaria and a small library of bacteria. These compounds show no activity in these assays suggesting they are *Wolbachia* specific. The benefit of this specificity would be to minimise 'off target' effects on microbiota and other bacterial pathogens. The next steps for these lead compounds is further prioritisation through cheminformatics as well as PKPD modelling to prioritise progression into *in vivo* models. In addition, investigations into the mode of action are on-going to further validate the improved *Wolbachia* kill dynamics.

The success of this project could not have been achieved without the close collaboration between AstraZeneca and A·WOL, through the sharing of knowledge and resources but also structural and additional data on these compounds. To put this HTS campaign into context, the screening of the primary 1.3 million compounds alone took just 2 months. The equivalent screen would have taken 35 years to complete in the A·WOL HCS assay. This project has created a paradigm shift in the number of compounds screened and hits identified, resulting in the discovery of superior lead compounds based on their kill rate in multiple diverse compound series.

This study was published in *Nature Communications* (Clare et al. 2019a).

4.6. Summary

- Through collaboration with AstraZeneca, our validated HTS assay was successfully deployed against their approximately 1.3 million compound library.
- This primary screen identified greater than 20,000 hit compounds.
- Cheminformatics were utilised to prioritise 6,000 compounds for secondary dose response screening, with the majority of these compounds maintaining good activity.
- From this secondary screen, 58 clusters were selected based on an overall manual assessment of anti-*Wolbachia* activity, mammalian toxicity, measured compound purity, cluster size, and chemical structure.
- Larval worm (mf) *in vitro* screening resulted in 5 clusters with similar EC50s to doxycycline and other A·WOL lead compounds.
- When further assessed in a *Wolbachia* time kill assay in mf with compounds removed on day 2, the ~70% *Wolbachia* reduction is maintained for these compounds in comparison to doxycycline which reduces to just ~50%.
- When tested after 24 hour of drug exposure all but one cluster maintains >25% reduction in *Wolbachia* compared to doxycycline at less than 10%.
- Two clusters reduce *Wolbachia* by >25% after just 12 hours of treatment.
- These results suggest that we have identified compounds with a faster rate of kill and potential different mode of action to current lead A·WOL compounds.

Chapter 5 : Summary and conclusions

5.1. Evolution of the A·WOL screening assays

This thesis has described the development and validation of two *in vitro* cellular screening assays (High Content Screen (HCS) Chapter 3 and High Throughput Screen (HTS) Chapter 4) and an *in vitro Wolbachia* time kill assay in mf. The development of these assays has provided improvements in the throughput and capacity of the original qPCR based *in vitro* cell screen developed at the beginning of the A·WOL Consortium in 2007. This assay was used to initiate a drug discovery programme through the creation of a stably infected *Wolbachia* cell line, C6/36 (*w*AlbB). This cell line was utilised as the starting point in the development of both the HCS and HTS assays. Through the HCS assay development, an increase in the *Wolbachia* load within the cells was established by increasing the FCS content of the media. This increase in *Wolbachia* load proved consistent and was important to achieve a robust screening assay through increasing the signal window between infected and uninfected cells. The visual microscopy element of the HCS screen was beneficial in enabling this development, as it allowed for the rapid assessment of *Wolbachia* loads within individual cells, compared to a time-consuming qPCR readout representing the overall cell population. In addition, this rapid *Wolbachia* load assessment allowed for cell populations to be either checked or selected before the initiation of the assay, thus reducing the number of failed assays providing a saving in both cost and time. During the HTS validation, the stability of the *Wolbachia* load was further progressed by creating a large-scale cryopreserved batch of cells, achieved through optimised methodology. This provided assay-ready cells, with consistent post-recovery host cell growth and *Wolbachia* loads. This improved stability has subsequently been built back into the ongoing screening in the HCS assay.

Although the cell line stability allowed for the development of both assays, the most important outcomes were the increase in throughput achieved by both screens. The original qPCR method initiated the A·WOL screening work, yet the throughput was low and labour intensive. Table 5.1 demonstrates the throughput of the BioFocus screen, which used this qPCR read out, with 10,000 compounds taking 12 months to be completed both in a primary screen with follow up secondary confirmation testing (Johnston et al. 2017). The monthly

Table 5.1. Throughput of the evolving A·WOL *in vitro* cell line screens. Primary screening is indicated by a *, with ** indicating secondary screening.

	qPCR screen	HCS screen	industrial scale HTS
	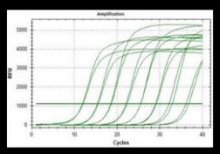	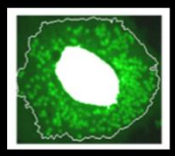	
	BioFocus * and **	MMV req. 1-4 * and **	AstraZeneca library * and 6,000**
Total compounds screened (time scale)	10,000 (12 months)	56,000 (18 months)	~1.3 million (3 months)
Monthly throughput	833	3111	433,333
		x4	x139

throughput of this work was 833 compounds completed by two/three FTEs due to the requirement for manual DNA extraction and qPCR analysis. In comparison, the employment of the HCS assay to screen 56,000 compounds from the MMV library at LSTM, in both primary and secondary dose response took 18 months by < 1 FTE. The increased screening of 3,111 compounds per month, scaled up the throughput 4-fold. In addition, the labour-intensive nature of this assay was reduced through the single staining method followed by automated imaging and analysis, which could now routinely complete dose response analysis. The completion of these 56,000 compounds would have taken over 5 years to complete in the qPCR screen.

The HTS assay, although more labour intensive (4 FTE) than the HCS assay, allowed for a dramatic shift in screening at a 139-fold increase in throughput from the HCS, through the completion of ~1.3 million compounds in just 3 months, including both primary and secondary dose response testing. To complete just the primary screen of the ~1.3 million compounds would have taken 35 years in the HCS assay. The throughput is further emphasised by the completion of the remaining MMV library in a single month, which would have taken over 13 years based on the time scale of the first 56,000 compounds.

Within the A·WOL drug discovery pipeline, hits from the primary cell assays described above are progressed into an *in vitro* worm assay. Historically, this utilised an *in vitro Onchocerca gutturosa* or *Brugia malayi* adult worm 5-day assay with qPCR and motility read outs. This

pipeline was later refined to maximise throughput by progressing hits from the HCS assay directly into newly validated *in vivo B. malayi* larval and adult mouse models (Johnston et al. 2014b). The nematode *in vitro* assays were subsequently removed to streamline the screening pathway as there was high consistency in activity from the primary HCS cell assay through to *in vitro* and *in vivo* nematode screens. However, once the A·WOL Consortium progressed to identifying new chemical entities the correlation became less consistent. Re-introduction of an *in vitro* mf nematode screen described in Chapter 4.3.8 identified that the disconnect was often between the cell line and nematode assays. This discrepancy could either be related to the origin of the *Wolbachia* (insect versus nematode) or related to the difference in the *Wolbachia* host e.g. the need to penetrate the cuticle of nematodes. The advantage of this *B. malayi* mf screen is the greater availability of mf from the in-house lifecycle over adult worms, thus providing a higher throughput over the previous *in vitro* adult worm screens. Reintroduction of this *in vitro* nematode screen avoids the unnecessary resources of progressing poor quality hits into low throughput *in vivo* screening (Taylor et al. 2014; Johnston et al. 2014b).

Although the standard *in vitro* mf screen can identify compounds with improved activity over 'gold' standards, it cannot predict compounds with a faster acting profile. The development of a *Wolbachia* time kill assay based on modifications of the cell line HCS assay, were unsuccessful due to the variable growth rates of *Wolbachia* between time points and compound treatments. As part of the HTS screen discussed in Chapter 4, this work was successfully revisited using *B. malayi* mf. Using the principles of the standard *B. malayi* mf screen, this novel *Wolbachia* time kill assay was able to assess for the first time compounds with more rapid activity compared to standard anti-*Wolbachia* drugs. This assay identified that after 2 days of treatment, followed by a 4 day wash out period, doxycycline reduced *Wolbachia* by less than 50% compared to a greater than 50% reduction for the A·WOL lead compounds TylAMac™ (Taylor et al. 2019), fusidic acid, moxifloxacin, AWZ 1066S (Hong et al. 2019) and the AstraZeneca lead series. This assay is now being utilised more readily, although limited to lead compounds, due to the low throughput of this screen, as it requires labour intensive wash steps as well as the prerequisite EC50 data from the standard mf screen. This time kill assay would therefore not replace the standard mf screen in the A·WOL pipeline.

In summary, the most recent evolution of the A·WOL screening funnel now includes a *Wolbachia* time kill screen prior to *in vivo* testing. This enables the identification of hits with equal or improved properties to the lead fast acting candidate AWZ 1066S. These improved hits are then tested at clinically relevant doses (informed by PK studies, as discussed in Chapter 1.3) *in vivo*, preliminary in a short term, L3-L4 larval *B. malayi* assay. Compounds with promising data are progressed into the longer-term adult *B. malayi* screen. Within the latter, the completion of further dose and time course refinement studies can ultimately inform clinical testing, with the ultimate aim of a less than 7 day, orally bioavailable and safe treatment. To address the requirement for a safe compound, in parallel further DMPK and toxicology studies are completed where necessary, providing information required for application for human trials.

5.2. Alternative anti-*Wolbachia in vitro* drug discovery assays

Another cell based 'high-throughput' assay for screening anti-*Wolbachia* drugs has been described in the literature (Serbus et al. 2012). In this assay a *Wolbachia* infected *Drosophila* cell line (JW18) was used, with the detection of *Wolbachia* reduction via fluorescent staining and whole cell imaging in a 384-well format. This is followed by customised software analysis which identifies "infected cells" based on the cytoplasmic DAPI fluorescent units per cell being above a determined threshold. A number of issues with this assay resulted in a lack of validation and concerns of the suitability of this assay for anti-*Wolbachia* drug discovery. Firstly, the lack of efficacy of doxycycline against the *Wolbachia* in this assay, suggests a problem either with the cell or *Wolbachia* strain. Furthermore, this results in the subsequent use of a *Wolbachia* uninfected cell population for the negative control rather than an anti-*Wolbachia* treatment control. Secondly, 'edge' effects appear to not have been taken into consideration and potentially compromise the outputs were controls are included in these outer wells. Thirdly, the misinterpretation of Z prime factor calculations suggests some of their plates would not be classed as valid. Finally, the use of concentrations of 100 µM are likely to deliver off-target toxicity and a high rate of false positive outputs. An example of this includes the false positive activity of albendazole sulfone, which is inactive in the HCS assay described in this thesis (Turner et al. 2017).

5.3. Comparison of the A·WOL screens to drug discovery for other fastidious bacteria

Mycobacterium tuberculosis (*Mtb*) is one of the top 10 causes of global mortality. The WHO estimates around 10 million new cases and 1.6 million deaths annually (World Health Organization 2018f). In several respects *Mtb* shares many of the challenges associated with drug screening against *Wolbachia,* such as a slow growing intracellular population, but has the added challenge of requiring containment facilities (Christophe et al. 2009; Zuniga et al. 2015). The main driver for *Mtb* drug discovery is also similar to *Wolbachia*, where the goal is to find faster acting treatments, which can be delivered in much shorter timeframes than the current lengthy 4-drug 6-month regimen.

Target-based screens have been widely used to identify new compound classes active against *Mtb* but have had limited success when translated to whole cell screens due to a variety of reasons relating to permeation, efflux and target accessibility (Payne et al. 2007; Ollinger et al. 2019). Phenotypic screens have been developed for *Mtb* drug discovery. These have exploited the availability of non-pathogenic related species such as *Mycobacterium smegmatis* or *Mycobacterium aurum* and fluorescent reporter strains of *Mtb* (Ollinger et al. 2019). The latter strains have allowed for the development of HTS assays utilising a variety of different culture conditions to try and mimic the complex environment inhabited by *Mtb* including nutrient starvation, stress and low oxygen (Ollinger et al. 2019). HTS campaigns completed at the Tuberculosis Antimicrobial Acquisition and Coordinating Facility (Ananthan et al. 2009; Maddry et al. 2009), have achieved the testing of 100,000 and 200,000 compounds against extracellular *Mtb*, using a single fluorescent read out. These HTS campaigns identified novel classes of compounds that display significant anti-*Mtb* activity, providing new leads for drug development.

Mtb drug screening activities have identified differences between extracellular and intracellular populations (within macrophages), including their growth rates, related drug efficacy as well as drug specificity (Christophe et al. 2009; Sundaramurthy et al. 2013; Stanley et al. 2014; Aljayyoussi et al. 2017b). These findings are of importance, as although the intracellular forms of *Mtb* are estimated at just 5% of the bacterial population in patients with an advanced disease state, this intracellular population is believed to cause the persistent form of this disease (Aljayyoussi et al. 2017b). This intracellular population is

at highest risk of developing drug resistance, due to the necessity for a longer treatment course required to kill this slower growing form. Consideration of the pathogen's environment has proved to be crucial to inform real life clinical implications for novel drug treatment (Christophe et al. 2009; Aljayyoussi et al. 2017b).

Overcoming the initial challenge of culturing *Mtb* (growth conditions in a category 3 laboratory) has allowed for the identification of novel compounds, using HTS methods, against extracellular *Mtb*. These achievements have also been aided by the benefit of minimal complexity in the read outs available for these assays, due to the ease of staining extracellular *Mtb* or availability of fluorescent strains. As previously discussed, however, hit compounds from extracellular screens should be tested against intracellular *Mtb*. Triaging of these extracellular hits could be built into the secondary screening phase of a drug discovery campaign, although this runs the risk of excluding compounds with a higher efficacy towards intracellular *Mtb.* Therefore, increasing the throughput of the HCS *Mtb* screens could be of great benefit to identify novel targets against persistent *Mtb.* HTS or HCS screening against other *Mycobacteria* such as the species causing leprosy (*Mycobacterium leprae*) and Buruli ulcer (*Mycobacterium ulcerans*) would also be of benefit, especially considering their reliance upon rifampicin within multidrug treatments (Scherr et al. 2016; Cambau et al. 2018; World Health Organization 2019a; 2019b).

The requirements of drugs to treat another persistent group of bacteria, *Chlamydia*, have similar properties to *Wolbachia*, related to their intracellular and intravacuolar lifestyle. These requirements include the need for the compounds to penetrate tissues and, pass through several eukaryotic membranes to reach the vacuoles harbouring the bacteria (Hahn et al. 2002; Hanski and Vuorela 2016). New treatments are required against this challenging bacterium, due to its propensity for persistence. Clinically *Chlamydia trachomatis* species replicate in both mucosal and conjunctival epithelial cells. The mucosal replicating form is the cause of the most common sexually transmitted disease (STD) worldwide (Dean 2009, World Health Organization 2016). The conjunctival infection causes trachoma, which is the most common form of preventable infectious blindness (Bhosai et al. 2012, World Health Organization 2019c). The airborne species, *Chlamydia pneumoniae* is responsible for 5-10% of community-acquired pneumonia cases and respiratory tract infections. This species is believed to infect the majority of people at least once in their lifetime, across both

developed and developing countries (Hahn et al. 2002, Hanski and Vuorela 2016). The intra-cellular/vacuolar complexity alongside the long development cycle and genetic intractability of *Chlamydia pneumoniae* has made large-scale drug discovery screening unattractive, slow and technically demanding (Hanski and Vuorela 2016). This has led to more focused and hypothesis-driven approaches. Following similarity searches to other bacterial genes, Alvesalo et al. (2006) used the crystal structure of a protein (ermC) from *Bacillus subtilis* which was homologous to a selected target for *C. pneumoniae*, which mediated essential functions in ribosomal methylation and structure. This homologous crystal structure was used to complete virtual screening of 300,000 compounds. From this screening 33 compounds were selected for growth inhibition assays on *C. pneumoniae*, resulting in eight previously unknown active compounds. Another virtual screening approach was undertaken by Karhu et al. (2016), based on the cheminformatic analysis of previously identified plant-based anti-chlamydial compounds, which identified 19 compounds clustered by physiochemical properties. Similarity searching of these properties was then carried out on a small natural product library. These prioritised compounds were subsequently tested *in vitro*, resulting in six new anti-chlamydial compounds, including mycophenolic acid (a clinically approved drug with known antibacterial activity). These virtual screening examples demonstrate the benefit of alternative approaches when HTS or HCS assays are not practical. Advances in computational screening of ultra-large virtual libraries have demonstrated the benefits of this approach in improving the efficiency and reducing the timeframes and costs associated with early stage conventional drug discovery (Gloriam 2019; Lyu et al. 2019).

A more recent global concern relating to fastidious bacteria, is the increased global distribution of scrub/bush typhus (Izzard et al. 2010; Balcells et al. 2011; Maina et al. 2016; Jiang and Richards 2018). This global disease is caused by intracellular bacterium *Orientia tsutsugamushi,* as well as newly identified *Orientia* species, which are transmitted through the bite of an infected larval *Leptotrombidium* mites (Luce-Fedrow et al. 2018; Centers for Disease Control of Prevention 2019; Tilak and Kunte 2019). Timely treatment with doxycycline leads to recovery, with more severe cases requiring rifampicin and azithromycin (Luce-Fedrow et al. 2018; Centers for Disease Control of Prevention 2019; Tilak and Kunte 2019). These drugs not only overlap with the treatment of the fastidious bacteria discussed

above but are also known to have anti-*Wolbachia* activity (doxycycline and rifampicin). Again, resistance is of concern and new drugs are required. Drug discovery is limited by the restriction to category 3 laboratories, and the requirement for intracellular culture (Luce-Fedrow et al. 2018). These challenges relate to those faced by anti-*Wolbachia*, *Mtb* and *Chlamydia* screening. However, there are many lessons that can be learned from the drug discovery discussed for these three bacterial groups. Firstly, the challenges of intracellular culture in a category 3 laboratory, does not make HTS screening for *Orientia* unfeasible, as seen by the completion of HTS campaigns for *Mtb* (category 3 laboratory) and *Wolbachia* (intracellular). Secondly, virtual screening can be utilised, for example through virtual screening of compounds against a crystal structure of a known target (Alvesalo et al. 2006) or computational screening of well characterised targets with ultra-large virtual libraries (Lyu et al. 2019). Alternatively, cheminformatics can be used to prioritise and limit the number of compounds to test *in vitro* (Karhu et al. 2017). The latter approach has been successfully implemented by the A·WOL Consortium as discussed in this thesis to prioritise the MMV library screening (Chapter 4.4.10) as well as the triaging of hits from the HTS screen (Chapter 4.3.7 and 4.4.5). Finally, there is the possibility that the similar niches (intracellular/intravacuolar) and slow growing nature of these fastidious bacteria, may provide an overlap in the activity of novel drugs or conserved drug targets. One example includes the anti-*Orientia* and anti-*Chlamydia* activity (Kock et al. 2018; Shima et al. 2018) for a novel compound, Corallopyronin A, which has known anti-*Wolbachia* activity (Schäberle et al. 2014). Testing of a selection of compounds from the A·WOL portfolio against phenotypic whole cell screens for *Orientia, Chlamydia* and *Mycobacteria* may prove fruitful and vice versa. Furthermore, although the diseases cause by these bacteria are principally an issue within developing countries, pharmaceutical development of such drugs could also be of benefit to pneumonia and the leading STDs, which are public health problems in developed countries.

5.4. The A·WOL drug portfolio expansion: 10 years on

Over the last decade the A·WOL drug portfolio has expanded dramatically. In 2007 the portfolio consisted of only doxycycline as a proof of concept (POC) treatment, as well as the

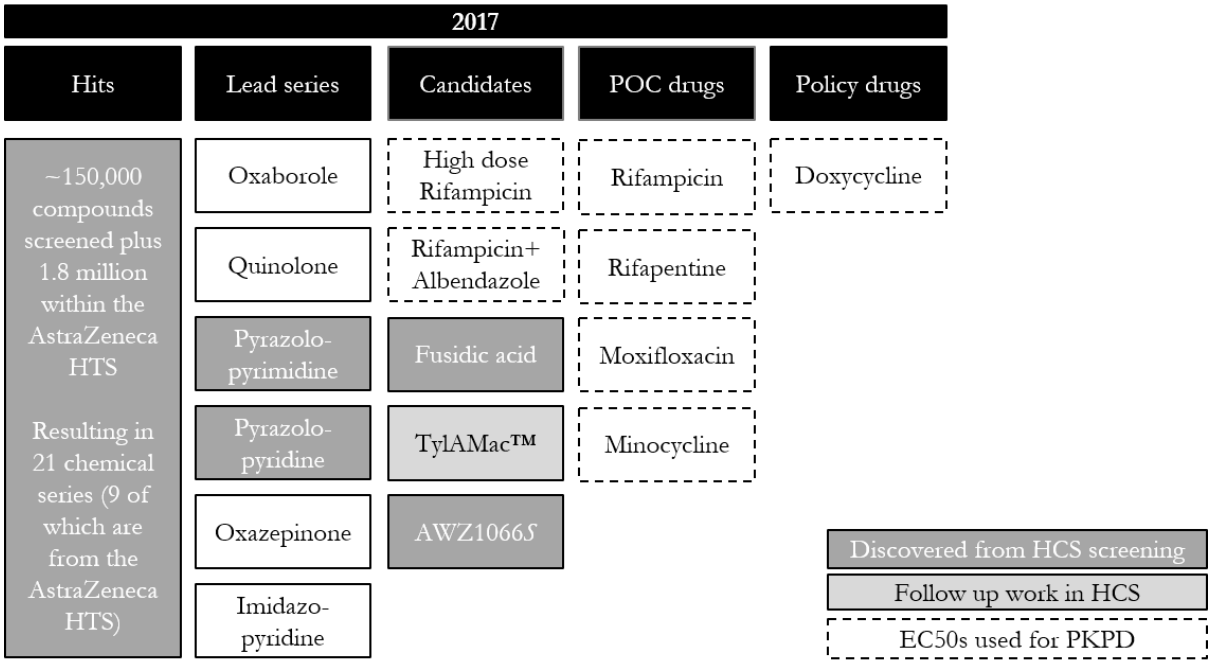

Figure 5.1. The A·WOL portfolio in 2017 highlighting the use of the HCS assay

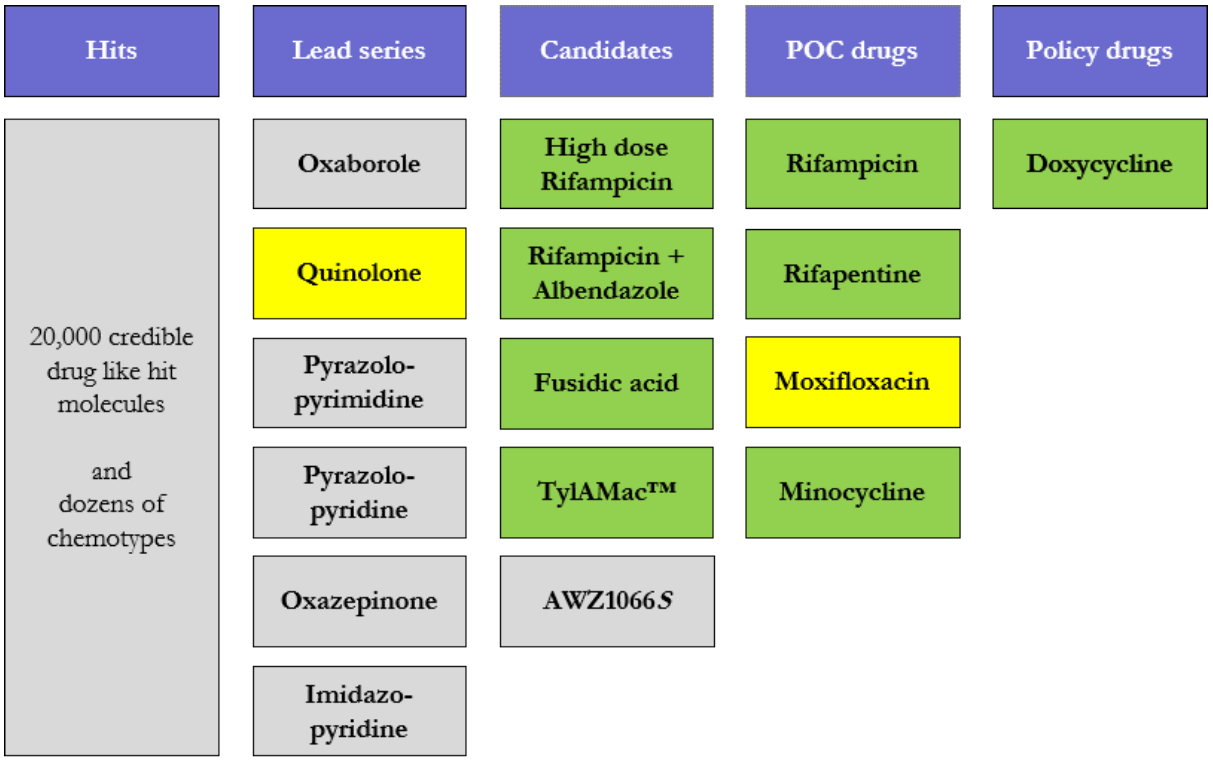

Figure 5.2. A·WOL Consortium's drug portfolio 2017 highlighted by drug target. Green boxes indicate compounds with predicted inhibition of protein synthesis. Yellow boxes indicate compounds with inhibition of DNA replication and repair, whilst those in grey boxes have unknown drug targets.

initiation of screening of medium sized compound libraries. By 2017, as seen in Figure 5.1, doxycycline had progressed to a policy drug alongside 4 new POC drugs: rifampicin (Specht et al. 2008), rifapentine, moxifloxacin and minocycline (Sharma et al. 2016). Furthermore the portfolio also has multiple candidates: high dose rifampicin (Aljayyoussi et al. 2017a), rifampicin in combination with albendazole (Turner et al. 2017), fusidic acid and the first designer macrofilaricidal drugs TylAMac™ (Taylor et al. 2019) and the back-up lead candidate AWZ 1066S (Hong et al. 2019). These designer drugs, as well as 6 additional lead series, have all been discovered through the paradigm shift in compound screening which the A·WOL Consortium has completed, soon to reach 2 million compounds resulting in over 21 anti-*Wolbachia* active chemical series. This growth of the portfolio has been accelerated by the new screens developed as part of this thesis. The HCS assay identified two lead series (pyrazolopyrimidine and pyrazolopyridine) and two candidates (fusidic acid and AWZ 1066S) from the screening of the MMV and BioFocus libraries (Figure 5.1). In addition, the ability for the HCS assay to be able to routinely produce EC50 analysis allowed for the initiation of a medicinal chemistry campaign as part of A·WOL II, which aided the progression of the lead candidate (TylAMac™ (Taylor et al. 2019)) as well as AWZ 1066S (Hong et al. 2019). The ability to create EC50 data also permitted PKPD modelling, which was used to recommend dosing regimens for the *in vivo* studies (as well as potential human trials) for A·WOL candidates (high dose rifampicin (Aljayyoussi et al. 2017a), rifampicin+albendazole (Turner et al. 2017), proof of concept drugs (rifampicin, rifapentine, moxifloxacin and minocycline (Sharma et al. 2016) and the policy drug (doxycycline). The future benefit to the portfolio of the HTS assay is clear with the identification (as discussed in Chapter 4.4.8) of 9 new chemical series, almost doubling the number of A·WOL series discovered over the last 10 years. In general, and in common with many antibiotic classes, the target for most anti-*Wolbachia* drugs in the A·WOL portfolio is the inhibition of protein synthesis (Figure 5.2). The tetracyclines (doxycycline and minocycline) target protein biosynthesis via the inhibition of the 30S subunit whilst the 50S subunit is predicted to be targeted by TylAMac™ (modified from the macrolide tylosin). The rifamycins (rifampicin and rifapentine) inhibit the early transcriptional stage of protein synthesis through DNA directed polymerase. However, fusidic acid inhibits the elongation factor G, later in the protein synthesis pathway (Figure 5.3). The only other known target within the A·WOL portfolio is the inhibition of DNA replication and repair identified through the quinolones (POC drug and lead series).

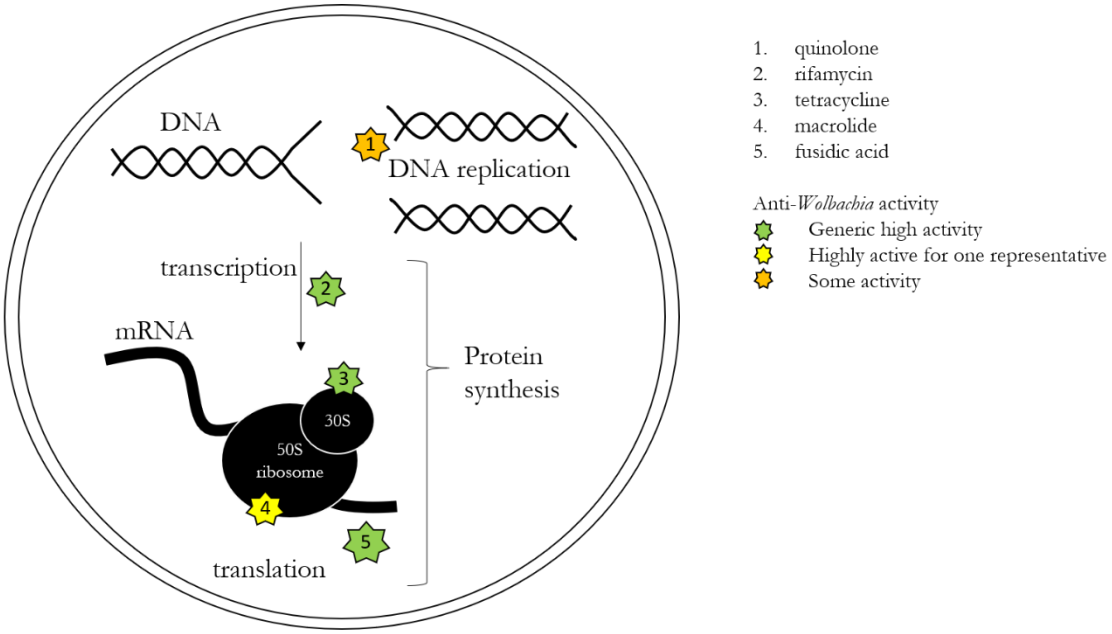

Figure 5.3. Predicted drug targets for registered antibiotics within the A·WOL drug portfolio.

However, the breadth of the portfolio drug targets maybe much wider as the drug target is unknown for the remaining candidate AWZ 1066S, all of the lead series except quinolones and the early stage series. Furthermore, the identification of the fast-acting series including AWZ 1066S and the AstraZeneca lead series, is suggestive of bactericidal activity. Experimental confirmation of this bactericidal activity is required and is likely to reveal a novel mode of action.

5.5. Future prospects for the A·WOL drug portfolio

A·WOL compounds which have progressed through to the drug candidate stage are awaiting progression for clinical development by DNDi. These product development partnerships (PDP) have become more common since the turn of the millennium. This model for the latter stages of the drug discovery process have certain advantages including spreading the financial cost and risk across a number of partners. In addition, as the return on investment is lives saved and not money made, commercial viability will not cause the failure of a drugs progress or cut short promising candidates. The final benefit is the collaborative aspect, which brings together knowledge from a variety of sources both academic and commercial as well as different expertise (Chatelain and Loset 2011; Burrows et al. 2014).

One of A·WOL's lead candidates, TylAMac™, has successfully completed phase I clinical trials and is progressing to phase II in a partnership between LSTM, Abbvie and DNDi (Taylor et al. 2019). The back-up drug candidate AWZ 1066S (Hong et al. 2019) is currently undergoing pre-clinical development.

Although target confirmation (fusidic acid, rifampicin and TylAMac™) or identification (AWZ 1066S) for these candidates is not a formal requirement, this work is currently being investigated within A·WOL to enable resistance management and monitoring. Protocols developed as part of this work for anti-*Wolbachia* target identification could subsequently be utilised against other A·WOL candidates or lead series. Target identification would be of interest to further profile A·WOL's "Fast Acting" lead chemotypes. These fast-acting chemotypes include AWZ 1066S and the 5 series discovered from the A·WOL-AstraZeneca screening campaign discussed in Chapter 4. All five of the A·WOL-AstraZeneca series show higher *Wolbachia* reduction after 2 days of treatment compared to all other A·WOL candidates. This difference in activity of the fast-acting compounds, as well as their chemically diversity suggests a potentially novel drug target. If a new anti-bacterial target is identified this could have benefits to the wider antibiotic discovery community.

The selection of additional candidates to the A·WOL portfolio would now be bench marked against the fast-acting back-up lead candidate AWZ 1066S. Work to date on the 5 series discovered from the A·WOL-AstraZeneca collaboration fall into this category. Progression of these hits will require PKPD modelling, followed by *in vivo* larval and adult *B. malayi* efficacy testing. These *in vivo* studies require the production of additional compound; therefore, prioritisation on the most promising candidates is necessary. As discussed in this thesis and by Clare et al. (2019a), cluster 139 (Cluster 5A in Clare et al. 2019a) is currently being prioritised. The prioritisation of Cluster 5A is due to its favourable chemistry for SAR and suitable all-round properties, including lower solubility and moderate metabolic stability, which are amenable to medicinal chemistry development. Progression of this series would first focus on the production of analogs to identified and further improved compounds from this series. Scale up in the quantity of the compounds would then allow testing in the *in vivo* screens.

5.6. Conclusion

This thesis presents the development of a HCS and HTS screen in a stably *Wolbachia* infected cell line, as well as the adaptation of a *B. malayi in vitro* assay to provide time kill data for the discovery of faster-acting anti-*Wolbachia* compounds. These assays have provided the tools to accelerate the A·WOL drug discovery programme. The HCS and HTS assays have increased the throughput of compound screening capabilities, which in turn has allowed for the expansion in the quantity of compounds being screened from thousands to millions. As well as providing abundant hits (>20,000) from the primary screening, these assays have provided EC50 data which has improved potency outputs to prioritise *in vivo* studies, but also the PKPD modelling to aid dosage predictions for *in vivo* studies and clinical trials. The development of the *Wolbachia* time kill assay in mf, has identified a new group of "Fast Acting" series including the 5 series from the final output of the HTS screening campaign. These 5 series have utilised all three assays and through cheminformatic prioritisation are predicted to further reduce the timeframe of anti-*Wolbachia* treatments.

The progression of these 5 fast-acting series of compounds will require additional medicinal chemistry and *in vivo* screening. Novel anti-*Wolbachia* treatments, especially those with a fast-acting profile (< 7 days) would be an important tool in three scenarios. Firstly, providing an alternative strategy for areas where existing MDA implementation is restricted e.g. co-endemicity with *Loa loa.* Secondly, in areas of high prevalence, hard to reach locations and in populations with evidence of sub-optimal responses to MDA drugs, where transmission hotspots required enhanced programmatic approaches. The curative nature of anti-*Wolbachia* treatments would dramatically shorten the number of rounds of treatments required in these settings and increasing the chances of elimination success. Thirdly, a curative drug regimen would improve 'mop-up' strategies in the endgame of during surveillance of endemic areas following the cessation of MDA programmes and provide a point-of-care treatment for individual cases.

References

African Programme for Onchocerciasis Control (APOC). 2012. Eighteenth session of the joint action forum. Final Communique. https://www.who.int/apoc/about/structure/jaf/Final_Communique_JAF_18_English_final_with_annexes.pdf?ua=1 [Accessed June 12, 2018].

Albers, A., Esum, M.E., Tendongfor, N., Enyong, P., Klarmann, U., Wanji, S., Hoerauf, A. and Pfarr, K. 2012. Retarded *Onchocerca volvulus* L1 to L3 larval development in the *Simulium damnosum* vector after anti-Wolbachial treatment of the human host. *Parasites & Vectors*, 5, 12.

Aliota, M.T., Walker, E.C., Yepes, A.U., Velez, I.D., Christensen, B.M. and Osorio, J.E. 2016a. The *w*Mel strain of *Wolbachia* reduces transmission of chikungunya virus in *Aedes aegypti*. *PLoS Neglected Tropical Diseases*, 10(4), e0004677.

Aliota, M.T., Peinado, S.A., Velez, I.D. and Osorio, J.E. 2016b. The *w*Mel strain of *Wolbachia* reduces transmission of Zika virus by *Aedes aegypti*. *Scientific Reports*, 6, 28792.

Aljayyoussi, G., Jenkins, V.A., Sharma, R., Ardrey, A., Donnellan, S., Ward, S.A. and Biagini, G.A. 2017a. Short-course, high-dose rifampicin achieves *Wolbachia* depletion predictive of curative outcomes in preclinical models of lymphatic filariasis and onchocerciasis. *Scientific Reports*, 8(1), 1384.

Aljayyoussi, G., Jenkins, V.A., Sharma, R., Ardrey, A., Donnellan, S., Ward, S.A. and Biagini, G.A. 2017b. Pharmacokinetic-pharmacodynamic modelling of intracellular *Mycobacterium tuberculosis* growth and kill rates is predictive of clinical treatment duration. *Scientific Reports*, 7(1), 502.

Alvesalo, J.K., Siiskonen, A., Vainio, M.J., Tammela, P.S. and Vuorela, P.M. 2006. Similarity based virtual screening: a tool for targeted library design. *Journal of Medicinal Chemistry*, 49(7), p.2353-2356.

Ananthan, S., Faaleolea, E.R., Goldman, R.C., Hobrath, J.V., Kwong, C.D., Laughon, B.E., Maddry, J.A., Mehta, A., Rasmussen, L., Reynolds, R.C. et al. 2009. High-throughput screening for inhibitors of *Mycobacterium tuberculosis* H37Rv. *Tuberculosis*, 89(5),

p.334-353.

Balasubramanian, V., Solapure, S., Iyer, H., Ghosh, A., Sharma, S., Kaur, P., Deepthi, R., Subbulakshmi, V., Ramya, V., Ramachandran, V. et al. 2014. Bactericidal activity and mechanism of action of AZD5847, a novel oxazolidinone for treatment of tuberculosis. *Antimicrobial Agents and Chemotherapy*, 58(1), p.495–502.

Balcells, M.E., Rabagliati, R., García, P., Poggi, H., Oddó, D., Concha, M., Abarca, K., Jiang, J., Kelly, D.J., Richards, A.L. et al. 2011. Endemic scrub typhus–like illness, Chile. *Emerging Infectious Diseases*, 17(9), p.1659-1663.

Bandi, C., Anderson, T.J., Genchi, C. and Blaxter, M.L. 1998. Phylogeny of *Wolbachia* in filarial nematodes. *Proceedings of the Royal Society of London: Series B, Biological Sciences*, 265(1413), p.2407-2413.

Bandi, C., McCall, J.W., Genchi, C., Corona, S., Venco, L. and Sacchi, L. 1999. Effects of tetracycline on the filarial worms *Brugia pahangi* and *Dirofilaria immitis* and their bacterial endosymbionts *Wolbachia*. *International Journal for Parasitology*, 29(2), p.357-364.

Bandi, C., Trees, A.J. and Brattig, N.W. 2001. *Wolbachia* in filarial nematodes: evolutionary aspects and implications for the pathogenesis and treatment of filarial diseases. *Veterinary Parasitology*, 98(1), p.215–238.

Barr, A.R. 1980. Cytoplasmic incompatibility in natural populations of a mosquito, *Culex pipiens* L. *Nature*, 283(5742), p.71-72.

Basáñez, M. G., Walker, M., Turner, H.C., Coffeng, L.E., de Vlas, S.J. and Stolk, W.A. 2016. River blindness: mathematical models for control and elimination. *Advances in Parasitology*, 94, p.247–341.

Bhosai, S.J., Bailey, R.L., Gaynor, B.D. and Lietman, T.M. 2012. Trachoma: an update on prevention, diagnosis, and treatment. *Current Opinion in Ophthalmology*, 23(4), p.288.

Bing, X.L., Xia, W.Q., Gui, J.D., Yan, G.H., Wang, X.W. and Liu, S.S. 2014. Diversity and evolution of the *Wolbachia* endosymbionts of *Bemisia* (*Hemiptera: Aleyrodidae*) whiteflies. *Ecology and Evolution*, 4(13), p.2714-2737.

Bland, J.M. and Altman, D. 1986. Statistical methods for assessing agreement between two methods of clinical measurement. *Lancet*, 327(8476), p.307-310.

Blagrove, M.S., Arias-Goeta, C., Di Genua, C., Failloux, A.B. and Sinkins, S.P. 2013. A *Wolbachia w*Mel transinfection in *Aedes albopictus* is not detrimental to host fitness and inhibits chikungunya virus. *PLoS Neglected Tropical Diseases*, 7(3), e2152.

Boatin, B. 2008. The onchocerciasis control programme in West Africa (OCP). *Annals of Tropical Medicine & Parasitology*, 102(sup1), p.13-17.

Bosshardt, S. C., McCall, J.W., Coleman, S.U., Jones, K.L., Petit, T.A. and Klei, T.R. 1993. Prophylactic activity of tetracycline against *Brugia pahangi* infection in jirds (*Meriones unguiculatus*). *The Journal of Parasitology*, 79(5), p.775-777.

Botto, C., Basañez, M.G., Escalona, M., Villamizar, N.J., Noya-Alarcón, O., Cortez, J., Vivas-Martínez, S., Coronel, P., Frontado, H., Flores, J., et al. 2016. Evidence of suppression of onchocerciasis transmission in the Venezuelan Amazonian focus. *Parasites & Vectors*, 9, 40.

Boussinesq, M., Fobi, G. and Kuesel, A.C. 2018. Alternative treatment strategies to accelerate the elimination of onchocerciasis. *International Health*, 10, p.40–48.

Bozdogan, B. and Appelbaum, P. C. 2004. Oxazolidinones: Activity, mode of action, and mechanism of resistance. *International Journal of Antimicrobial Agents*, 23(2), p.113–119.

Burnham, G. 1998. Onchocerciasis. *Lancet*, 351, p.1341–6.

Burrows, J. N., Elliott, R.L., Kaneko, T., Mowbray, C.E. and Waterson, D. 2014. The role of modern drug discovery in the fight against neglected and tropical diseases. *MedChemComm*, 5(6), p.688-700.

Büttner, D. W., Wanji, S., Bazzocchi, C., Bain, O. and Fischer, P. 2003. Obligatory symbiotic *Wolbachia* endobacteria are absent from *Loa loa*. *Filaria Journal*, 2(1), 10.

Cambau, E., Saunderson, P., Matsuoka, M., Cole, S.T., Kai, M., Suffys, P., Rosa, P.S., Williams, D., Gupta, U.D., Lavania, M. et al. 2018. Antimicrobial resistance in leprosy: results of the first prospective open survey conducted by a WHO surveillance network for the

period 2009–15. *Clinical Microbiology and Infection*, 24, p.1305-1310.

Cano, J., Rebollo, M.P., Golding, N., Pullan, R.L., Crellen, T., Soler, A., Kelly-Hope, L.A., Lindsay, S.W., Hay, S.I., Bockarie, M.J., et al. 2014. The global distribution and transmission limits of lymphatic filariasis: Past and present. *Parasites & Vectors*, 7, 466.

Centers for Disease Control and Prevention (CDC). 2019. Scrub Typhus. https://www.cdc.gov/typhus/scrub/index.html#treatment. [Accessed February 12, 2019].

Chatelain, E. and Loset, J. R. 2011. Drug discovery and development for neglected diseases: The DNDi model. *Drug Design, Development and Therapy*, 5, p.175–181.

Christophe, T., Jackson, M., Jeon, H.K., Fenistein, D., Contreras-Dominguez, M., Kim, J., Genovesio, A., Carralot, J.P., Ewann, F., Kim, E.H., et al. 2009. High content screening identifies decaprenyl-phosphoribose 2′ epimerase as a target for intracellular antimycobacterial inhibitors. *PLoS Pathogens*, 5(10), e1000645.

Clare, R. H., Cook, D.A., Johnston, K.L., Ford, L., Ward, S.A. and Taylor, M.J. 2014. Development and validation of a high-throughput anti-*Wolbachia* whole-cell screen: a route to macrofilaricidal drugs against onchocerciasis and lymphatic filariasis. *Journal of Biomolecular Screening*, 20(1), p.64–69.

Clare, R.H., Bardelle, C., Harper, P., Hong, W.D., Börjesson, U., Johnston, K.L., Collier, M., Myhill, L., Cassidy, A., Plant, D., Plant, H., et al. 2019a. Industrial scale high-throughput screening delivers multiple fast acting macrofilaricides. *Nature Communications*, 10(1), 11.

Clare, R.H., Clark, R., Bardelle, C., Harper, P., Collier, M., Johnston, K.L., Plant, H., Plant, D., McCall, E., Slatko, B.E., et al. 2019b. Development of a high-throughput cytometric screen to identify anti-*Wolbachia* compounds: the power of public–private partnership. *SLAS Discovery*, 2019, in press

Clark, R., Harper, P. and Wigglesworth, M. 2013. Technological and sociological advances in HTS: evolution and revolution? *European Pharmaceutical Review*, 18(6), p.55–60.

Convit, J., Schuler, H., Borges, R., Olivero, V., Domínguez-Vázquez, A., Frontado, H. and

Grillet, M.E. 2013. Interruption of *Onchocerca volvulus* transmission in Northern Venezuela. *Parasites & Vectors*, 6, 289.

Cruz, D. J. M., Koishi, A.C., Taniguchi, J.B., Li, X., Bonotto, R.M., No, J.H., Kim, K.H., Baek, S., Kim, H.Y., Windisch, M.P., et al. 2013. High content screening of a kinase-focused library reveals compounds broadly-active against dengue viruses. *PLoS Neglected Tropical Diseases*, 7(2), e2073.

Darby, A.C., Armstrong, S.D., Bah, G.S., Kaur, G., Hughes, M.A., Kay, S.M., Koldkjær, P., Rainbow, L., Radford, A.D., Blaxter, M.L. and Tanya, V.N. 2012. Analysis of gene expression from the *Wolbachia* genome of a filarial nematode supports both metabolic and defensive roles within the symbiosis. *Genome Research*. 22, p.2467-2477.

De Rycker, M., Rigoreau, L., Dowding, S. and Parker, P.J. 2009. A high-content, cell-based screen identifies micropolyin, a new inhibitor of microtubule dynamics. *Chemical Biology and Drug Design*, 73(6), p.599–610.

De Rycker, M., Hallyburton, I., Thomas, J., Campbell, L., Wyllie, S., Joshi, D., Cameron, S., Gilbert, I.H., Wyatt, P.G., Frearson, J.A., et al. 2013. Comparison of a high-throughput high-content intracellular *Leishmania donovani* assay with an axenic amastigote assay. *Antimicrobial Agents and Chemotherapy*, 57(7), p.2913–2922.

De Rycker, M., Baragaña, B., Duce, S.L. and Gilbert, I.H. 2018. Challenges and recent progress in drug discovery for tropical diseases. *Nature*, 559, p.498–506.

Dean, D. 2009. *Chlamydia trachomati*s today: treatment, detection, immunogenetics and the need for a greater global understanding of *chlamydial* disease pathogenesis. *Drugs of today*, 45(Suppl B), p.25-31.

Debrah, A. Y. 2006a. Doxycycline reduces plasma VEGF-C/sVEGFR-3 and improves pathology in lymphatic filariasis. *PLoS Pathogens*, 2(9), e92.

Debrah, A. Y., Mand, S., Marfo-Debrekyei, Y., Larbi, J., Adjei, O. and Hoerauf, A.. 2006b. Assessment of microfilarial loads in the skin of onchocerciasis patients after treatment with different regimens of doxycycline plus ivermectin. *Filaria Journal*, 5, p.1–10.

Debrah, A. Y., Mand, S., Marfo-Debrekyei, Y., Batsa, L., Pfarr, K., Buttner, M., Adjei, O.,

Buttner, D. and Hoerauf, A. 2007. Macrofilaricidal effect of 4 weeks of treatment with doxycycline on *Wuchereria bancrofti*. *Tropical Medicine & International Health*, 12(12), p.1433–1441.

Debrah, A. Y., Mand, S., Marfo-Debrekyei, Y., Batsa, L., Pfarr, K., Lawson, B., Taylor, M., Adjei, O. and Hoerauf, A. 2009. Reduction in levels of plasma vascular endothelial growth factor-A and improvement in hydrocele patients by targeting endosymbiotic *Wolbachia* sp. in *Wuchereria bancrofti* with doxycycline. *The American Journal of Tropical Medicine and Hygiene*, 80(6), p.956–63.

Debrah, A. Y., Mand, S., Marfo-Debrekyei, Y., Batsa, L., Albers, A., Specht, S., Klarmann, U., Pfarr, K., Adjei, O. and Hoerauf, A. et al. 2011. Macrofilaricidal activity in *Wuchereria bancrofti* after 2 weeks treatment with a combination of rifampicin plus doxycycline. *Journal of Parasitology Research*, 2011, p.1–9.

Debrah, A. Y., Specht, S., Klarmann-Schulz, U., Batsa, L., Mand, S., Marfo-Debrekyei, Y., Fimmers, R., Dubben, B., Kwarteng, A., Osei-Atweneboana, M., et al. 2015. Doxycycline leads to sterility and enhanced killing of female *Onchocerca volvulus* worms in an area with persistent microfilaridermia after repeated ivermectin treatment: A randomized, placebo-controlled, double-blind trial. *Clinical Infectious Diseases*, 61(4), p.517–26.

Dobson, S.L., Marsland, E.J., Veneti, Z., Bourtzis, K. and O'Neill, S.L. 2002. Characterization of *Wolbachia* host cell range via the *in vitro* establishment of infections. *Applied and Environmental Microbiology*, 68(2), p.656-660.

Dreyer, G., Noroes, J., Figueredo-Silva, J. and Piessens, W.F. 2000. Pathogenesis of lymphatic disease in Bancroftian filariasis: a clinical perspective. *Parasitology Today*, 16(12), p.544-548.

Drugs for Neglected Diseases Initiative. 2018. Portfolio. *www.dndi.org/diseases-projects/portfolio*. [Accessed October 20, 2018].

Dutra, H.L.C., Rocha, M.N., Dias, F.B.S., Mansur, S.B., Caragata, E.P. and Moreira, L.A. 2016. *Wolbachia* blocks currently circulating Zika virus isolates in Brazilian *Aedes aegypti* mosquitoes. *Cell Host & Microbe*, 19(6), p.771-774.

Eisai. 2014. Access to Medicines. *http://atm.eisai.co.jp/english/)*. [Accessed November 11,

2018].

Engel, J. C., Ang, K.K., Chen, S., Arkin, M.R., McKerrow, J.H. and Doyle, P.S. 2010. Image-based high-throughput drug screening targeting the intracellular stage of *Trypanosoma cruzi*, the agent of Chagas' disease. *Antimicrobial Agents and Chemotherapy*, 54(8), p.3326–3334.

Fallon, A.M. 2008. Cytological properties of an *Aedes albopictus* mosquito cell line infected with *Wolbachia* strain *w*AlbB. *In Vitro Cellular & Developmental Biology-Animal*, 44(5-6), p.154-161.

Fallon, A.M. and Witthuhn, B.A. 2009. Proteasome activity in a naïve mosquito cell line infected with *Wolbachia pipientis w*AlbB. *In Vitro Cellular & Developmental Biology-Animal*, 45(8), p.460-466.

Fenollar, F., La Scola, B., Inokuma, H., Dumler, J.S., Taylor, M.J. and Raoult, D. 2003a. Culture and phenotypic characterization of a *Wolbachia pipientis* isolate. *Journal of Clinical Microbiology*, 41(12), p.5434-5441.

Fenollar, F., Maurin, M. and Raoult, D. 2003b. *Wolbachia pipientis* growth kinetics and susceptibilities to 13 antibiotics determined by immunofluorescence staining and real-time PCR. *Antimicrobial Agents and Chemotherapy*, 47(5), p.1665-1671.

Fischer, K., Beatty, W.L., Jiang, D., Weil, G.J. and Fischer, P.U. 2011. Tissue and stage-specific distribution of *Wolbachia* in *Brugia malayi*. *PLoS Neglected Tropical Diseases*, 5(5), e1174.

Fischer, P. U., King, C.L., Jacobson, J.A. and Weil, G.J. 2017. Potential value of triple drug therapy with ivermectin, diethylcarbamazine, and albendazole (IDA) to accelerate elimination of lymphatic filariasis and onchocerciasis in Africa. *PLoS Neglected Tropical Diseases*, 11(1), e0005163.

Foster, J., Ganatra, M., Kamal, I., Ware, J., Makarova, K., Ivanova, N., Bhattacharyya, A., Kapatral, V., Kumar, S., Posfai, J. et al. 2005. The *Wolbachia* genome of *Brugia malayi*: endosymbiont evolution within a human pathogenic nematode. *PLoS Biology*, 3(4), e121.

Francis, H., Awadzi, K. & Ottesen, E. A. 1985. The mazzotti reaction following treatment infection intensity. *American Journal of Tropical Medicine and Hygiene*, 34(3), p.529–536.

Frempong, K. K., Walker, M., Cheke, R.A., Tetevi, E.J., Gyan, E.T., Owusu, E.O., Wilson, M.D., Boakye, D.A., Taylor, M.J., Biritwum, N.K., et al. 2016. Does increasing treatment frequency address suboptimal responses to ivermectin for the control and elimination of river blindness? *Clinical Infectious Diseases*, 62(11), p.1338–1347.

Frentiu, F.D., Robinson, J., Young, P.R., McGraw, E.A. and O'Neill, S.L. 2010. *Wolbachia*-mediated resistance to dengue virus infection and death at the cellular level. *PLoS One*, 5(10), e13398.

Gardon, J., Gardon-Wendel, N., Kamgno, J., Chippaux, J.P. and Boussinesq, M. 1997. Serious reactions after mass treatment of onchocerciasis with ivermectin in an area endemic for *Loa loa* infection. *Lancet*, 350(9070), p.18-22.

Gayen, P., Nayak, A., Saini, P., Mukherjee, N., Maitra, S., Sarkar, P. and Babu, S.P.S. 2013. A double-blind controlled field trial of doxycycline and albendazole in combination for the treatment of Bancroftian filariasis in India. *Acta Tropica*, 125(2), p.150–156.

Gedge, L. M., Bettis, A.A., Bradley, M.H., Hollingsworth, T.D. and Turner, H.C. 2018. Economic evaluations of lymphatic filariasis interventions: a systematic review and research needs. *Parasites & Vectors*, 11, 75.

Geary, T.G., Mackenzie, C.D. and Silber, S.A. 2019. Flubendazole as a macrofilaricide: history and background. *PLoS Neglected Tropical Diseases*, 13(1), e0006436.

Glaser, R.L. and Meola, M.A. 2010. The native *Wolbachia* endosymbionts of *Drosophila melanogaster* and *Culex quinquefasciatus* increase host resistance to West Nile virus infection. *PLoS One*, 5(8), e11977.

Gloriam, D.E. 2019. Bigger is better in virtual drug screens. *Nature*, 566(7743), p.193-194.

Glowska, E., Dragun-Damian, A., Dabert, M. and Gerth, M. 2015. New *Wolbachia* supergroups detected in quill mites (*Acari: Syringophilidae*). *Infection, Genetics and Evolution*, 30, p.140-146.

Griffiths, K. G., Alworth, L.C., Harvey, S.B. and Michalski, M.L. 2010. Using an intravenous catheter to carry out abdominal lavage in the gerbil. *Lab Animal*, 39(5), p.143-148.

Grobler, Y., Yun, C.Y., Kahler, D.J., Bergman, C.M., Lee, H., Oliver, B. and Lehmann, R. 2018. Whole genome screen reveals a novel relationship between *Wolbachia* levels and *Drosophila* host translation. *PLoS Pathogens*, 14(11), e1007445.

Gustavsen, K. M., Colatrella, B.D. and McCoy, T. 2018. For as long as necessary: examining 30 years of MSD's focus on achieving elimination of onchocerciasis and lymphatic filariasis. *International Health*, 10, i3–i6.

Hahn, D.L., Azenabor, A.A., Beatty, W.L. and Byrne, G.I. 2002. *Chlamydia pneumoniae* as a respiratory pathogen. *Frontiers in Bioscience*, 7, e66-76.

Hall, L.R. and Pearlman, E. 1999. Pathogenesis of onchocercal keratitis (river blindness). *Clinical Microbiology Reviews*, 12(3), p.445-453.

Hansen, R.D., Trees, A.J., Bah, G.S., Hetzel, U., Martin, C., Bain, O., Tanya, V.N. and Makepeace, B.L. 2011. A worm's best friend: recruitment of neutrophils by *Wolbachia* confounds eosinophil degranulation against the filarial nematode *Onchocerca ochengi. Proceedings of the Royal Society of London: Series B, Biological Sciences,* 278, p.2293-2302.

Hanski, L. and Vuorela, P. 2016. Lead discovery strategies for identification of *chlamydia* pneumoniae inhibitors. *Microorganisms*, 4(4), e43.

Hawking F, Thurston JP. 1951. The periodicity of microfilariae: I. The distribution of microfilariae in the body. *Transactions of the Royal Society of Tropical Medicine and Hygiene*, 45(3), p.307-28.

Hawking F. 1967. The 24-hour periodicity of microfilariae: biological mechanisms responsible for its production and control. *Proceedings of the Royal Society of London: Series B, Biological Sciences*, 169(1014), p59-76.

Hermans, P.G., Hart, C.A. and Trees, A.J. 2001. *In vitro* activity of antimicrobial agents against the endosymbiont *Wolbachia pipientis*. *Journal of Antimicrobial Chemotherapy*, 47(5), p.659-663.

Hilgenboecker, K., Hammerstein, P., Schlattmann, P., Telschow, A. and Werren, J.H. 2008. How many species are infected with *Wolbachia*?–a statistical analysis of current data. *FEMS microbiology letters*, 281(2), p.215-220.

Hoerauf, A. et al. 1999. Tetracycline therapy targets intracellular bacteria in the filarial nematode *Litomosoides sigmodontis* and results in filarial infertility. *Journal of Clinical Investigation*, 103(1), p.11–18.

Hoerauf, A., Volkmann, L., Hamelmann, C., Adjei, O., Autenrieth, I.B., Fleischer, B. and Büttner, D.W. 2000a. Endosymbiotic bacteria in worms as targets for a novel chemotherapy in filariasis. *Lancet*, 355(9211), p.1242–1243.

Hoerauf, A., Volkmann, L., Nissen-Paehle, K., Schmetz, C., Autenrieth, I., Büttner, D.W. and Fleischer, B. 2000b. Targeting of *Wolbachia* endobacteria in *Litomosoides sigmodontis*: Comparison of tetracyclines with chloramphenicol, macrolides and ciprofloxacin. *Tropical Medicine and International Health*, 5(4), p.275–279.

Hoerauf, A., Mand, S., Adjei, O., Fleischer, B. and Büttner, D.W. 2001. Depletion of *Wolbachia* endobacteria in *Onchocerca volvulus* by doxycycline and microfilaridermia after ivermectin treatment. *Lancet*, 357(9266), p.1415–1416.

Hoerauf, A., Mand, S., Volkmann, L., Büttner, M., Marfo-Debrekyei, Y., Taylor, M., Adjei, O. and Büttner, D.W. 2003a. Doxycycline in the treatment of human onchocerciasis: Kinetics of *Wolbachia* endobacteria reduction and of inhibition of embryogenesis in female *Onchocerca* worms. *Microbes and Infection*, 5(4), p.261–273.

Hoerauf, A., Mand, S., Fischer, K., Kruppa, T., Marfo-Debrekyei, Y., Debrah, A.Y., Pfarr, K.M., Adjei, O. and Büttner, D.W. 2003b. Doxycycline as a novel strategy against Bancroftian filariasis depletion of *Wolbachia* endosymbionts from *Wuchereria bancrofti* and stop of microfilaria production. *Medical Microbiology and Immunology*, 192(4), p.211–216.

Hoerauf, A., Marfo-Debrekyei, Y., Büttner, M., Debrah, A.Y., Konadu, P., Mand, S., Adjei, O. and Büttner, D.W. 2008a. Effects of 6-week azithromycin treatment on the *Wolbachia* endobacteria of *Onchocerca volvulus*. *Parasitology Research*, 103(2), p.279–286.

Hoerauf, A., Specht, S., Büttner, M., Pfarr, K., Mand, S., Fimmers, R., Marfo-Debrekyei, Y., Konadu, P., Debrah, A.Y., Bandi, C., et al. 2008b. *Wolbachia* endobacteria depletion by

doxycycline as antifilarial therapy has macrofilaricidal activity in onchocerciasis: A randomized placebo-controlled study. *Medical Microbiology and Immunology*, 197(3), p.295–311.

Hoerauf, A., Specht, S., Marfo-Debrekyei, Y., Büttner, M., Debrah, A.Y., Mand, S., Batsa, L., Brattig, N., Konadu, P., Bandi, C. et al. 2009. Efficacy of 5-week doxycycline treatment on adult *Onchocerca volvulus*. *Parasitology Research*, 104(2), p.437–447.

Hong, W.D., Benayoud, F., Nixon, G.L., Ford, L., Johnston, K.L., Clare, R.H., Cassidy, A., Cook, D.A., Siu, A., Shiotani, M., et al. 2019. AWZ1066S, a highly specific anti-*Wolbachia* drug candidate for a short-course treatment of filariasis. *Proceedings of the National Academy of Sciences*, 116(4), p.1414-1419.

Hopkins, A.D. 2016. Neglected tropical diseases in Africa: a new paradigm. *International Health*, 8(suppl_1), i28-i33.

Hotez, P. J., Fenwick, A., Savioli, L. and Molyneux, D.H. 2009. Rescuing the bottom billion through control of neglected tropical diseases. *Lancet*, 373(9674), p.1570–1575.

Hotez, P. J., Pecoul, B., Rijal, S., Boehme, C., Aksoy, S., Malecela, M., Tapia-Conyer, R. and Reeder, J.C. 2016. Eliminating the neglected tropical diseases: translational science and new technologies. *PLoS Neglected Tropical Diseases*, 10(3), e0003895.

Hughes, J. P., Rees, S., Kalindjian, S.B. and Philpott, K.L. 2011. Principles of early drug discovery. *British Journal of Pharmacology*, 162(6), p.1239–49.

Hussain, M., Lu, G., Torres, S., Edmonds, J.H., Kay, B.H., Khromykh, A.A. and Asgari, S. 2013. Effect of *Wolbachia* on replication of West Nile virus in a mosquito cell line and adult mosquitoes. *Journal of Virology*, 87(2), p.851-858.

Iversen, P. W., Beck, B., Chen, Y.F., Dere, W., Devanarayan, V., Eastwood, B.J., Farmen, M.W., Iturria, S.J., Montrose, C., Moore, R.A. 2004. HTS Assay Validation. In *Assay Guidance Manual*. p. 1–30.

Izzard, L., Fuller, A., Blacksell, S.D., Paris, D.H., Richards, A.L., Aukkanit, N., Nguyen, C., Jiang, J., Fenwick, S., Day, N.P. et al. 2010. Isolation of a novel *Orientia species* (*O. chuto* sp.

nov.) from a patient infected in Dubai. *Journal of Clinical Microbiology*, 48(12), p.4404-4409.

James, S.L., Abate, D., Abate, K.H., Abay, S.M., Abbafati, C., Abbasi, N., Abbastabar, H., Abd-Allah, F., Abdela, J., Abdelalim, A., et al. 2018. Global, regional, and national incidence, prevalence, and years lived with disability for 354 diseases and injuries for 195 countries and territories, 1990–2017: a systematic analysis for the Global Burden of Disease Study 2017. *Lancet*, 392(10159), p.1789-1858.

Jiang, J. and Richards, A., 2018. Scrub typhus: no longer restricted to the Tsutsugamushi Triangle. *Tropical Medicine and Infectious Disease*, 3(1), 11.

Johnston, K. L., Ford, L., Umareddy, I., Townson, S., Specht, S., Pfarr, K., Hoerauf, A., Altmeyer, R. and Taylor, M.J. 2014a. Repurposing of approved drugs from the human pharmacopoeia to target *Wolbachia* endosymbionts of onchocerciasis and lymphatic filariasis. *International Journal for Parasitology: Drugs and Drug Resistance*, 4(3), p.278–286.

Johnston, K. L., Ford, L. and Taylor, M. J. 2014b. Overcoming the challenges of drug discovery for neglected tropical diseases: The A·WOL experience. *Journal of Biomolecular Screening*, 19(3), p.335–343.

Johnston, K. L., Cook, D.A., Berry, N.G., Hong, W.D., Clare, R.H., Goddard, M., Ford, L., Nixon, G.L., O'Neill, P.M., Ward, S.A. 2017. Identification and prioritization of novel anti-*Wolbachia* chemotypes from screening a 10,000-compound diversity library. *Science Advances*, 36, p.1–11.

Kamgno, J., Pion, S.D., Chesnais, C.B., Bakalar, M.H., D'ambrosio, M.V., Mackenzie, C.D., Nana-Djeunga, H.C., Gounoue-Kamkumo, R., Njitchouang, G.R., Nwane, P. et al. 2017. A test-and-not-treat strategy for onchocerciasis in *Loa loa* – endemic areas. *New England Journal of Medicine*, 377(21), p.2044-2052.

Kamgno, J., Nana-Djeunga, H.C., Pion, S.D., Chesnais, C.B., Klion, A.D., Mackenzie, C.D., Nutman, T.B. and Boussinesq, M. 2018. Operationalization of the test and not treat strategy to accelerate the elimination of onchocerciasis and lymphatic filariasis in Central Africa. *International Health*, 10, i49–i53.

Karhu, E., Isojärvi, J., Vuorela, P., Hanski, L. and Fallarero, A. 2017. Identification of privileged antichlamydial natural products by a ligand-based strategy. *Journal of Natural Products*, 80(10), p.2602-2608.

Katsuno, K., Burrows, J.N., Duncan, K., Van Huijsduijnen, R.H., Kaneko, T., Kita, K., Mowbray, C.E., Schmatz, D., Warner, P. and Slingsby, B.T. 2015. Hit and lead criteria in drug discovery for infectious diseases of the developing world. *Nature Reviews Drug Discovery*. 14(11), p.751-758.

Keiser, P. B., Reynolds, S.M., Awadzi, K., Ottesen, E.A., Taylor, M.J. and Nutman, T.B. 2002. Bacterial endosymbionts of *Onchocerca volvulus* in the pathogenesis of posttreatment reactions. *Journal of Infectious Diseases*, 185(6), p.805–811.

Khare, S., Nagle, A.S., Biggart, A., Lai, Y.H., Liang, F., Davis, L.C., Barnes, S.W., Mathison, C.J., Myburgh, E., Gao, M.Y., et al. 2016. Proteasome inhibition for treatment of leishmaniasis, Chagas disease and sleeping sickness. *Nature*, 537, 229-233.

King, C.L., Suamani, J., Sanuku, N., Cheng, Y.C., Satofan, S., Mancuso, B., Goss, C.W., Robinson, L.J., Siba, P.M., Weil, G.J., et al. 2018. A trial of a triple-drug treatment for lymphatic filariasis. *New England Journal of Medicine*, 379(19), p.1801-1810.

Klarmann-Schulz, U., Specht, S., Debrah, A.Y., Batsa, L., Ayisi-Boateng, N.K., Osei-Mensah, J., Mubarik, Y., Konadu, P., Ricchiuto, A., Fimmers, R. et al. 2017. Comparison of doxycycline, minocycline, doxycycline plus albendazole and albendazole alone in their efficacy against onchocerciasis in a randomized, open-label, pilot trial. *Clinical Infectious Diseases*, 60(8), e0005156.

Kock, F., Hauptmann, M., Osterloh, A., Schäberle, T.F., Poppert, S., Frickmann, H., Menzel, K.D., Peschel, G., Pfarr, K., Schiefer, A. et al. 2018. *Orientia tsutsugamush*i is highly susceptible to the RNA polymerase switch region inhibitor corallopyronin A *in vitro* and *in vivo*. *Antimicrobial Agents and Chemotherapy*, 62(4), e01732-17.

Kozek, W. J. and Marroquin, H. F. 1977. Intracytoplasmic bacteria in *Onchocerca volvulus*. *American Journal of Tropical Medicine and Hygiene*, 26(4), p.663–678.

Kozek, W. J. 1977. Transovarially-transmitted intracellular microorganisms in adult and larval stages of *Brugia malayi*. *The Journal of Parasitology*, 63(6), p.992–1000.

Lachau-Durand, S., Lammens, L., Van Gompel, J., Bailey, G., Engelen, M. and Lampo, A. 2019. Preclinical toxicity and pharmacokinetics of a new orally bioavailable flubendazole formulation and the impact for clinical trials and risk/benefit to patients. *PLoS Neglected Tropical Diseases*, 13(1), e0007026.

Landmann, F., Foster, J.M., Slatko, B. and Sullivan, W. 2010. Asymmetric *Wolbachia* segregation during early *Brugia malayi* embryogenesis determines its distribution in adult host tissues. *PLoS Neglected Tropical Diseases*, 4(7), e758.

Landmann, F., Voronin, D., Sullivan, W. and Taylor, M.J. 2011. Anti-filarial activity of antibiotic therapy is due to extensive apoptosis after *Wolbachia* depletion from filarial nematodes. *PLoS Pathogens*, 7(11), e1002351.

Lefoulon, E., Bain, O., Makepeace, B.L., d'Haese, C., Uni, S., Martin, C. and Gavotte, L. 2016. Breakdown of coevolution between symbiotic bacteria *Wolbachia* and their filarial hosts. *PeerJ*, 4, e1840.

Lo, N., Paraskevopoulos, C., Bourtzis, K., O'Neill, S.L., Werren, J.H., Bordenstein, S.R. and Bandi, C. 2007. Taxonomic status of the intracellular bacterium *Wolbachia pipientis*. *International Journal of Systematic and Evolutionary Microbiology*, 57(3), p.654-657.

Lu, I.M., Kassis, T., Rogers, A.M., Schudel, A., Weil, J., Evans, C.C., Moorhead, A.R., Thomas, S.N., Dixon, J.B. 2018. Optimization of culture and analysis methods for enhancing long-term *Brugia malayi* survival, molting and motility *in vitro*. *Parasitology Open*, 4, e3.

Luce-Fedrow, A., Lehman, M., Kelly, D., Mullins, K., Maina, A., Stewart, R., Ge, H., John, H., Jiang, J. and Richards, A., 2018. A review of scrub typhus (*Orientia tsutsugamushi* and related organisms): then, now, and tomorrow. *Tropical Medicine and Infectious Disease*, 3(1), 8.

Lyu, J., Wang, S., Balius, T.E., Singh, I., Levit, A., Moroz, Y.S., O'Meara, M.J., Che, T., Algaa, E., Tolmachova, K. et al. 2019. Ultra-large library docking for discovering new chemotypes. *Nature*, 566, 224-229.

Maddry, J.A., Ananthan, S., Goldman, R.C., Hobrath, J.V., Kwong, C.D., Maddox, C., Rasmussen, L., Reynolds, R.C., Secrist III, J.A., Sosa, M.I. et al. 2009. Antituberculosis

activity of the molecular libraries screening center network library. *Tuberculosis*, 89(5), p.354-363.

Maina, A.N., Farris, C.M., Odhiambo, A., Jiang, J., Laktabai, J., Armstrong, J., Holland, T., Richards, A.L. and O'Meara, W.P., 2016. Q fever, scrub typhus, and *rickettsial* diseases in children, Kenya, 2011–2012. *Emerging Infectious Diseases*, 22(5), p.883-886.

Makepeace, B.L., Rodgers, L. and Trees, A.J. 2006. Rate of elimination of *Wolbachia pipientis* by doxycycline *in vitro* increases following drug withdrawal. *Antimicrobial Agents and Chemotherapy*, 50(3), p.922-927.

Mand, S., Pfarr, K., Sahoo, P.K., Satapathy, A.K., Specht, S., Klarmann, U., Debrah, A.Y., Ravindran, B. and Hoerauf, A. 2009. Macrofilaricidal activity and amelioration of lymphatic pathology in Bancroftian filariasis after 3 weeks of doxycycline followed by single-dose diethylcarbamazine. *The American Journal of Tropical Medicine Hygiene*, 81(4), p.702–711.

Mand, S., Debrah, A.Y., Klarmann, U., Batsa, L., Marfo-Debrekyei, Y., Kwarteng, A., Specht, S., Belda-Domene, A., Fimmers, R., Taylor, M. et al. 2012. Doxycycline improves filarial lymphedema independent of active filarial infection: a randomized controlled trial. *Clinical Infectious Diseases*, 55(5), p.621–630.

Marcellino, C., Gut, J., Lim, K.C., Singh, R., McKerrow, J., Sakanari, J. 2012. WormAssay: a novel computer application for whole-plate motion-based screening of macroscopic parasites. *PLoS Neglected Tropical Diseases*. 6, e1494.

Martin-Plaza, J. and Chatelain, E. 2015. Novel therapeutic approaches for neglected infectious diseases. *Journal of Biomolecular Screening*, 20(1), p.3–5.

McGarry, H. F., Pfarr, K., Egerton, G., Hoerauf, A., Akue, J.P., Enyong, P., Wanji, S., Kläger, S.L., Bianco, A.E., Beeching, N.J. et al. 2003. Evidence against *Wolbachia* symbiosis in *Loa loa*. *Filaria Journal,* 2(1), 9.

McGarry, H. F., Egerton, G.L. and Taylor, M.J. 2004. Population dynamics of *Wolbachia* bacterial endosymbionts in *Brugia malayi*. *Molecular and Biochemical Parasitology*, 135(1), p.57–67.

Mclaren, D. J., Worms, M.J., Laurence, B.R. and Simpson, M.G. 1975. Micro-organisms in filarial larvae (Nematoda). *Transactions of the Royal Society of Tropical Medicine and Hygiene*, 69(5-6), p.509-514.

Medicines Development for Global Health. 2018. Moxidectin package insert. https://www.accessdata.fda.gov/drugsatfda_docs/label/2018/210867lbl.pdf.

Melrose, W.D. 2002. Lymphatic filariasis: new insights into an old disease. *International Journal for Parasitology*, 32(8), p.947-960.

Molyneux, D. H., Bradley, M., Hoerauf, A., Kyelem, D. and Taylor, M.J. 2003. Mass drug treatment for lymphatic filariasis and onchocerciasis. *Trends in Parasitology*, 19(11), p.516–522.

Molyneux, D. H. 2004. "Neglected" diseases but unrecognised successes - challenges and opportunities for infectious disease control. *Lancet*, 364(9431), p.380–383.

Molyneux, D. H. 2012. The "Neglected Tropical Diseases": now a brand identity; responsibilities, context and promise. *Parasites & Vectors*, 5, 23.

Molyneux, D. H. 2017. The london declaration on neglected tropical diseases: 5 years on. *Transactions of the Royal Society of Tropical Medicine and Hygiene*, 375, p.239–47.

Molyneux, D. H., Savioli, L. and Engels, D. 2017. Neglected tropical diseases: progress towards addressing the chronic pandemic. *Lancet*, 389(10066), p.312–325.

Moon, S., Siqueira-Neto, J.L., Moraes, C.B., Yang, G., Kang, M., Freitas-Junior, L.H. and Hansen, M.A. 2014. An image-based algorithm for precise and accurate high throughput assessment of drug activity against the human parasite *Trypanosoma cruzi*. *PLoS One*, 9(2), e87188.

Nissink, J.W.M., Schmitt, S., Blackburn, S. and Peters, S. 2014. Stratified high-throughput screening sets enable flexible screening strategies from a single plated collection. *Journal of Biomolecular Screening*, 19(3), p.369–378.

Ollinger, J., Kumar, A., Roberts, D.M., Bailey, M.A., Casey, A. and Parish, T. 2019. A high-throughput whole cell screen to identify inhibitors of *Mycobacterium tuberculosis*. *PLoS One*, 14(1), e0205479.

O'Neill, S.L., Giordano, R., Colbert, A.M., Karr, T.L. and Robertson, H.M. 1992. 16S rRNA phylogenetic analysis of the bacterial endosymbionts associated with cytoplasmic incompatibility in insects. *Proceedings of the National Academy of Sciences*, 89(7), p.2699-2702.

O'Neill, S.L., Pettigrew, M., Sinkins, S.P., Braig, H.R., Andreadis, T.G. and Tesh, R.B. 1997. *In vitro* cultivation of *Wolbachia pipientis* in an *Aedes albopictus* cell line. *Insect Molecular Biology*, 6(1), p.33–39.

Opoku, N. O., Bakajika, D.K., Kanza, E.M., Howard, H., Mambandu, G.L., Nyathirombo, A., Nigo, M.M., Kasonia, K., Masembe, S.L., Mumbere, M. et al. 2018. Single dose moxidectin versus ivermectin for *Onchocerca volvulus* infection in Ghana, Liberia, and the Democratic Republic of the Congo: a randomised, controlled, double-blind phase 3 trial. *Lancet*, 392(10154), p.1207-1216.

Osei-Atweneboana, M.Y., Awadzi, K., Attah, S.K., Boakye, D.A., Gyapong, J.O. and Prichard, R.K. et al. 2011. Phenotypic evidence of emerging ivermectin resistance in *Onchocerca volvulus*. *PLoS Neglected Tropical Diseases*, 5(3), e998.

Ottesen, E.A., Vijayasekaran, V., Kumaraswami, V., Pillai, S.P., Sadanandam, A., Frederick, S., Prabhakar, R. and Tripathy, S.P. 1990. A controlled trial of ivermectin and diethylcarbamazine in lymphatic filariasis. *New England Journal of Medicine*, 322(16), p.1113–1117.

Ottesen, E.A. 2000. The global programme to eliminate lymphatic filariasis. *Tropical Medicine & International Health*, 5(9), p.591-594.

Ottesen, E.A. 2006. Lymphatic filariasis: treatment, control and elimination. *Advances in Parasitology*, 61, p.395–441.

Panic, G., Duthaler, U., Speich, B. and Keiser, J. 2014. Repurposing drugs for the treatment and control of helminth infections. *International Journal for Parasitology: Drugs and Drug Resistance*, 4(3), p.185–200.

Paveley, R. A., Mansour, N.R., Hallyburton, I., Bleicher, L.S., Benn, A.E., Mikic, I., Guidi, A., Gilbert, I.H., Hopkins, A.L. and Bickle, Q.D. 2012. Whole organism high-content screening by label-free, image-based bayesian classification for parasitic diseases. *PLoS*

Neglected Tropical Diseases, 6(7), e1762.

Payne, D.J., Gwynn, M.N., Holmes, D.J. and Pompliano, D.L. 2007. Drugs for bad bugs: confronting the challenges of antibacterial discovery. *Nature Reviews Drug Discovery*, 6(1), p.29-40.

Pena, I., Manzano, M.P., Cantizani, J., Kessler, A., Alonso-Padilla, J., Bardera, A.I., Alvarez, E., Colmenarejo, G., Cotillo, I., Roquero, I., et al. 2015. New compound sets identified from high throughput phenotypic screening against three kinetoplastid parasites: an open resource. *Scientific Reports,* 5(1), 8771.

Plaisier, A., van Oortmarssen, G., Remme, J. and Habbema, D. 1991. The reproductive lifespan of *Onchocerca volvulus* in West African savanna. *Acta tropica*, 48(4), p.271-284.

Remme, J., Baker, R.H., De Sole, G., Dadzie, K.Y., Walsh, J.F., Adams, M.A., Alley, E.S., Avissey, H.S. 1989. A community trial of ivermectin in the onchocerciasis focus of Asubende, Ghana. I. Effect on the microfilarial reservoir and the transmission of *Onchocerca volvulus*. *Tropical Medicine and Parasitology.* 40 (3), p.367-374.

Remme, J., De Sole, G., Dadzie, K.Y., Alley, E.S., Baker, R.H., Habbema, J.D.F., Plaisier, A.P., van Oortmarssen, G.J., Samba, E.M. 1990. Large scale ivermectin distribution and its epidemiological consequences. *Acta Leiden*. 59(1-2), p.177-191.

Richards, F.O., Amann, J., Arana, B., Punkosdy, G., Klein, R., Blanco, C., Lopez, B., Mendoza, C., Domínguez, A., Guarner, J. et al. 2007. No depletion of *Wolbachia* from *Onchocerca volvulus* after a short course of rifampin and/or azithromycin. *American Journal of Tropical Medicine and Hygiene*, 77(5), p.878–882.

Ros, V.I., Fleming, V.M., Feil, E.J. and Breeuwer, J.A. 2009. How diverse is the genus *Wolbachia*? Multiple-gene sequencing reveals a putatively new *Wolbachia* supergroup recovered from spider mites (*Acari: Tetranychidae*). *Applied and Environmental Microbiology*, 75(4), p.1036-1043.

Rousset, F., Bouchon, D., Pintureau, B., Juchault, P. and Solignac, M. 1992. *Wolbachia* endosymbionts responsible for various alterations of sexuality in arthropods.

Proceedings of the Royal Society of London: Series B, *Biological Sciences,* 250(1328), p.91-98.

Sanprasert, V., Sujariyakul, A. and Nuchprayoon, S. 2010. A single dose of doxycycline in combination with diethylcarbamazine for treatment of Bancroftian filariasis. *Southeast Asian Journal of Tropical Medicine and Public Health*, 41(4), p.800–812.

Sauerbrey, M. 2008. The onchocerciasis elimination program for the Americas (OEPA). *Annals of Tropical Medicine & Parasitology*, 102, p.25-29.

Savioli, L. and Daumerie, D. 2012. Accelerating work to overcome the global impact of neglected tropical diseases: a roadmap for implementation. *Geneva: World Health Organization*, p.1–42.

Schäberle, T.F., Schiefer, A., Schmitz, A., König, G.M., Hoerauf, A. and Pfarr, K. 2014. Corallopyronin A–A promising antibiotic for treatment of filariasis. *International Journal of Medical Microbiology*, 304(1), p.72-78.

Scherr, N., Pluschke, G. and Panda, M. 2016. A comparative study of activities of a diverse set of anti-mycobacterial agents against *Mycobacterium tuberculosis* and *Mycobacterium ulcerans*. *Antimicrobial Agents and Chemotherapy*, 60(5), 3132-3137.

Senyonjo, L., Oye, J., Bakajika, D., Biholong, B., Tekle, A., Boakye, D., Schmidt, E. and Elhassan, E. 2016. Factors associated with ivermectin non-compliance and its potential role in sustaining *Onchocerca volvulus* transmission in the West region of Cameroon. *PLoS Neglected Tropical Diseases*, 10(8), e0004905.

Serbus, L. R., Landmann, F., Bray, W.M., White, P.M., Ruybal, J., Lokey, R.S., Debec, A. and Sullivan, W. 2012. A cell-based screen reveals that the albendazole metabolite, albendazole sulfone, targets *Wolbachia*. *PLoS Pathogens*, 8(9), e1002922.

Sharma, R., Aljayyoussi, G., Tyrer, H.E., Gamble, J., Hayward, L., Guimaraes, A.F., Davies, J., Waterhouse, D., Cook, D.A., Myhill, L.J. et al. 2016. Minocycline as a re-purposed anti-*Wolbachia* macrofilaricide: superiority compared with doxycycline regimens in a murine infection model of human lymphatic filariasis. *Scientific Reports*, 6, 23458.

Shima, K., Ledig, S., Loeper, N., Schiefer, A., Pfarr, K., Hoerauf, A., Graspeuntner, S. and

Rupp, J. 2018. Effective inhibition of rifampicin-resistant *Chlamydia trachomatis* by the novel DNA-dependent RNA polymerase inhibitor corallopyronin A. *International Journal of Antimicrobial Agents*, 52(4), p.523-524.

Sironi, M., Bandi, C., Sacchi, L., Di Sacco, B., Damiani, G. and Genchi, C. 1995. Molecular evidence for a close relative of the arthropod endosymbiont *Wolbachia* in a filarial worm. *Molecular and Biochemical Parasitology*, 74, p.223–227.

Slatko, B. E., Taylor, M. J. and Foster, J. M. 2010. The *Wolbachia* endosymbiont as an anti-filarial nematode target. *Symbiosis*, 51(1), p.55–65.

Slatko, B.E., Luck, A.N., Dobson, S.L. and Foster, J.M. 2014. *Wolbachia* endosymbionts and human disease control. *Molecular and Biochemical Parasitology*, 195(2), p.88–95.

Somani, J., Bhullar, V.B., Workowski, K.A., Farshy, C.E. and Black, C.M. 2000. Multiple drug-resistant *Chlamydia trachomatis* associated with clinical treatment failure. *The Journal of Infectious Diseases*, 181(4), p.1421-1427.

Specht, S., Mand, S., Marfo-Debrekyei, Y., Debrah, A.Y., Konadu, P., Adjei, O., Büttner, D.W. and Hoerauf, A. 2008. Efficacy of 2-and 4-week rifampicin treatment on the *Wolbachia* of *Onchocerca volvulus*. *Parasitology International*, 103, p.1303–1309.

Srinivasan, G. and Shobha, G. 2008. Statistical texture analysis. *Proceedings of World Academy of Science, Engineering and Technology*, 36, p.1264–1269.

Stanley, S.A., Barczak, A.K., Silvis, M.R., Luo, S.S., Sogi, K., Vokes, M., Bray, M.A., Carpenter, A.E., Moore, C.B., Siddiqi, N. et al. 2014. Identification of host-targeted small molecules that restrict intracellular *Mycobacterium tuberculosis* growth. *PLoS Pathogens*, 10(2), e1003946.

Starkuviene, V. and Pepperkok, R. 2007. The potential of high-content high-throughput microscopy in drug discovery. *British Journal of Pharmacology*, 152(1), p.62–71.

Stolk, W. A., Stone, C. and de Vlas, S. J. 2015. Modelling lymphatic filariasis transmission and control: modelling frameworks, lessons learned and future directions. *Advances in Parasitology*, 87, p.249-291

Storey, B., Marcellino, C., Miller, M., Maclean, M., Mostafa, E., Howell, S., Sakanari, J.,

Wolstenholme, A. and Kaplan, R. 2014. Utilization of computer processed high definition video imaging for measuring motility of microscopic nematode stages on a quantitative scale: "The Worminator". *International Journal for Parasitology: Drugs and Drug Resistance*, 4(3), p233-43.

Stouthamer, R., Breeuwer, J.A.J., Luck, R.F. and Werren, J.H. 1993. Molecular identification of microorganisms associated with parthenogenesis. *Nature*, 361(6407), p.66.

Sundaramurthy, V., Barsacchi, R., Samusik, N., Marsico, G., Gilleron, J., Kalaidzidis, I., Meyenhofer, F., Bickle, M., Kalaidzidis, Y. and Zerial, M. 2013. Integration of chemical and RNAi multiparametric profiles identifies triggers of intracellular mycobacterial killing. *Cell Host & Microbe*, 13(2), p.129-142.

Supali, T., Djuardi, Y., Pfarr, K.M., Wibowo, H., Taylor, M.J., Hoerauf, A., Houwing-Duistermaat, J.J., Yazdanbakhsh, M. and Sartono, E. 2008. Doxycycline treatment of *Brugia malayi* infected persons reduces microfilaremia and adverse reactions after diethylcarbamazine and albendazole treatment. *Clinical Infectious Diseases*, 46(9), p.1385–1393.

Sykes, M. L. and Avery, V. M. 2013. Approaches to protozoan drug discovery: phenotypic screening: miniperspectives series on phenotypic screening for anti-infective targets. *Journal of Medicinal Chemistry*, 56(20), p.7727–7740.

Tamarozzi, F., Halliday, A., Gentil, K., Hoerauf, A., Pearlman, E. and Taylor, M.J. 2011. Onchocerciasis: The role of *Wolbachia* bacterial endosymbionts in parasite biology, disease pathogenesis, and treatment. *Clinical Microbiology Reviews*, 24(3), p.459–468.

Tamarozzi, F., Tendongfor, N., Enyong, P.A., Esum, M., Faragher, B., Wanji, S. and Taylor, M.J. 2012. Long term impact of large scale community-directed delivery of doxycycline for the treatment of onchocerciasis. *Parasites & Vectors*, 5, 53.

Taylor, M. J., Bilo, K., Cross, H.F., Archer, J.P. and Underwood, A.P. 1999a. 16S rDNA phylogeny and ultrastructural characterization of *Wolbachia* intracellular bacteria of the filarial nematodes *Brugia malayi*, *B. pahangi*, and *Wuchereria bancrofti*. *Experimental Parasitology*, 91(4), p.356–361.

Taylor, M. J. and Hoerauf, A. 1999b. *Wolbachia* bacteria of filarial nematodes. *Parasitology*,

15(11), p.437–442.

Taylor, M. J., Makunde, W.H., McGarry, H.F., Turner, J.D., Mand, S. and Hoerauf, A. 2005. Macrofilaricidal activity after doxycycline treatment of *Wuchereria bancrofti*: a double-blind, randomised placebo-controlled trial. *Lancet*, 365(9477), p.2116–2121.

Taylor, M.J., Awadzi, K., Basáñez, M.G., Biritwum, N., Boakye, D., Boatin, B., Bockarie, M., Churcher, T.S., Debrah, A., Edwards, G. and Hoerauf, A. 2009. Onchocerciasis control: vision for the future from a Ghanian perspective. *Parasites & Vectors*, 2, 7.

Taylor, M. J., Hoerauf, A. and Bockarie, M. 2010. Lymphatic filariasis and onchocerciasis. *Lancet*. 376(9747), p. 1175–1185.

Taylor, M. J., Voronin, D., Johnston, K.L. and Ford, L. 2013. *Wolbachia* filarial interactions. *Cellular Microbiology*, 15(4), p.520–526.

Taylor, M. J., Hoerauf, A., Townson, S., Slatko, B.E. and Ward, S.A. 2014. Anti-*Wolbachia* drug discovery and development: safe macrofilaricides for onchocerciasis and lymphatic filariasis. *Parasitology*, 141(1), p.119–27.

Taylor, M.J., Bordenstein, S.R. and Slatko, B. 2018. Microbe profile: *Wolbachia*: a sex selector, a viral protector and a target to treat filarial nematodes. *Microbiology*, 164(11), p.1345-1347.

Taylor, M. J., von Geldern, T.W., Ford, L., Hübner, M.P., Marsh, K., Johnston, K.L., Sjoberg, H.T., Specht, S., Pionnier, N., Tyrer, H.E. et al. 2019. New macrolides as short-course oral anti-*Wolbachia* therapy for filariasis. *Science Translational Medicine*, in press.

Thorne, N., Auld, D. S. and Inglese, J. 2010. Apparent activity in high-throughput screening: origins of compound-dependent assay interference. *Current Opinion in Chemical Biology*, 14(3), p.315–324.

Tilak, R. and Kunte, R. 2019. Scrub typhus strikes back: Are we ready?. *Medical Journal Armed Forces India*, 75, 8-17.

Turner, H.C., Churcher, T.S., Walker, M., Osei-Atweneboana, M.Y., Prichard, R.K. and Basáñez, M.G. 2013. Uncertainty surrounding projections of the long-term impact of ivermectin treatment on human onchocerciasis. *PLoS Neglected Tropical Diseases*, 7(4),

e2169.

Turner, H. C., Walker, M., Churcher, T.S. and Basáñez, M.G. 2014. Modelling the impact of ivermectin on River Blindness and its burden of morbidity and mortality in African savannah: EpiOncho projections. *Parasites & Vectors*, 7, 241.

Turner, H.C., Walker, M., Attah, S.K., Opoku, N.O., Awadzi, K., Kuesel, A.C. and Basáñez, M.G. 2015. The potential impact of moxidectin on onchocerciasis elimination in Africa: an economic evaluation based on the Phase II clinical trial data. *Parasites & Vectors*, 8, 167.

Turner, J.D., Mand, S., Debrah, A.Y., Muehlfeld, J., Pfarr, K., McGarry, H.F., Adjei, O., Taylor, M.J. and Hoerauf, A. 2006a. A randomized, double-blind clinical trial of a 3-week course of doxycycline plus albendazole and ivermectin for the treatment of *Wuchereria bancrofti* infection. *Clinical Infectious Diseases*, 42, p.1081–89.

Turner, J.D., Langley, R.S., Johnston, K.L., Egerton, G., Wanji, S. and Taylor, M.J. 2006b. *Wolbachia* endosymbiotic bacteria of *Brugia malayi* mediate macrophage tolerance to TLR- and CD40-specific stimuli in a MyD88/TLR2-dependent manner. *Journal of Immunology*, 177(2), p.1240–1249.

Turner, J.D., Langley, R.S., Johnston, K.L., Gentil, K., Ford, L., Wu, B., Graham, M., Sharpley, F., Slatko, B., Pearlman, E., et al. 2009. *Wolbachia* lipoprotein stimulates innate and adaptive immunity through toll-like receptors 2 and 6 (TLR2/6) to induce disease manifestations of filariasis. *Journal of Biological Chemistry*. 284(33), p.22364-22378.

Turner, J.D., Tendongfor, N., Esum, M., Johnston, K.L., Langley, R.S., Ford, L., Faragher, B., Specht, S., Mand, S., Hoerauf, A. et al. 2010. Macrofilaricidal activity after doxycycline only treatment of *Onchocerca volvulus* in an area of *Loa loa* co-endemicity: a randomized controlled trial. *PLoS Neglected Tropical Diseases*, 4(4), e660.

Turner, J.D., Sharma, R., Aljayyoussi, G., Tyrer, H.E., Gamble, J., Hayward, L., Priestley, R.S., Murphy, E.A., Davies, J., Waterhouse, D., et al. 2017. Albendazole and antibiotics synergize to deliver short-course anti-*Wolbachia* curative treatments in preclinical models of filariasis. *Proceedings of the National Academy of Sciences*, 114(45), e9712–9721.

Van den Hurk, A.F., Hall-Mendelin, S., Pyke, A.T., Frentiu, F.D., McElroy, K., Day, A., Higgs, S. and O'Neill, S.L. 2012. Impact of *Wolbachia* on infection with chikungunya and yellow fever viruses in the mosquito vector *Aedes aegypti*. *PLoS Neglected Tropical Diseases*, 6(11), e1892.

Venard, C.P., Crain, P.R. and Dobson, S.L. 2011. SYTO11 staining vs FISH staining: a comparison of two methods to stain *Wolbachia pipientis* in cell cultures. *Letters in Applied Microbiology*, 52(2), p.168-176.

Verver, S., Walker, M., Kim, Y.E., Fobi, G., Tekle, A.H., Zouré, H.G., Wanji, S., Boakye, D.A., Kuesel, A.C., de Vlas, S.J. et al. 2018. How can onchocerciasis elimination in Africa be accelerated? Modelling the impact of increased frequency of ivermectin distribution and complementary vector control. *Clinial Infectious Diseases*, 66, p.267–274.

Walker, T.J., Johnson, P.H., Moreira, L.A., Iturbe-Ormaetxe, I., Frentiu, F.D., McMeniman, C.J., Leong, Y.S., Dong, Y., Axford, J., Kriesner, P. et al. 2011. The *w*Mel *Wolbachia* strain blocks dengue and invades caged *Aedes aegypti* populations. *Nature*, 476(7361), p.450.

Walker, M., Specht, S., Churcher, T.S., Hoerauf, A., Taylor, M.J. and Basáñez, M.G. 2015. Therapeutic efficacy and macrofilaricidal activity of doxycycline for the treatment of river blindness. *Clinical Infectious Diseases*, 60(8), p.1199-1207.

Wanji, S., Tendongfor, N., Nji, T., Esum, M., Che, J.N., Nkwescheu, A., Alassa, F., Kamnang, G., Enyong, P.A., Taylor, M.J., et al. 2009. Community-directed delivery of doxycycline for the treatment of onchocerciasis in areas of co-endemicity with loiasis in Cameroon. *Parasites & Vectors*, 2, 39.

Wanji, S., Kengne-Ouafo, J.A., Esum, M.E., Chounna, P.W., Adzemye, B.F., Eyong, J.E., Jato, I., Datchoua-Poutcheu, F.R., Abong, R.A., Enyong, P. et al. 2015. Relationship between oral declaration on adherence to ivermectin treatment and parasitological indicators of onchocerciasis in an area of persistent transmission despite a decade of mass drug administration in Cameroon. *Parasites & Vectors*, 8, 667.

White, P.M., Pietri, J.E., Debec, A., Russell, S., Patel, B. and Sullivan, W. 2017. Mechanisms of horizontal cell-to-cell transfer of *Wolbachia* spp. in *Drosophila melanogaster*. *Applied and Environmental Microbiology*, 83(7), e03425-16.

Wigglesworth, M.J., Murray, D.C., Blackett, C.J., Kossenjans, M. and Nissink, J.W.M. 2015. Increasing the delivery of next generation therapeutics from high throughput screening libraries. *Current Opinion in Chemical Biology*, 26, p.104–110.

World Health Organization. 2012. African programme for onchocerciasis control: meeting of national onchocerciasis task forces. *Weekly Epidemiological Record*, 49/50, p.494–508.

World Health Organization. 2016. WHO guidelines for the treatment of *Chlamydia trachomatis. https://www.who.int/reproductivehealth/publications/rtis/chlamydia-treatment-guidelines/en/* [Accessed February 08, 2019].

World Health Organization. 2017. Global programme to eliminate lymphatic filariasis: progress report, 2016. *Weekly Epidemiological Record*, 92, p.594–608.

World Health Organization. 2018a. Lymphatic filariasis fact sheet. *http://www.who.int/en/news-room/fact-sheets/detail/lymphatic-filariasis*. [Accessed June 12, 2018].

World Health Organization. 2018b. Lymphatic filariasis status of mass drug administration: 2018. *http://apps.who.int/neglected_diseases/ntddata/lf/lf.html*. [Accessed October 18, 2018].

World Health Organization. 2018c. Onchocerciasis fact sheet. *http://www.who.int/news-room/fact-sheets/detail/onchocerciasis*. [Accessed June 12, 2018].

World Health Organization. 2018d. Onchocerciasis status of endemicity of onchocerciasis: 2018. *http://apps.who.int/neglected_diseases/ntddata/oncho/onchocerciasis.html*. [Accessed October 18, 2018].

World Health Organization. 2018e. Neglected tropical diseases. *http://www.who.int/neglected_diseases/diseases/en/*. [Accessed June 12, 2018].

World Health Organization. 2018f. Tuberculosis fact sheet. https://www.who.int/en/news-room/fact-sheets/detail/tuberculosis. [Accessed February 08, 2019].

World Health Organization. 2019a. Leprosy. https://www.who.int/lep/en/. [Accessed February 08, 2019].

World Health Organization. 2019b. Buruli ulcer. https://www.who.int/buruli/en/. [Accessed

February 08, 2019].

World Health Organization. 2019c. Trachoma. *https://www.who.int/trachoma/disease/en/.* [Accessed February 08, 2019].

World Mosquito Program. Our research. http://www.eliminatedengue.com/our-research/*Wolbachia.* [Accessed February 1, 2019].

Wu, B., Novelli, J., Foster, J., Vaisvila, R., Conway, L., Ingram, J., Ganatra, M., Rao, A.U., Hamza, I. and Slatko, B. 2009. The heme biosynthetic pathway of the obligate *Wolbachia* endosymbiont of *Brugia malayi* as a potential anti-filarial drug target. *PLoS Neglected Tropical Diseases*, 3(7), e475.

Yarrow, J., Feng, Y., Perlman, Z.E., Kirchhausen, T. and Mitchison, T.J. 2003. Phenotypic screening of small molecule libraries by high throughput cell imaging. *Combinatorial Chemistry & High Throughput Screening*, 6(4), p.279–286.

Zanella, F., Lorens, J. B. and Link, W. 2010. High content screening: seeing is believing. *Trends in Biotechnology*, 28(5), p.237–245.

Zhang, J.H., Chung, T.D.Y. and Oldenburg, K.R. 1999. A simple statistical parameter for use in evaluation and validation of high throughput screening assays. *Journal of Biomolecular Screening*, 4(2), p.67–73.

Zug, R. and Hammerstein, P. 2012. Still a host of hosts for *Wolbachia*: analysis of recent data suggests that 40% of terrestrial arthropod species are infected. *PLoS One*, 7(6), e38544.

Zuniga, E.S., Early, J. and Parish, T. 2015. The future for early-stage tuberculosis drug discovery. *Future Microbiology*, 10(2), p.217-229.

Appendix

Primer design for the qPCR analysis in the tertiary screen developed by A·WOL. The primers are based on either *Brugia malayi wsp* (surrogate for *Wolbachia* quantification) or *Brugia malayi gst* (surrogate for worm quantification).

Primer name	Sequence position	Sequence	Product size	Melting temperature
BMWSP _forward	456	5' CCCTGCAAAGGCACAAGTTATTG 3'	117	65
BMWSP _ reverse	572	5' CGAGCTCCAGCAAAGAGTTTAATTT 3'	117	63
BMGST_ forward	1368	5' GAGACATCTTGCTCGCAAAC 3'	264	59
BMGST_ reverse	1632	5' ATCACGGACGCCTTCACAG 3'	264	59